U.PORTO

FACULDADE DE FARMÁCIA
UNIVERSIDADE DO PORTO

Development of a proliposome formulation as a drug carrier for a novel antitumor drug

Ana Daniela Coutinho Alves

Dissertation of the 2nd Cycle of Studies Conducting the Degree of Master in Pharmaceutical Chemistry, Faculty of Pharmacy, University of Porto

Dissertação do 2º Ciclo de Estudos Conducente ao Grau de Mestre em Química Farmacêutica, Faculdade de Farmácia, Universidade do Porto

Under the scientific guidance of/ Sob orientação do:
 Professor Doutor Paulo Jorge Cardoso da Costa
 Professor Doutor Domingos Carvalho Ferreira

2016/2017

ACCORDING TO THE LEGISLATION, THE REPRODUCTION OF ANY PART OF THIS DISSERTATION IS NOT AUTHORIZED.

AUTHOR'S DECLARATION:

Under the terms of the Decree-Law no 216/92, of October 13th, is hereby declared that the author afforded a major contribution to the conceptual design and technical execution of the work and interpretation of the results included in this dissertation. Under the terms of the referred Decree-Law, is hereby declared that the following articles/communications were prepared in the scope of this dissertation.

The results presented in this dissertation are part of the following scientific communications:

Ana D. Coutinho Alves, E. Sousa, Madalena M. M Pinto, Marta Correia-da-Silva, D. Ferreira, P. Costa. "Development of HPLC method for the quantification of a new glycosylated xanthone with cell growth inhibitory activity". 10th Meeting of Young Researchers of University of Porto, Porto, Portugal, 08-10 February 2017.

ACKNOWLEDGMENTS

The making of this dissertation has been a fantastic learning experience, not only regarding academic and scientific knowledge, but mainly for personal aspects I developed.

My first special thanks are dedicated to my supervisor Prof. Dr. Paulo Jorge Cardoso da Costa. I don't have enough words to express my gratitude. He always showed willingness to listen to my doubts and always managed to solve them and showed incredible patience and dedication. He was my main adviser, and more importantly, I sincerely thank Prof. Dr. Paulo Costa for always believing in the success of my work and for recognizing my effort. I am grateful to have the opportunity to work with him, and for all the teachings I could learn.

I want to thank my co-supervisor, Prof. Dr. Domingos Ferreira de Carvalho. During my work, he showed an immense availability and a constant concern with my work. Thank you for all the teachings and wisdom he shared and will certainly continue to share with me. I really appreciate the opportunity that was given to work on this ambitious project and to deal with its inherent subjects.

I also want to thank the following persons.

- Prof. Dr.ª Maria Madalena de Magalhães Pinto for all the help she has given.
- The teachers of Organic and Pharmaceutical Chemistry for the knowledge transmitted in the Master, especially the Prof. Dr.ª Emília Sousa and Prof. Dr.ª Marta Correia da Silva for all the assistance given during this year.
- Prof. Dr.ª Salette Reis (Laboratório de Química Aplicada da Faculdade de Farmácia da Universidade do Porto) and his collaboration team but especially to Prof. Dr.ª Claúdia Nunes, for the help given.
- Prof. Dr. Hassan Bousbaa (Instituto Superior de Ciências da Saúde –Norte, ISCS-N), and his collaboration team, especially Dr.ª Patrícia Silva, for the help in the viability cells study that have made my work more rewarding.
- Centro de Materiais da Universidade do Porto (CEMUP) for the morphology analasys (SEM and CryoSEM).
- My colleagues in the Master's Degree in Pharmaceutical Chemistry for the friendship and support, with special recognition to Ana Joyce, João Carmo, Francisca Carvalhal, Isabel Barbosa, Ivanna Hk, Giulia Esposito and João

Campos for his help in my work and for always taking the time to listen to me.

- For my incredible family, especially my father, my mother, my sister and my amazing boyfriend, thank you for being my core, my shelter, for always believing in me, in my value and potential, more than myself, and for being at my side as I give this step in my life. Thus, this dissertation is especially dedicated to them.

NORTE-01-0145-FEDER-000035

ABSTRACT

The use of nanotechnology in cancer is progressing, thus increasing the effectiveness and/or tolerability of new drug candidates. Nanotechnology can significantly contribute to create differentiated products and improve clinical outcomes. Nanoparticles give us the possibility to encapsulate poorly water soluble drugs, protect therapeutic molecules, and modify their blood circulation and tissue distribution.

Liposomes may incorporate hydrophilic and/or lipophilic substances, where they can stand in the aqueous compartment, be inserted in the lipophilic phase or adsorbed on the membrane surface. They have been widely explored for the delivery of drugs. However, these systems have problems of stability, limiting its storage for a long period of time. The proliposomes were developed to overcome the stability problems of the liposomes.

The xanthone classes bear different types of substituents that are able to interact with several biological targets and exert different pharmacological actions. There is a diversity of biological activities described for natural and synthetic xanthones, and the growth inhibitor in tumor cell lines seems to be quite important as they exert their effect on a wide range of different tumor cell lines.

In this dissertation, proliposomal formulations were developed to encapsulate the synthetic xanthonic compound XGA, being the method used to produce proliposomes the *Spray Drying*. After their production, proliposomes were hydrated to form liposomes. This method proved to be efficient at encapsulating the compound. Liposomes have also been developed and have been shown to be efficient in the encapsulation of XGA, however the stability showed to be limited. It was found that after 15 days, 1 month and 3 months of the production date, the proliposomes presented good physical stability, being this method a promising strategy to improve stability. Toxicity was evaluated in 3 tumor cell lines, where it was found that the encapsulated compound was able to inhibit them.

Keywords: Xanthone; Cancer; Tumor cell lines; Nanotechnology; Liposomes; Proliposomes; XGA.

RESUMO

A utilização da nanotecnologia no cancro está a progredir, aumentando assim a eficácia e / ou tolerabilidade de novos candidatos a medicamentos. A nanotecnologia pode contribuir significativamente para criar produtos diferenciados e melhorar o resultado clínico. As nanopartículas dão-nos a possibilidade de encapsular medicamentos pouco solúveis em água, de proteger moléculas com interesse terapêutico e modificar a sua circulação sanguínea e a sua distribuição nos tecidos.

Os lipossomas podem incorporar substâncias hidrofílicas e / ou lipofílicas, permanecendo no compartimento aquoso, ser inseridos na fase lipofílica ou adsorvidos na superfície da membrana. Estes sistemas têm vindo a ser amplamente explorados para a vectorização e a libertação de fármacos. No entanto, têm problemas de estabilidade, limitando o seu armazenamento por um longo período de tempo. Os prolissomas foram descobertos e tem vindo a ser desenvolvidos para superar os problemas de estabilidade dos lipossomas.

As classes de xantonas possuem diferentes tipos de substituintes capazes de interagir com vários alvos biológicos que exercem diferentes ações, permitindo-lhes interagir com diferentes alvos farmacológicos. Há uma diversidade de atividades biológicas descritas para xantonas naturais e sintéticas, e o inibidor de crescimento em linhas celulares tumorais parece ser bastante importante, pois exercem o seu efeito em uma ampla gama de diferentes linhas celulares tumorais.

Nesta dissertação, formulações prolipossomais foram desenvolvidas para encapsular o composto xantônico XGA, sendo o método utilizado para a produção de prolipossomas a atomização e secagem. Após a sua produção, os prolipossomas foram hidratados para formar lipossomas. Este método mostrou-se eficiente no encapsulamento do composto. Os lipossomas também foram desenvolvidos e demonstraram ser eficientes no encapsulamento de XGA, mas sendo a sua estabilidade limitada. Verificou-se que 15 dias, 1 mês e 3 meses após a produção dos prolipossomas, eles apresentaram boa estabilidade física, sendo uma estratégia promissora. A toxicidade foi avaliada em 3 linhas celulares tumorais, onde se descobriu que o composto encapsulado inibe essas linhas tumorais.

Palavras-chave: Xantona; Cancro; Linhas celulares tumorais; Nanotecnologia; Lipossomas; Prolipossomas; XGA.

TABLE OF CONTENTS

INDEX OF FIGURES

INDEX OF TABLES

LIST OF ABBREVIATIONS

α - Separation coefficient

BBB - Blood-brain barrier

DAD – Diode Array Detector

DDS - Drug Delivery System

DPI - Dry powder inhalers

DSC - Differential Scanning Calorimetry

FTIR - Fourier transform infrared spectroscopy

HPLC - High performance liquid chromatography

K - Retention factor

LUV – Large unilamellar vesicles

MLV - Multilamellar vesicles

MPS - Mononuclear Phagocyte System

N - Number of theoretical plates

PC – Phosphatidylcholine

PCS - Photon correlation spectroscopy

PE - Phosphatidylethanolamine

PI - Polydispersion Index

pMDI - Pressurized metered dose Inhalers

PS - Phosphatidylserine

RES - Reticuloendothelial system

R_s – Resolution

SCF - Super critical anti-solvent method

SD – Spray Drying

SEM - Scanning electron microscopy

SM - Sphingomyelin

SUV - Small unilamellar vesicles

T – Tailing factor

TEM - Transmission electron microscopy

t_r - Retention time

UV – Unilamellar vesicles

ZP – Zeta Potential

OUTLINE OF THE DISSERTATION

The present dissertation consists of seven chapters. On the first Chapter a small introduction of the themes is done. In the second Chapter the main objectives of the work are presented. In the third Chapter the materials and methods used are described. In the fourth Chapter the results are presented and discussed. In the fifth Chapter the general conclusions of the work are presented. Finally we have in the sixth and seventh Chapters the bibliographical references and the appendices respectively.

CHAPTER 1 – INTRODUCTION

The introductory Chapter of the present dissertation is divided in four sections. In the first part, a briefly overview about the effects of nanotechnology in cancer will be presented. The second part will be focused on liposomes as drug delivery systems suitable for application in cancer nanotechnology, with their advantages and drawbacks being highlighted. In the third part, proliposomes will be presented as a promising strategy to overcome the drawbacks presented by liposomes. In the fourth part, a brief introduction to xanthone derivatives will be given and their use in nanosystems will be justified.

CHAPTER 2 – AIMS

The main objectives of the present dissertation are described in this Chapter.

CHAPTER 3 - MATERIAL AND METHODS

In this Chapter, methods of producing proliposomes and their characterization will be described in detail. Hydration of the proliposomes and characterization of the liposomes obtained will also be described. The conditions used for the stability tests of the proliposomes will be specified. HPLC conditions for the development of a method for quantifying XGA will be detailed. The software and the statistical tests will be identified.

CHAPTER 4 - RESULTS AND DISCUSSION

Results are subdivided in five sections. In the first part, the characterization of the liposomes obtained by hydration of proliposomes and stability results of proliposomes will be show. The second part will show the results of the analysis of thermal behavior of proliposomes. The third part will present the results of the HPLC method for the quantification of XGA. The fourth part will show the results of cell culture. The fifth part will show the morphology of proliposomes.

CHAPTER 5 – CONCLUSIONS

This chapter includes the general conclusions of the present dissertation.

CHAPTER 6 – REFERENCES

The references will be presented at the end of this dissertation. The references followed the Vancouver reference style. The main bibliographic research motors were ScienceDirect, Pubmed, Scopus, and Google.

CHAPTER 7 – APPENDICES

This section will include the complete of data for the characterization of conventional liposomes and the liposomes obtained by hydration of proliposomes that were used to construct the box and whiskers plots used to present the results and the data obtained from t-student, Shapiro-Wilk and Levene statistic tests. It will also include the complete data of the histograme of the sizes and zeta potential the liposomes and proliposomes.

1 Introduction

1.1 Cancer nanotechnology

Nanotechnology can be described as the control and manipulate structured matter at an atomic and molecular level, allowing the development of devices, functional materials and systems with significantly different properties from those observed in micro or macroscopic scale (1).

Cancer is defined as a large group of diseases that can affect any part of the body. A defining feature of cancer is the rapid creation of abnormal cells that grow beyond normal limits, which can invade parts of the body and spread to other organs (2).

Cancer nanotherapeutics is advancing, as the research and development in this field has been in exponential growth since the beginning of XXI century (3). Cancer nanotechnology is emerging as a new field of interdisciplinary research and is expected to lead to breakthroughs in the detection, diagnosis and treatment of cancer (4). The idea of creating more effective cancer treatments gives us the possibility of encapsulating poor water soluble drugs, protecting therapeutic molecules and modifying their blood circulation and tissue distribution without serious damage to normal cells (5).

Cancer and normal cells present different chemical, structural and biophysical characteristics. While no pattern has been explained, such modifications can be accountable for cancer cell sensitivity or resistance to several anticancer drugs (6). Some tumor cells exhibit greater membrane flexibility, in opposing, other cancer cells, present lower membrane fluidity because there is a decreased degree of fatty acid unsaturation and increased cholesterol (7, 8).

The surrounding environment also suffers multiple changes. Tumor microenvironment is harsh and essentially determined by a disordered vasculature that creates an heterogeneous blood supply (9). As a result, several regions are hypoxic and have a high glucose use rates, resulting in an acidic extracellular pH (pH_e) in malignant tumors (pH = 6.2 – 6.9) compared to normal tissue (pH_e= 7.3 - 7.4), figure 1 (10-12). Many studies showed that this pH_e benefits the malignant cells and is a standard intrinsic feature of cancer phenotype (13). Since this can influence the ionization state of the drugs and, consequently, their partition with membranes, this feature should be taken in account (13).

The characteristics of the membrane impacts the drug permeation, lipid conformation and/or location within membrane and, consequently, their ability to reach the

therapeutic target (14). Also, drugs can have distinctive effects on the membrane, such as modifications in lipid conformation, surface charge, lipid domains and packing, membrane fluidity and curvature and, consequently, cell function (15). The study of the interactions of chemotherapeutic compounds with biological membranes is vital, since it is directly correlated with the therapeutic activity and toxicity of drugs (16).
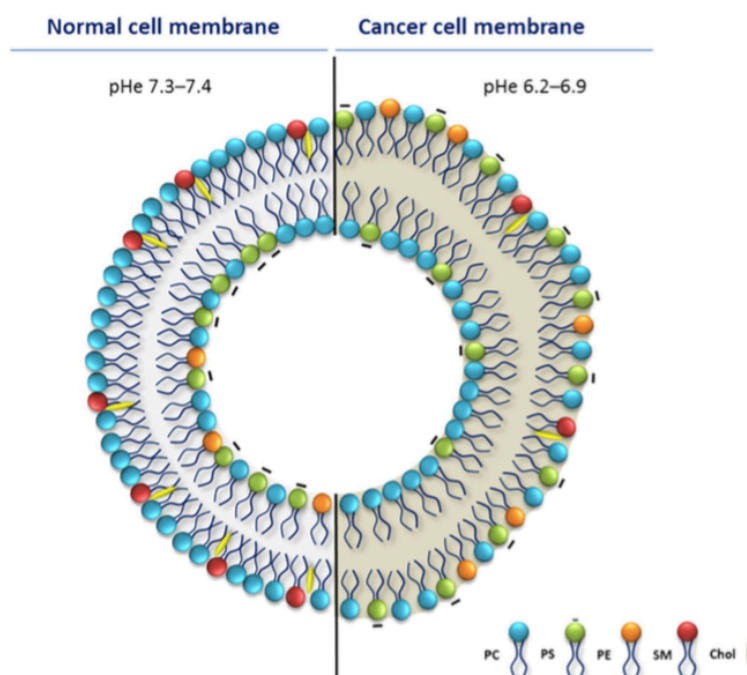
Figure 1 – Schematic representation of normal and cancer cell membranes (16).

1.2   Liposomes

Liposomes, first reported by Bangham in 1965, are microscopic vesicles composed of one or more concentric lipid bilayers separated by internal and external aqueous environment. It can be created from natural non-toxic phospholipids and cholesterol, they may incorporate hydrophilic and/or lipophilic substances, where they can stand in the aqueous compartment, be inserted in the lipophilic phase or adsorbed on the membrane surface (17-19). Hydrophobic molecules are inserted into the bilayer membrane, and hydrophilic molecules can be entrapped in the aqueous center (Figure 2) (20, 21).
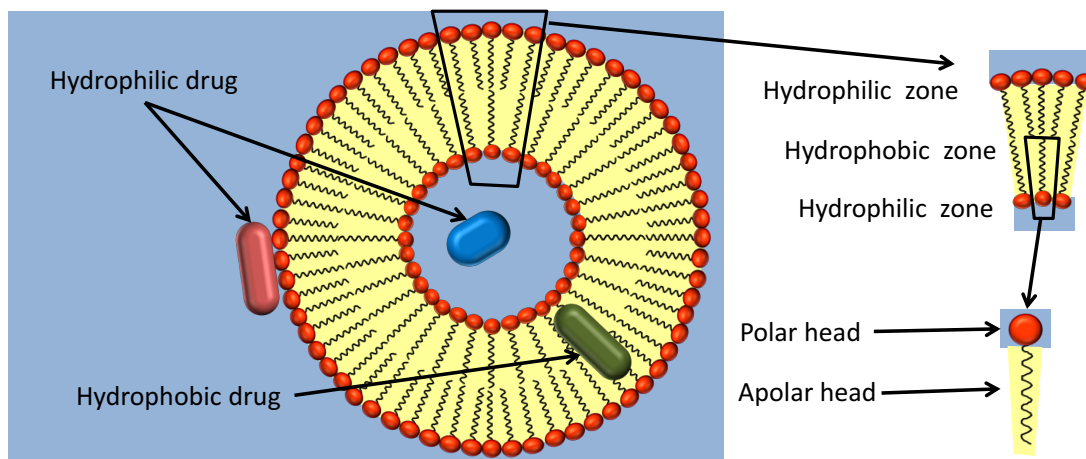
Figure 2 - Schematic representation of a liposomes.

These vesicles are composed of phospholipids (Figure 2), and can be synthetic or have a natural origin (22). The most used lipids in the liposome formulations are those which have a cylindrical shape as phosphatidylcholines, phosphatidylserine, phosphatidylglycerol and sphingomyelin, which lead to the formation of a stable bilayer in aqueous solution. Phosphatidylcholines are the main lipids used in liposome formulation studies and therefore exhibit great stability to pH variations and salt concentration in the medium (23).

Phospholipids are characterized by a phase transition temperature known as Tc, in which the membrane moves from a gel stage to a crystal-liquid stage where the molecules are more loose to movements and grouped hydrophilic radicals become fully hydrated (24). The length and saturation of the lipid chain influence the value of Tc, therefore, different membranes composed of different lipids can contain different levels of flowability at equal temperature (18).

Liposome properties vary with lipid composition, surface charge, size and the method of preparation. They can be prepared by various processes such as agitation, sonication, extrusion, lyophilization, freezing and thawing, reverse phase evaporation, among others (25, 26). However, these different types of liposomes (Figure 3) can contain a single lipid bilayer or multiple bilayers around the interior aqueous compartment and, thus, are categorized as unilamellar and multilamellar, respectively (27). As for the size, unilamellar vesicles can be small or large, characterized as small unilamellar liposomes, called SUV (small unilamellar vesicles), of a diameter between 45 and 80 nm, and large unilamellar liposomes, designated as LUVs (large unilamellar vesicles), with diameters greater than 100 nm. Micelles are a different type of particles because they are only composed by a single monolayer (25, 27).
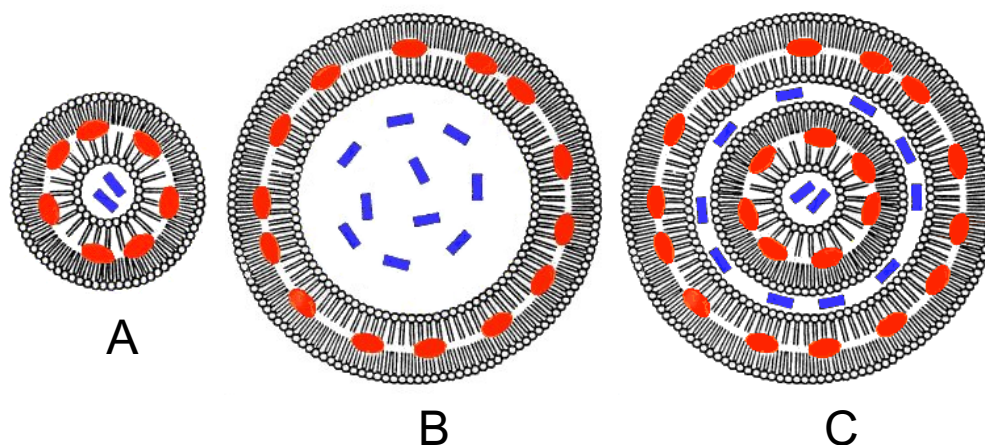
Figure 3 - Schematic representation of the different types of structures formed by phospholipids: SUV (A), LUV (B), MLV (C).

1.2.1 Advantages and drawbacks of liposomes

Liposomes are biocompatible, biodegradable, non-toxic and non-immunogenic, they are suitable for the delivery of hydrophobic, hydrophilic and amphipathic drugs, they protect the encapsulated drug from the external environment, they reduce toxicity of some drugs, have an increased therapeutic effect and reduce the exposure of sensitive tissue to toxic drugs (28). In addition, the liposomes also have an increased efficacy and therapeutic index, improved stability via encapsulation, decreased local effects evasion, improved pharmacokinetic effects (reduced elimination and high circulation half-life) and flexibility to fit with the location of specific ligands to achieve active targeting (29).

However, liposomes also have disadvantages, such as high cost of production, fusion and leakage of encapsulated drugs, short half-life and low stability (30).

The natural and synthetic phospholipids have both advantages and disadvantages. The advantages of synthetic phospholipids are good stability and high purity, however they are expensive. The advantage of natural phospholipids is that the price is relatively low, but disadvantages are that purity is difficult to control, and nature is relatively unstable (29).

The liposome stability may be affected by chemical, physical and biological processes. Depending on its composition, the final formulations of liposomes may exhibit a short half-life time, in part due to physical and chemical instability. The stability

assessment should include the characterization of the final product and monitoring of the storage stability of the liposomal formulation (18).

The chemical instability is process dependent on the composition of the liposomes, which means preventing hydrolysis of the ester and oxidation of the unsaturation located in the lipid chain, which can be seen in Figure 4 (31).
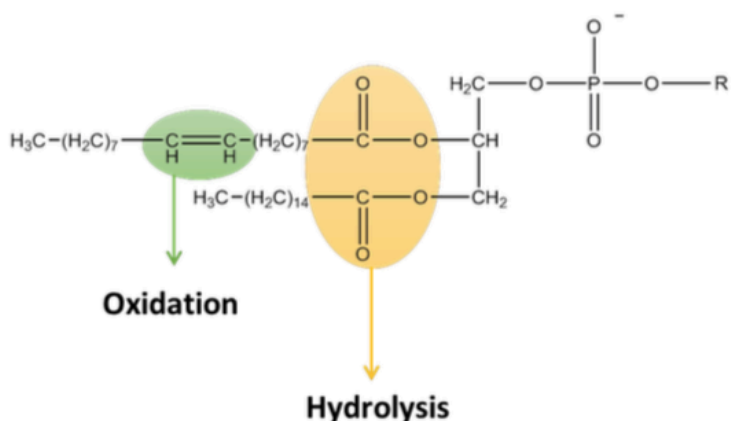
Figure 4 - Representation of molecular moieties of phospholipids associated with the chemical instability of liposomes.

Chemical instability is associated with tendency of phospholipids in liposomal formulations to suffer hydrolysis and oxidation (Figure 4). Hydrolysis may occur in ester bonds linking the glycerol backbone to the fatty acids, leading to the disconnection of the hydrophobic chains. In the case of phosphatidylcholine, the hydrolysis might cause the formation of lysophosphatidylcholine (Figure 5), increasing the permeability of liposomes.
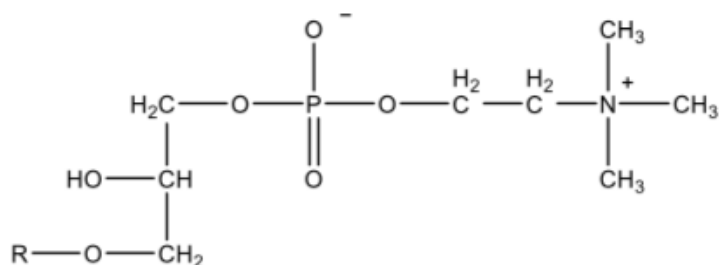
Figure 5 - Structure of lysophosphatidylcholine; R = Fatty acid acyl chain.

Therefore, it is important to keep the levels of lysophospholipids to a minimum during preparation and storage of liposomes. Oxidation might occur in the presence of

unsaturated acyl chains, which could change the permeability of liposomes and their shelf life.

Oxidation of phospholipids might be minimized by protecting them from light or by the addition of antioxidants to the liposomes (32, 33). Oxidation and hydrolysis of lipids can originate the formation of short-chain lipids and then less hydrophobic derivatives appear in the bilayers, compromising the quality of the liposomes. Besides, the described stability problems can cause quicker liposome breakdown and altered drug release profile.

In addition, in plasma, liposomes are destabilized due to the lipid exchange between liposome and HDLs, leading to aggregation and leakage of the entrapped material (33).

For the physical instability, some of the most important processes that cause instability of the liposomes are the fusion and agreggation of vesicles and extravasation of encapsulated drug (34). The physical instability of these systems can be caused by the formation of ice crystals in the liposome, which conduces to the destabilization of bilayers resulting in drug leakage.

However, biological stability it is one of the major prerequisites for the use of liposomes as carriers *in vivo* drugs is that they should circulate and keep the drug long enough for effective access and interaction with the target, usually in the blood, the walls of the capillaries and, in some cases, at extravascular cell areas (31).

Indeed, there is a necessity of developing strategies to improve the characteristics of liposomes and, consequently, expanding their applications.

The major drawback of conventional liposomes has been their quick removal of blood because of the adsorption to plasma proteins (opsonin) in the phospholipid membrane, triggering the recognition and capture of liposomes by the Mononuclear Phagocyte System (MPS) (18).

Various physical-chemical parameters influence the removal of liposomes from the circulation, including the size of the vesicles, the lipid nature of the components, the electric charge of the surface by complementary recognition system and recognition by macrophages (35).

1.2.2   Liposomes in cancer nanotechnology

More than 100 chemotherapy drugs are actually to treat cancer, either alone or in combination with other drugs or treatments. These types of drugs are very different in their chemical composition, administration route, posology and side effects. These chemotherapy drugs target cells at different phases of the cell cycle (36). For instance, cisplatin fixes to the DNA and causes inhibition of its production and cell proliferation (37), paclitaxel compounds stabilizes tubulin against depolymerization by binding to them to

tubulin, which will result in inhibition of cell division (38). While chemotherapy drugs operate through several mechanisms to lead to cell apoptosis, their focal targets are intracellular, hence, they must enter the plasma membrane and, ultimately, the nuclear membrane, so they will be able to develop a pharmacological action.

Liposomal drugs have demonstrated to be useful in the clinical for their capability to gather at sites of amplified vasculature permeability when their average size is near 200 nm due to Enhanced Permeability and Retention (EPR) effect. Also, liposomes have reduced extravasation into tissues where tight endothelial junctions are observed. This can result in an important decrease in the side effects of the encapsulated drug paralleled to the free drug (25). This has resulted in a general growth in the therapeutic index, measuring efficacy over toxicity (25, 39).

Table I shows the approved liposomal products in the market and Table II shows the products in clinical trials.

Table I - Marketed liposomal and lipid-based products adapted from (40).

Product	Drug	Indications	Year approved	Reference
AmBisome	Amphotericin B	Fungal infections Leishmaniasis	1990 (Europe), 1997 (USA)	(41)
Doxil/Caelyx	Doxorubicin	Kaposi's sarcoma	1995	(42)
		Ovarian cancer	1999	
		Breast cancer	2003	
		Multiple myeloma + velcade	(Europe, Canada) 2007	
DaunoXome	Daunorubicin	Kaposi's sarcoma	1996 (Europa, USA)	(43)
Myocet	Doxorubicin	Breast cancer + cyclophosphamide	2000 (Europe)	(43)
Amphotec	Amphotericin B	Invasive aspergillosis	1996	(44)
Abelcet	Amphotericin B	Aspergillosis	1995	(45)
Visudyne	Verteporphin	Wet macular degeneration	2000 (USA), 2003 (Japan)	(46)
DepoDur	Morphine sulfate	Pain following surgery	2004	(47)
DepoCyt	Cytosine Arabinoside	Lymphomatous meningites Neoplastic meningites	1999	(48)
Diprivan	Propofol	Anesthesia	1986	(46)
Estrasorb	Estrogen	Menopausal therapy		(49)
Lipo-Dox	Doxorubicin	Kaposi's sarcoma, breast and ovarian cancer	2001	(46)
Marqibo	Vincristine	Acute lymphoblastic leukemia	2012 (USA)	(50)

Table II - Selection of products in clinical trials; adapted from (40).

Product	Drug	Indications	Year approved	Reference
SPI-077	Cis-platin	Solid tumor	Phase II	(51)
CPX-351	Cytarabin: daunorubicin	Acute myeloid leukemia	Phase II	(52)
CPX-1	Irinotecan HCl: floxuridine	Colorectal cancer	Phase II	(40)
MM-302	ErbB2/ ErbB3 – targeted doxorubicin	ErbB2 – positive breast cancer	Phase I	(53)
MBP - 436	Transferrin – targeted oxaliplatin	Gastric cancer and gastro-esophageal junction	Phase II	(46)
Brakiva	Topotecan	Relapsed solid tumors	Phase I	(54)
Alocrest	Vinorelbine	Newly diagnosed or relapsed solid tumors	Phase I	(46)
Lipoplatin	Cisplatin	Non-small cell lung cancer	Phase III	(46)
L-annamycin	Annamycin	Adult relapsed all and acute myelogenous leukemia	Phase I	(55)
ThermoDox	Thermosensitive doxorubicin	Primary hepatocellular carcinoma	Phase III	(56)
Endo-tag-1	Cationic liposomal paclitaxel	Pancreatic cancer, triple negative breast cancer	Phase II	(46)
ALN-TTR ALN-PCS ALN-VSP	SiRNA targeting transthyretin (TTR), siRNA targeting liver cancer	TTR amyloidosis, Hypocholesterolemia, Liver cancer and liver metastases	Phase I	(57)
TKM-PLK1 TKM-ApoB	RNAi targeting polo-like kinase 1, RNAi targeting Apo B	Liver tumors, High levels of LDL cholesterol	Phase I	(46)
Stimuvax	Anti-MUC1	Non-small cell lung	Phase I	(58)

	cancer vaccine	cancer		
Exparel	Bupivacaine	Nerve block, Epidural	Phase II	(59)

1.3   Proliposomes

Although liposomes have been widely used for drug delivery, the drawbacks cited above limit their application for medicinal purposes.

The proliposomes were developed to overcome the stability problems of the liposomes. These were discovered by Payne in 1986 in an attempt to overcome the inherent instability to liposomes, presenting an alternative to conventional liposomal formulations (60).

The proliposomes are a new generation drug delivery system (DDS), having several advantages over conventional liposomes. They have shown improved stability and ease of sterilization on a large scale (19, 61). The maximum amount of drug encapsulation aids the penetration of the drug and produces a sustained release effect at the administration site. The therapeutic benefits of the proliposome include a high retention of hydrophilic material, improved bioavailability, reduced toxicity and taste masking, as also they are relatively inexpensive and convenient to prepare. However, the disadvantages of the proliposome are related to the preparation methods, due to the need for additional measures or sometimes the need of cryo-protective material. The use of organic solvents also brings regulatory problems, as the final products may contain residues of this solvents (62).

We can define proliposomes as free-flowing particles which can form the liposomal suspension immediately upon contact with water (Figure 6). They are dry, free flowing, granular products composed of a mixture of drugs and phospholipids that will form a suspension of multilamellar liposomes, that, when dispersed in water, is suitable for administration by different routes (63). This solid formulation offers the advantage of being physically and chemically more stable in storage than liposomes (62). There are several ways to form liposomes from proliposomes, such as the use of an aqueous buffer or pure water, with manual or mechanical agitation or heating (62, 64, 65).
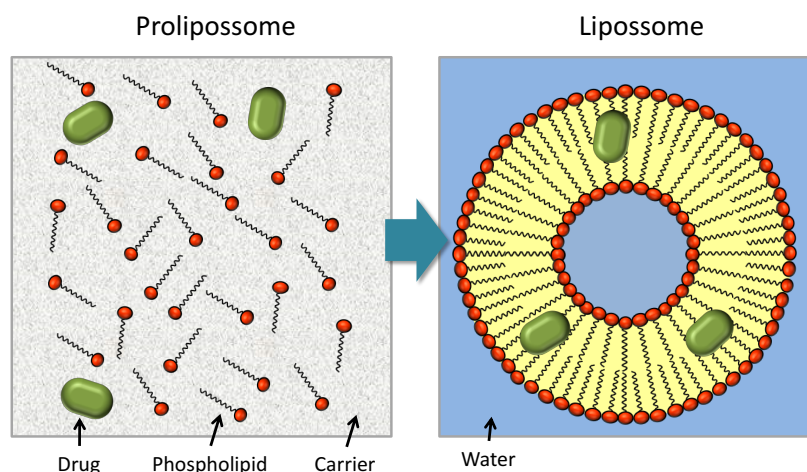
Figure 6 - Proliposomes are free-flowing particles which can form the liposome immediately upon contact with water and incorporate the drug.

Sterilized proliposomes can be stored in a dry state and then dissolved in aqueous solution to form a isotonic liposomal suspension when necessary (62).

The conversion of proliposomes to liposomes may be accomplished *in vivo* by the effect of physiological fluids or *in vitro* prior to administration using a convenient hydrating fluid (66).

The carriers selected for the preparation of the proliposome must have high surface area and porosity, so that the amount of vehicle needed can be adjusted easily to withstand the lipids. Moreover, the proliposomes are composed of a carrier, which is a water soluble porous powder where phospholipids and drugs dissolved in a solvent might be loaded. Some of the used carriers include maltodextrin, sorbitol, microcrystalline cellulose, magnesium, aluminum silicate and mannitol (Figure 7) (61).
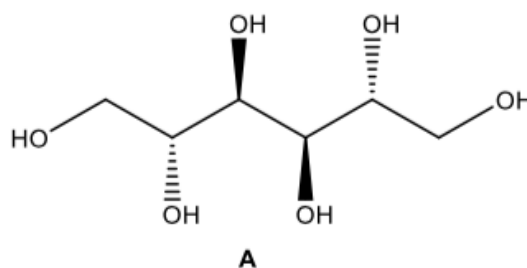
Figure 7 - The chemical structure of mannitol.

1.3.1 Administration routes

An overall review of scientific papers published in this area showed that the main focus is on the development of proliposome for administration by oral, pulmonary and parenteral administration.

1.3.1.1 Oral drug delivery

The oral route is the preferred choices for administration of drugs (67). However, many active substances suffer from bioavailability problems due to its low solubility and stability in gastrointestinal fluids, poor permeation through this barrier or hepatic metabolization (68).

In the future there will be focus on the delivery of this complex molecules through different ways, including oral, nasal, pulmonary, vaginal, rectal, among others (69). Numerous studies showed that proliposome may be a possible strategy. Since they are solid particles, they may be formulated into dosage forms such as tablets and capsules, occurring subsequent formation of the liposomes *in vivo* upon contact with biological fluids (28). Thus, the proliposome provide a unique synergy between the ability of the liposomes encapsulate and protect the drugs, and the increased stability that is provided by solid dosage forms (69).

In the delivery systems of conventional oral drugs, there is very little control over the drug release (70). The effective concentration at the target site can be achieved by intermittent administration of excessive doses, leading to marked side effects (69). A drug delivery system for oral administration should continuously deliver a measurable and reproducible amount of drug to the target site over a prolonged period (70).

Typically, they provide numerous advantages, including greater effectiveness in the treatment of chronic conditions, reduced side effects, greater convenience, and higher levels of patient compliance due to a simplified dosing scheme (69).

The oral delivery of some lipoproteins could be improved by increasing the ability of the liposomes to maintain their integrity at the site of absorption, that can be achieved by formulating them in proliposomes (71). Several studies have been reported to demonstrate the usefulness of oral proliposomes to provide the adequate solubility and bioavailability of insoluble/poorly soluble drugs (72).

Silymarin proliposomals formulations (prevention and treatment of liver diseases and primary liver cancer) were prepared for oral administration and were reported to be stable and to increase the gastrointestinal absorption of silymarin (73).

The insoluble glyburide (treatment type 2 diabetes) was incorporated into a proliposomal formulation and a threefold increase in drug dissolution was observed (74).

Exemestane proliposomals formulations (aromatase inhibitor steroid) showed that the *in vitro* evaluation, using various models such as bowel rat permeability test of the parallel artificial membrane (PAMPA) and Caco-2 cell line, provided useful information to improve oral bioavailability due to higher solubility, higher permeability, and thus higher absorption (75).

The improvement of the efficacy of indomethacin (nonsteroidal anti-inflammatory) through oral liposomes has the objective of preventing the most common side effect of gastric mucosal injury. The concept of proliposomes initially given (76) was adopted to avoid the problems of physical stability (77).

1.3.1.2 **Pulmonary drug delivery**

Liposomes have emerged as a promising carrier for delivering antitubercular drugs directly to the lung. They proved that the peripheral region of the lung can be penetrated by nebulization of liposomal dispersion (78). However, the potential instability of liposomes includes the drug loss due to hydrolysis/oxidation, leading to physical instability, sedimentation and aggregation, and fusion of liposomes during storage. *In situ* liposome formation could overcome the problems associated with the aqueous dispersion of liposomes (79, 80).

The proliposome can provide an efficient delivery system for the treatment of lung diseases, offering many advantages, such as that they are biocompatible, biodegradable, and relatively non-toxic. They also increase the therapeutic index of the drugs because of their promotion of cell delivery and slow clearance, which minimizes or eliminates side effects, reducing the dosage or frequency of dosage, the systemic toxicity and the cost of therapy. Proliposome levofloxacin for use with dry powder inhalers were prepared by a spray drying method using mannitol, as the porous carrier proliposome core has a low density and high porosity (80). It was expected that the porous mannitol would improve drug delivery to the lung (80). As density decreased, aerodynamic diameter decreased accordingly, and increased penetration into the alveolus (81, 82). *In vivo* tests were made on rats administered with proliposomes by intratracheal instillation to confirm the safety of the formulations. Proliposome levofloxacin shown to be nontoxic to cells and problems associated with the absence of renal and pulmonary toxicity associated with the administration of the proliposome, good antimycobacterial activity against *Mycobacterium bovis*, *M. tuberculosis* and *M. bovis* in intracellular macrophages (80).

Studies with amphotericin B, salbutamol sulphate and beclomethasone dipropionate suggested that the use of proliposomes to prepare liposomes is an advantageous strategy to incorporate hydrophilic and hydrophobic drug (79, 83). They concluded that liposomes coated with chitosan produced from proliposomal formulations were potential carriers for drug delivery systems that use spraying (83).

Furthermore, since proliposomes are in a state of dry powder, they are also suitable for liposomal delivery by dry powder inhalers (DPI). DPI proliposomal systems based formulations have been developed for drug delivery in the treatment of tuberculosis, isoniazid and pyranizamide (79).

1.3.1.3   **Parenteral drug delivery**

The application of drug delivery systems for parenteral administration must be sterile. However, common sterilization techniques, used in pharmaceutical products, such as steam sterilization, gamma radiation and sterilization by filtration cannot be suitable for liposome preparations, since they can cause the physical disruption of the lipid membrane, thus affecting the intrinsic properties of these vesicular structures (63).

Another technique for sterilization is aseptic manufacturing, which is applied less frequently, because it is expensive and presents difficulties in the validation (84).

The use of proliposomes to produce liposomes simplifies the process of sterilization, providing an improvement in its application for the parenteral administration (85). Proliposomes can be sterilized by X-ray irradiation. This sterilization technique has limited application to liposomes due to the formation of hydroxyl radicals from water exposure to radiation (63). Since proliposomes are available in dry form, the application of this sterilization technique has the advantage of generating free radicals (63). They reported that intravenous administration of drugs in proliposomal formulation can reduce the side effects produced when the free drug methotrexate is administered in this way (86).

These systems have been used to improve the applicability of drugs with adverse side effects and toxicity such as indomethacin, carboplatin, polymyxin E and docetaxel (87-89). In such cases, it has been demonstrated that these formulations lead to an altered pharmacokinetic behavior of the drug (89). There was a decrease in toxicity of polymyxin formulation and adverse side effects of indomethacin. An increase in therapeutic efficacy for both carboplatin and indomethacin were observed, and carboplatin bioavailability was enhanced (87, 88).

Additionally, liposomes prepared from proliposomal formulations have also been used to direct the indomethacin to the joints and the docetaxel to the lungs. (87, 89). It

was also reported an increased terbutaline sulfate location in the lungs for treatment of asthma, when these systems were used (90).

Liposomes coated polyethylene glycol were prepared to increase the circulation time in blood of indomethacin and glycyrrhetinic acid (91).

1.4   Xanthone

Xanthones (or xanthen-9-ones) constitute a class of O-heterocycles with a dibenzo-γ-pyrone scaffold (Figure 8) commonly found as secondary metabolites in higher plants, fungi and lichens (92). These oxygenated heterocycles are structurally related to other natural compounds with the γγ-pyrone scaffold: flavonoids and chromones (93).

They can also be obtained by synthesis and several strategies to achieve this goal have been described in the literature (93). The xanthone classes bear different types of substituents that are able to interact with several biological targets exerting different actions. Indeed, the xanthone core is a rigid heteroaromatic tricyclic platform which may be considered as a privileged structure since it can provide potent and selective ligands through modification of functional groups, allowing them to interact with different pharmacological targets (94).

Naturally occurring xanthone derivatives are subdivided into six major groups: single oxygenated xanthones, glycosylated xanthones, prenylated xanthones and their derivatives, xanthone dimers, xanthonolignoids and varied, depending on the nature of the substituents on the dibenzo-γ-pyrone scaffold. By chemical synthesis, simple functional groups such as hydroxyl, methoxy, methyl and carboxyl have been introduced into the xanthone nucleus as well as more complex substituents such as epoxide, azole, aminoalcohol, sulfamoyl and dihydropyridine (94). There is a diversity of biological activities described for natural and synthetic xanthones, and the growth inhibitor in tumor cell lines seems to be quite important as they exert their effect on a wide range of different tumor cell lines (95, 96).
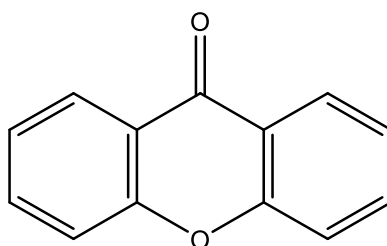
Figure 8 - The chemical structure of xanthone.

Invasive brain glioma is the most lethal type of cancer and is highly infiltrating. This leads to an extremely poor prognosis and makes complete surgical removal of the tumor virtually impossible (97).

Patients with gliomas have an extremely poor prognosis due to the highly infiltrating nature of gliomas (98). The mean survival time is lower than 16 months (99). They are even in the contralateral hemisphere, they hide in the areas of the brain and are protected by blood-brain barrier (BBB) (100). Therefore, complete removal of gliomas by surgery is practically impossible. Conventional surgical methods and / or radiotherapy alone cannot completely eliminate cancer cells from the brain (101), and relapse is inevitable. Therefore, a crucial challenge is to effectively deliver therapeutic agents to the nucleus of cancerous cells as well as migrating cells in the infiltration zone (100). Chemotherapy for gliomas is difficult due to two major obstacles: one obstacle is the BBB in brain cancer, which separates blood from brain tissue and avoids drug penetration into the central nervous system (CNS) and the other obstacle is the heterogeneity of brain cancer.

For many compounds, the BBB prevents drug delivery to the cerebral parenchyma, since systemic administration of the drug is ineffective for the treatment of CNS disorders (102). For highly debilitating diseases, an infusion of drugs directly into the brain (intra cranial) may be the only viable route of administration. However, agents directly infused into the brain in a small volume do not disperse easily from the infusion site. The diffusion coefficients are too low to allow even small molecules to move more than a few millimeters. Thus, diffusion requires a high concentration gradient to generate effective drug concentrations over a long distance (103). Such high drug concentrations generally lead to dose-limiting neurotoxicity (102).

The development of nanotechnology offers powerful tools for therapies to target sites. Anchoring them with specific ligands can provide the nanotherapeutics with the proper properties to circumvent the BBB (104).

2 Objectives

The main objectives of the present dissertation are:

- To develop and optimize proliposomal formulations using: egg phosphatidylcholine, cholesterol, mannitol, XGA;

- To develop an HPLC method for the quantification of XGA in proliposomal formulations;

- To evaluate size, morphology and crystalline state of proliposomal powders;

- To evaluate size, zeta potential, entrapment efficiency and morphology of liposomes obtained by hydration of proliposomes;

- To evaluate the stability of proliposomes;

- To test the feasibility of using proliposomes in the cell growth inhibitory activity of tumor cell lines using a promising new xanthone derivative.

3 Experimental part

3.1 Materials and Methods

3.1.1 Materials

The materials used in this work are presented in Table III. Lipoid E80 (egg phospholipids with 80% of phosphatidylcholine) was acquired by Lipoid, cholesterol was purchased from Acofarma and methanol used in HPLC was purchased from VWR chemicals, with HPLC grade. Mannitol and all the other reagents and solvents were purchased from Sigma Aldrich. XGA was obtained by synthesis.

Table III - Materials used in the experimental work.

Materials	Description	Batch number
Egg phosphatidylcholine	LIPOID E80 – LIPOID GMBH	4. D-67065
Cholesterol	Acorfarma®	150840-J-1
Mannitol	D-Mannitol ≥98%, SIGMA ALDRICH®	150965-P-1
XGA	Synthesized by the Laboratory of Organic and Pharmaceutical Chemistry FFUP/CIIMAR	
Ethanol	Panreac, AppliChem GmBH	
Methanol	AnalaR NORMAPUR; BDH PROLABO®, VWR CHEMICAL	
Methanol (HPLC)	HiPerSolv CHROMANORM; HPLC gradient grade; BDH PROLABO®, VWR CHEMICALS	
Ultrapure water	Type I; 18.2 μΩ at 25ºC; Milli-Q®; Merck Millipore	

3.1.2 Methods

3.1.2.1 Preparation of proliposomes and liposomes

The chosen method for the preparation of liposomes was the lipid film hydration.

The chosen method for the preparation of proliposomes was Spray-Drying (SD), since it showed a great potential to combine particle engineering and drying in one step, being able to produce particles with a spherical morphology.

Regarding the raw materials (105, 106), phosphatidylcholine, is one of the most abundant lipids in biological membranes, and explains why it is widely used in the preparation of liposomes. It has the ability to mimic the behavior of membranes, is biocompatible and biodegradable. The presence of cholesterol in the membranes of the liposomes is advantageous, as it allows their stabilization, reducing leakage of the drug from the interior, decreases membrane fluidity, and provides favorable drug retention properties.

Proliposome formulations are comprised of a lipid part and a carrier material. For this study, the lipid part was composed by a mixture of egg phospholipids with 80% of phosphatidylcholine (PC) and cholesterol (CH), and the carrier material used was mannitol (the carrier was only used in proliposomes).

3.1.2.1.1   Preparation of proliposomes

Choosing the best mass ratio PC:CH and lipids:mannitol (Table IV) previously obtained (106), proliposomes with and without XGA were produced using SD method, with 1% of the drug tested (XGA) in relation to the mass of lipids.

Table IV - Constituents used in the preparation of proliposomes.

Formulation	PC:CH	Lipid: Mannitol	PC (mg)	CH (mg)	Mannitol (mg)
1	3:1	1:10	142.52 mg	24.17 mg	1666.90 mg

The PC and CH were dissolved in ethanol and the mannitol was dissolved in water, and both substances were transferred to a 100 mL volumetric flask and make up to volume. In the preparation of the formulations with XGA, the drug was dissolved in absolute ethanol along with the lipids. The proliposome formulation was prepared, followed by drying with the SD technique; the experimental conditions used were as follows: Temperature: 80ºC, Compressed air flow: 90 L/min, Pressure: 30 mbar, Spray nozzle membrane: 5.5 μm

The SD method is used primarily when particles of uniform size and shape are required. It has a relatively low cost and is suitable for production proliposomes in a single large scale. A characteristic of the drying process lies in its ability to involve either the formation of particles and the drying in a single continuous step, allowing better control of

particle (107). SD is not limited to aqueous solutions, but may also be used for non-aqueous systems for preparing particles (63, 108).

The SD process involved four stages (107): atomization of the product by a spray nozzle, spray-air contact, drying of the sprayed droplets and collection of the solid.

Initially, the liquid dispersions containing pure lipid (or lipids) and the carrier solvent were prepared and pumped into the drying chamber (Figure 9). The dispersions were atomized into the drying chamber using a spray nozzle, dried in a concurrent air flow and then collected in a reservoir (63, 108).
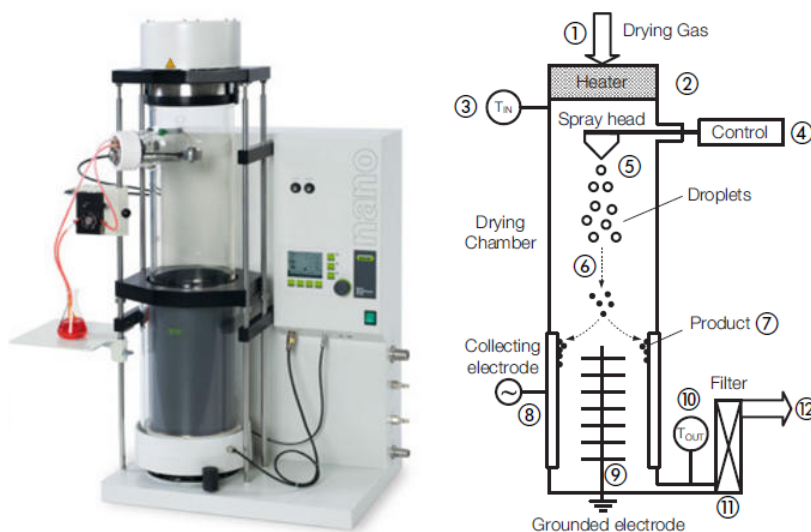
Figure 9 - Apparatus for the preparation of proliposomes by SD: 1 - drying gas inlet, 2 - electrical heater, 3 - inlet temperature sensor, 4 - display/control, 5 - spray head, 6 - spray cylinder and drying section, 7 - finished product at particle collecting electrode, 8 - particle collecting electrode, 9 - grounded electrode, 10 - outlet temperature sensor, 11 - outlet filter, 12 - drying gas outlet (109).

The Nano Spray Dryer B-90 (Buchi Labortechnik, Switzerland) uses piezotechnology to generate precisely controlled micro droplets from bulk liquids without the use of propellants. The spray head includes a piezoelectric actuator with a thin stainless steel membrane. The membrane has an array of micron-sized holes (spray meshes of 4.0, 5.5 or 7.0 µm hole size) and vibrates at ultrasonic frequency (60 kHz). Because of these vibrations the membrane ejects precisely sized droplets at high speed (109).
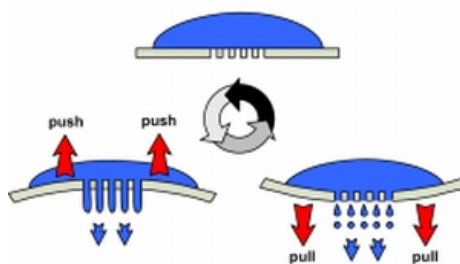
Figure 10 - The spray head membrane mechanism (110).

After the process was completed, the apparatus was dismantled to remove the inner cylinder, where the particles were collected with the aid of a scraper (nanoparticle scraper). At the end of the process, the proliposomes were collected into glass vials and stored in a desiccator.

3.1.2.1.2   Preparation of liposomes

For the preparation of liposomes by thin lipid film hydration method, the lipids, CH and egg phosphatidylcholine were mixed in chloroform: methanol in a 3:2 ratio. In a round-bottomed flask, the preparation was dried by rotary evaporation (R-210 Buchi, Canada) during 30 minutes under reduced pressure. Hydration of the film was done with phosphate buffer solution (PBS), pH=7.4, and 5 mL of this solution were measured. The liposomes were vortexed to remove the lipid film. Then, the liposomes were extruded (Lipex, Canada), three times through a three different filters, 600 nm and 200 nm, and then 10 times through a 100 nm filter. Thus, the liposomes were obtained with and without XGA with a size of approximately 100 nm.

3.1.3   Characterization of proliposomes and liposomes

The characterization of the proliposome and liposomes can be done by numerous ways as shown below.

3.1.3.1   Hydration study

The ability of the proliposome to form liposomes on hydration involves placing a small amount of proliposome powder on a glass slide and slowly adding water dropwise and then observing microscopically to visualize the formation of vesicles. Liposomes are

quickly formed in hydration during the process of dissolution and disintegration. This involves hydrating the lipid surface to form liposomes that are formed by the core of the proliposome. The process is subjected to lipid hydration and dissolution of the carrier (111).

The proliposome powders were hydrated using purified water and agitated to obtain liposomal dispersions, and then filtered through a 5 µm filter, in order to destroy possible aggregates.

Proliposomes and liposomes were prepared with and without XGA. The results of the mean diameter, polydispersity index and zeta potential. A statistical analysis was performed to determine if the differences between the zeta potential and the mean diameter with and without drug were statistically significant, that is, whether the XGA influenced these parameters or not.

3.1.3.2 **Particle size**

3.1.3.2.1 **Dynamic Light Scattering**

Dynamic Light Scattering (DLS) or Photon Correlation Spectroscopy (PCS) is a technique that, when light strikes the small particles, disperses it in all directions (Rayleigh scattering). If the light source is a laser, and thus is monochromatic and coherent, scattering intensity fluctuates over time. This variation is due to the fact that small molecules in solution are subjected to random motion of particles suspended in a fluid, and thus the distance between the scatters in the solution is constantly changing with time (Figure 11). This scattered light then passes through any constructive or destructive interference by the surrounding particles, and within this intensity variation, information is contained on the disperser circulation time scale. The sample preparation or filtration or centrifugation is critical to remove dust and articles from solution (112). A detector measures the change in the intensity of scattered light. Fluctuations in scattered light are induced by random Brownian motion of particles, and according to the Stokes-Einstein equation, are inversely related to particle diameter. Therefore, these fluctuations are faster in small particles and slower in the case of larger particles (44):

$$d = \frac{KT}{3\pi\eta D} \qquad \qquad \text{Equation 1}$$

where "d" is the hydrodynamic diameter, "D" is the translational diffusion coefficient, "k" is the Boltzmann's constant, "T" is the absolute temperature, and "η" is the viscosity of the

surrounding medium. However, this technique is suitable for estimating the polydispersity index (PI), which is a measure of homogeneity of the particle size distribution. DLS was applied to liposomal formulations prepared from proliposomal to measure the size of the vesicles (113, 114).
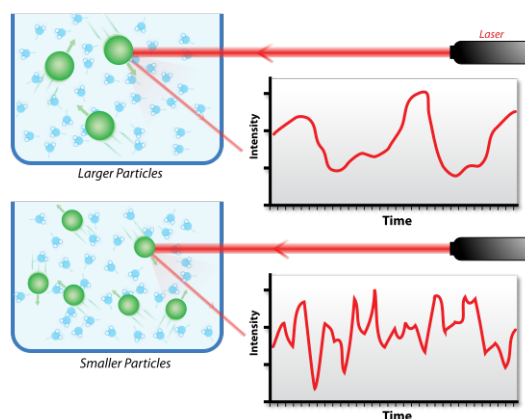
Figure 11 - The DLS technique is the variations in the intensity of the light dispersed by the particles, which are related to their size, that is, smaller particles correspond to higher velocities in the fluctuation of light intensity (115).

The effective diameters were evaluated by DLS, using an apparatus which is suitable to measure the diameter of particles until 5 µm (Brookhaven Instruments Corporation, Holtsville, NY, USA). Thus, particles with a higher diameter were not counted for the mean values of effective diameter. Thus, after hydration of the proliposomic formulations, the dispersion was filtered through a 5 µm filter; however for the liposomal formulations, the filter used in the extrusion was 100 nm. Considering this, the range of measured diameters seems to be appropriated to measure the obtained liposomes.

The data collected by the software Particle sizer (Version 5, Brookhaven Instruments Corporation, Holtsville, NY, USA) was expressed in mean ± standard deviation.

3.1.3.2.2   Scanning Electron Microscopy

The Scanning Electronic Microscopy (SEM) is capable of producing high-resolution images of a surface on the scale of nanometers to micrometers. The SEM microscope uses an electron beam finely focused to irradiate the sample to analyze. When the electron beam strikes the sample, elements at the surface release electrons and protons, whose intensity is used to produce the SEM image. Due to the way in which the image is

created, the SEM images have a characteristic three-dimensional appearance and are useful for evaluating the sample surface structure (116).

SEM is mainly used to visualize the surface morphology of the proliposome powder (117). SEM can also reveal the surface morphology of the dried powders proliposomes (118).

The SEM / EDS exam was performed using a High resolution Scanning Electron Microscope with X-Ray Microanalysis and CryoSEM experimental facilities: JEOL JSM 6301F/ Oxford INCA Energy 350/ Gatan Alto 2500. The specimen was rapidly cooled (plunging it into sub-cooled nitrogen – slush nitrogen) and transferred under vacuum to the cold stage of the preparation chamber. The specimen was fractured, sublimated ('etched') for 90 sec. at -90°C, and coated with Au/Pd by sputtering for 45 sec. The sample was then transferred into the SEM chamber. The sample was studied at a temperature of -150°C.

The SEM / EDS exam was performed using a High resolution (Schottky) Environmental Scanning Electron Microscope with X-Ray Microanalysis and Electron Backscattered Diffraction analysis: Quanta 400 FEG ESEM / EDAX Genesis X4M. Samples were coated with an Au/Pd thin film, by sputtering, using the SPI Module Sputter Coater equipment. Each image contains a data bar with the most important analysis conditions.

3.1.3.3 Particle stability

3.1.3.3.1 Zeta Potential

Particulate potential dispersion exposure zeta it's a physical property that allows indirect measurement of surface charge (119). The magnitude of this property gives an idea of the long-term stability of the colloidal dispersion. In addition, the Zeta Potential (ZP) can provide information regarding the electrostatic interactions of liposomes with cell membranes. The stability of colloidal dispersions depends mainly on two factors: the steric repulsion, which requires the addition of a polymer, and electrostatic or charge stabilization (120). This parameter is related to the repulsion of particles that can be sufficiently high to prevent flocculation or coagulation. If the ZP of liposomes dispersion has a high absolute value (generally higher than 30), there is a tendency for the repulsion between the nanoparticles (121).

The distribution of ions around the liposome in an aqueous medium is affected by the load on its surface. It forms a double electric layer, which has two separate parts: an inner part containing adsorbed ions, and a diffuse part, where the ions are less firmly

associated (Figure 12). In this part, the ion distribution is influenced by electrical forces and random thermal motion. There is an adherent layer of solvation to the surface formed by a certain amount of solvent bound to the ions and the surface. The boundary of this layer, called cutting plane, is a boundary representation for the relative motion between the solid, with the retained material, and liquid. The liposomes are dispersed in an electrolyte and an electric field is applied to them, which move at a constant speed to the oppositely charged electrode. This speed is measured and expressed in field strength unit as their mobility and when this value is known, the ZP ("ζ") can be calculated by the equation of Smoluchowski (122, 123):

$$\zeta = \frac{\eta}{\varepsilon} \mu_e \hspace{4cm} \text{Equation 2}$$

where the "μ_e" is the electrophoretic mobility, "η" is the viscosity of the medium and ε is the dielectric constant (61).
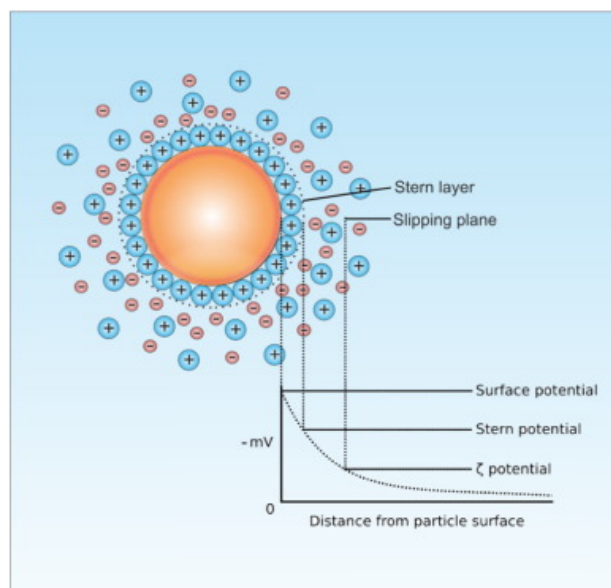
Figure 12 – Potential difference as a function of distance from the charged surface of a particle dispersed in a liquid medium (124).

The sample was placed in a cuvette, where an electrode is inserted, ZetaPALS equipment (Brookhaven Instruments Corporation, Holtsville, NY, USA). The results analised by the software PALS Zeta Potential Analyzer (Version 5, Brookhaven Instruments Instruments Corporation, Holtsville, NY, USA) were expressed in mean ± standard deviation.

3.1.3.4   **Thermal behavior of proliposome powders**

The study of the drug–excipient and excipient-excipient compatibility studies was performed using a DSC 200F3 Maia (Netzsh–Gerätebau GmbH, Germany).

Individual samples (drug and excipients) as well as the formulations of proliposomes and liposomes were weighed directly in DSC aluminum pans and scanned in the temperature range of -40 to 340°C under nitrogen atmosphere with flow of 40 mL /min.

A heating rate of 10°C/min was used and the obtained thermograms were observed for any interaction. An empty aluminum pan was used as reference. The onset temperatures were calculated using Proteus Analysis software (Version 6.1, Netzsh-Gerätebau GmbH, Germany).

The DSC cell was calibrated (sensitivity and temperature calibration) with Hg (m.p. -38.8°C), In (m.p. 156.6°C), Sn (m.p. 231.9°C), Bi (m.p. 271.4°C), Zn (m.p. 419.5°C) and CsCl (m.p. 476.0°C) as standards.

3.1.3.5   **Assay of XGA**

XGA was metered using a reverse phase High Performance Liquid Chromatography (HPLC) method. The apparatus used was the Dionex Ultimate 3000 (Thermo Scientific, Germany) with a column *ACE 5 C18* (internal particles diameter: 3 µm; dimensions: 15 x 0.46 cm). The chromatograms were analyzed using Chromeleon software (version 6.80, Dionex, EUA) and the elution used was isocratic. The methanol and water were chosen as eluents (72:28), at a flow of 1.0 mL/min. Then, calibration curves were prepared the drug solution with the five different concentrations 20, 30, 40, 50 and 60 µg/mL and was injected 5 times (125). The chromatographic parameters were calculated: retention time (t_r), peak area (mAU.min), retention factor (K), number of theoretical plates (N), resolution (R_s) and tailing factor (T) (126).

$$k = \frac{t_R - t_0}{t_0}$$

Equation 3

$$N = \frac{L}{H}$$

Equation 4

$$R_S = \frac{2(t_{r2} - t_{r1})}{w_1 + w_2}$$

Equation 5

$$T = \frac{w_{0.05}}{2d}$$

Equation 6

To determine the detection wavelength of the XGA, a drug solution in methanol/water (72:28) was prepared and an absorption spectrum was drawn between the wavelength of 200 and 400 nm in a spectrophotometer (Jasco v-650, Germany) using a proper software (Spectra Manager Version 2, Jasco, Germany).

3.1.3.5.1 Entrapment efficiency

220 mg of proliposomes were weighed and diluted in 2 mL of ultra-pure water. The diluted samples were filtered through a 5 μm nitrocellulose membrane filter to reject unincorporated XGA. Subsequently, methanol dilution of 1:8 and subsequent manual shaking was performed to allow the release of the XGA which was encapsulated in the liposomes. The obtained mixture was centrifuged (5000 rpm for 15 min) (Model 5804, Eppendorf, USA) and the filtered supernatant (0.45 μm PTFE filter, OlimPeak®) to obtain an XGA solution. The obtained samples were then evaluated by HPLC, and each sample was injected three times.

HPLC analysis of the samples was done under the same XGA assay conditions. By interpolation of the calibration curve, the actual XGA concentration was obtained. The theoretical concentration of XGA was calculated by taking into account the amount of XGA placed during the production of the proliposomes and the dilutions effected throughout the procedure for the determination of the incorporation efficiency. Thus, the encapsulation efficiency (EE) was calculated by the following formula:

$$EE(\%) = \frac{C_{filtrate}}{C_{formulation}} \times 100 \qquad \text{Equation 7}$$

where $C_{filtrate}$ is the concentration of the drug in the filtrate (μg/mL) and $C_{formulation}$ is the concentration of the drug in the formulation (μg/mL).

3.1.3.6 Cell viability

The assays related to the inhibition of the 3 tumor lines of the glioma where realized out under the supervision of Prof. Dr. Hassan Bousbaa and Drª Patricia Silva.

U251, U373 and U87-MG glioblastoma cells were grown in DMEM culture medium supplemented with 10% fetal bovine serum (FBS, Biochrom) and were maintained at 37°C in a 5% CO_2 humidified incubator. All experiments were performed when exponentially growing cells presented more than 95% viability.

Cell viability was determined with MTT (3-(4, 5-dimethylthiazolyl-2)-2,5-diphenyltetrazolium bromide) assay (Sigma-Aldrich). A total of 5×10^4 glioblastoma cells were seeded in 96-well plate, allowed to attach for 24 h. Cells were then treated for 48 h with XGA, proliposomes with and without XGA and liposomes with and without XGA. 48 h later, cells were placed in fresh FBS-free medium and 20 μL MTT reagent (5 mg/mL in PBS) was added and incubated at 37ºC and 5% CO_2 for 4 h. The purple formazan crystals were solubilized with a detergent solution (89% v/v) 2-propanol, 10% (v/v) Triton X-100, 1% (v/v) HCl 3.7%), for 2 h. Optical density was measured at 570 nm in a microplate reader (Biotek Synergy 2, Winooski, VT, USA). Cell viability was calculated relative to untreated cells.
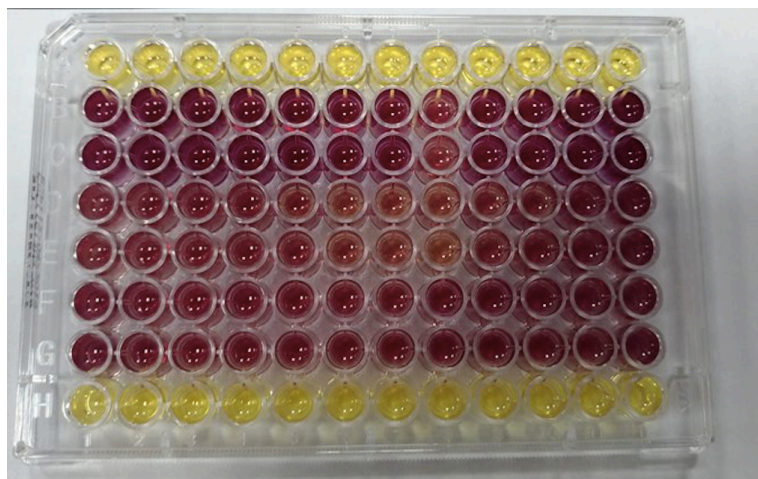
Figure 13 - Preparation of the 96 well plate with the XGA formulations, liposomes, XGA liposomes, proliposomes and XGA proliposomes at concentrations of 0.1 µM, 1 µM, 10 µM and 100 µM.

3.2   Statistical analysis

The results were statistically analyzed using the t-student test, after confirming the normality and homogeneity of the variance with the Shapiro-Wilk and Levene tests. Significance was set at p <0.05. All the statistical analyzes were performed with the software, IBM SPSS Statistics for Macintosh (Version 24.0. Armonk, NY: IBM Corp., USA).

4   Results and discussion

4.1   Preparation of proliposomes and liposomes

According to previous studies (105, 106), it was found that the molar ratios that presented the best results were the PC:CH (3:1) molar ratio and the carrier:lipid (10:1). Empty proliposomes were prepared and results obtained by DLS can be seen in Table V. These results obtained showed that the proliposomes, after hydration, formed liposomes.

Table V - Results of empty proliposome formulations by DLS.

Formulation	Effective diameter (nm)	PI	ZP (mV)
Empty proliposomes	178.63 $\pm$ 45.07	0.27 $\pm$ 0.03	-47.16 $\pm$ 1.53

4.1.1   Particle size and zeta potential

The effective diameter, the PI and ZP values of the proliposome formulations, and liposomes with and without XGA are shown in the Table VI.

Table VI - Results obtained from the mean diameter (nm), polydispersity index and zeta potential (mV), for formulations prepared by SD, using proliposomic and liposomal formulations, with and without XGA.

Formulation	Effective diameter (nm)	PI	ZP (mV)
Prolipo+XGA	199.37 $\pm$ 20.55	0.26 $\pm$ 0.01	-39.28 $\pm$ 7.06
Proliposome	178.63 $\pm$ 45.07	0.27 $\pm$ 0.03	-47.15 $\pm$ 1.51
Lipo+XGA	102.37 $\pm$ 2.11	0.10 $\pm$ 0.01	-25.62 $\pm$ 2.60
Liposome	117.10 $\pm$ 5.80	0.33 $\pm$ 0.01	-44.10 $\pm$ 8.44

Figure 14 and Table VI shows the results obtained from the mean diameter (nm), PI (mV) and ZP, for formulations prepared by SD, using proliposomal and liposomal formulations, with and without XGA. The mean diameter in the presence of XGA was 199.37 $\pm$ 20.55 nm, compared to the drug-free formulation, 178.63 ± 45.07 nm. However, this difference was not statistically significant ($p \geq 0.05$) (Appendix I and VI) (127).

The effective diameter of the liposomes with and without XGA is shown in Figure 15 and Table VI. The drugless formulation has an effective diameter of 117.10±5.80 nm and

for the drug formulations the effective diameter value is 102.37 ± 2.11 nm. The effective diameter decreased significantly when the drug was placed in the formulation ($p \leq 0.05$), probably because XGA, in some way, affected the physical structure of the lipid organization (Appendix II and VI) (128).
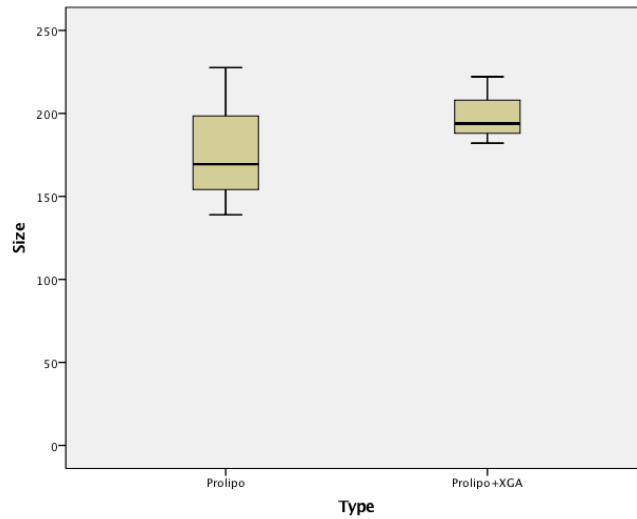
Figure 14 – Box and whisker plot of effective diameter of liposomes formed by hydration of proliposomes produced by SD, with and without XGA (p = 0.509).

Figure 15 - Box and whisker plot of effective diameter of liposomes with and without XGA (p = 0.017).

For all the studied formulations, ZP was more negative than -30 mV, indicating eventual electrostatic stability.

Figure 16 and Table VI shows that, for drugless proliposome formulations, the ZP was between -47.15 ± 1.51 mV, whereas for the XGA formulations the ZP values ranged from -39.28 ± 7.06 mV. The presence of XGA didn't affected the ZP of liposomes (p = 0.132) (Appendix VII).
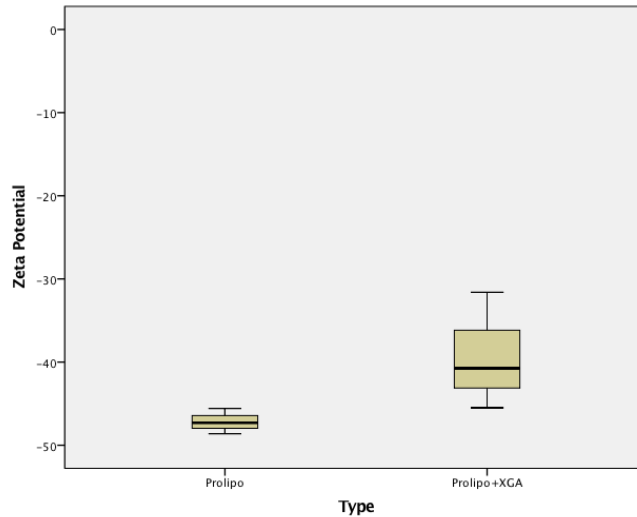
Figure 16 - Box and whisker plot of ZP of liposomes formed by hydration of proliposomes produced by SD, with and without XGA (p = 0.132).

Finally, in Figure 17, for the drugless liposome formulations, the ZP was between -44.10 ± 8.44 mV whereas for the formulations with XGA the ZP values ranged between -25.62 ± 2.60 mV. These differences were statistically significant (Appendix VII).
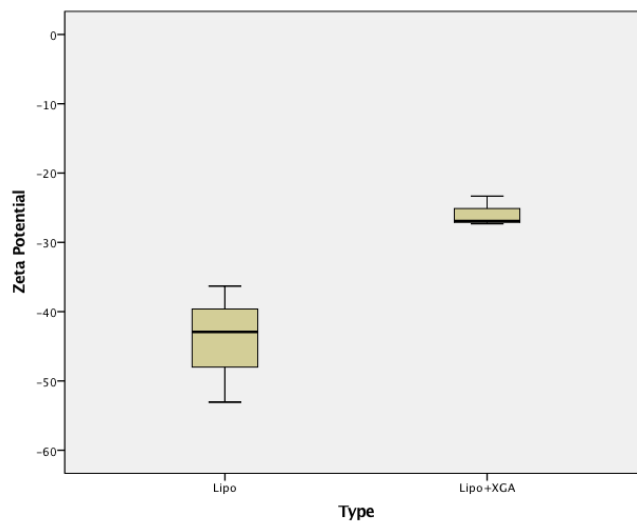
Figure 17 - Box and whisker plot of ZP of liposome with and without XGA (p = 0.022).

4.1.2 Stability of proliposomes

The proliposomes with and without XGA were tested in order to determine their stability, after 15 days, 1 month and 3 months from the first reading in the DLS. After producing proliposomes, they were kept in a desiccator at room temperature. Proliposomes were analyzed by DLS and hydrated to characterize the obtained liposomes.

a) 15 days after

Figures 18 and 19 shows the variation in size and ZP of the liposomes obtained after hydration of the proliposomes by the SD method 15 days after its production. No statistically significant changes were found in the effective diameter after 15 days of proliposome production. Also, the PI were similar to those measured on the day of production (Table VII, Appendix III).

Table VII - Results obtained from the mean diameter (nm), PI and ZP (mV), for formulations prepared by SD, using proliposomic and liposomal formulations, with and without XGA, after 15 days.

Formulation	Effective diameter (nm)	PI	ZP (mV)
Prolipo+XGA	195.53 ± 22.09	0.29 ± 0.03	-42.05 ± 3.72
Proliposome	206.53 ± 37.58	0.26 ± 0.01	-36.72 ± 5.78

The proliposomes with and without drug had a size of 195.53 ± 22.09 nm and 206.53 ± 37.58 nm, respectively (Figure 18, Table VII). With respect to ZP (Figure 19) the values were close to -30 mV, with no statistically significant differences (Appendix VI and VII).
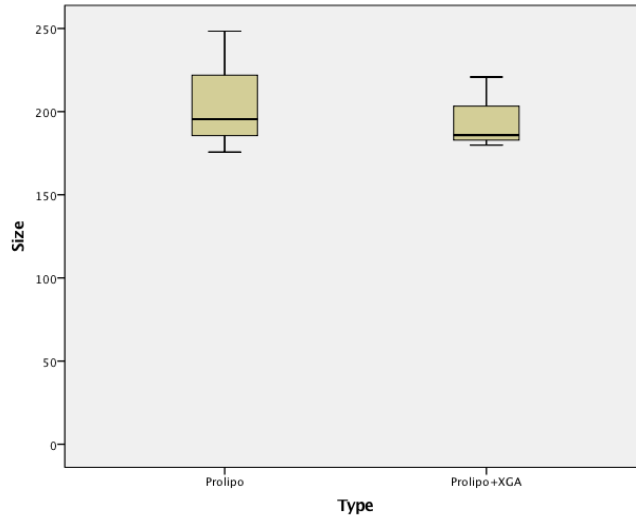
Figure 18 - Box and whisker plot of effective diameter of liposomes formed by hydration of proliposomes produced by SD, with XGA and with no XGA, at the day of production and at day 15 (p = 0.685).
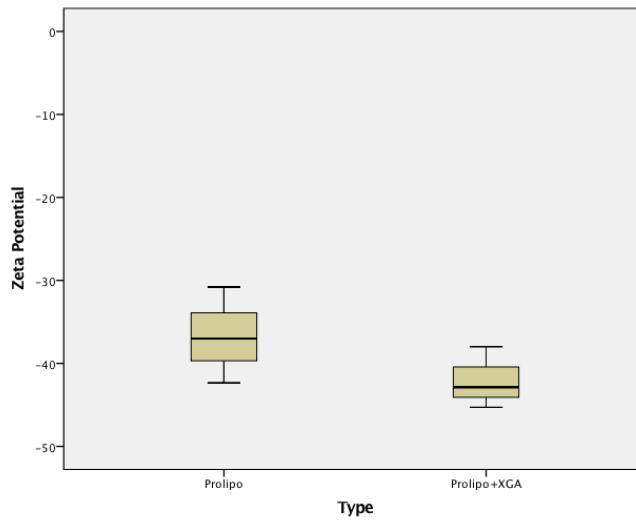
Figure 19 - Box and whisker plot of ZP of liposomes formed by hydration of proliposomes produced by SD, with XGA and with no XGA, at the day of production and at day 15 (p = 0.250).

b) 1 month after

Figure 20 and 21 shows the production of the proliposomes after 1 month. The proliposomes with and without drug had a size of 225.63 ± 54.74 nm and 275.50 ± 6.78

nm, respectively (Figure 20, Table VIII). With respect to ZP (Figure 21) the values were close to -30 mV, with no statistically significant differences (Appendix IV).

Table VIII: Results obtained from the mean diameter (nm), PI (mV) and ZP, for formulations prepared by SD, using proliposomic and liposomal formulations, with and without XGA, after 1 month.

Formulation	Effective diameter (nm)	PI	ZP (mV)
Prolipo+XGA	225.63 ± 54.74	0.20 ± 0.17	-27.96 ± 10.65
Proliposome	275.50 ± 6.78	0.24 ± 0.06	-39.43 ± 2.29
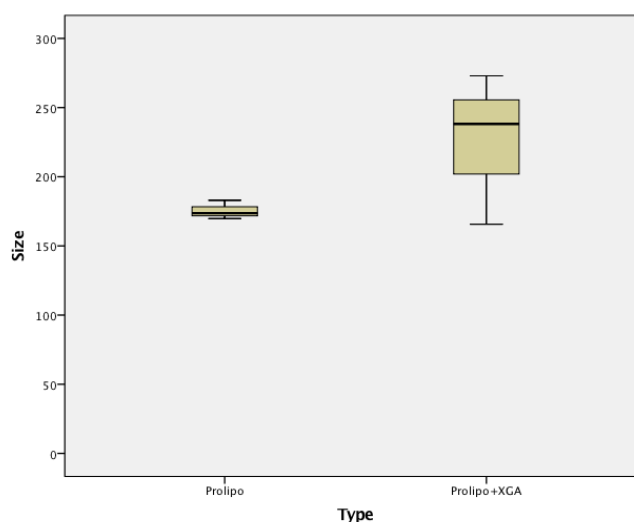
Figure 20 - Box and whisker plot of effective diameter of liposomes formed by hydration of proliposomes produced by SD, with XGA and without XGA, at the day of production and at 1 month (p = 0.191).
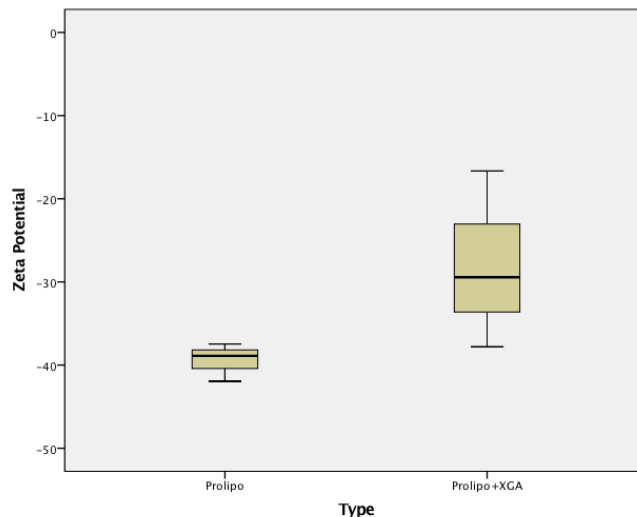
Figure 21 - Box and whiskers plot of zeta potential of liposomes formed by hydration of proliposomes produced by SD, with XGA and without XGA, at the day of production and at 1 month (p = 0.142).

c) 3 months after

The production of proliposomes after 3 months can be seen in Figures 22 and 23. The proliposomes with and without drug, had a mean size of 176.97 ± 40.51 nm and 194.73 ± 63.41 nm, respectively (Figure 22, Table IX). With respect to ZP (Figure 23) the values were close to -30 mV, with no statistically significant differences (Appendix V).

Table IX: Results obtained from the mean diameter (nm), PI (mV) and ZP, for formulations prepared by SD, using proliposomic and liposomal formulations, with and without XGA, after 3 months.

| Formulation	Effective diameter (nm)	PI	ZP (mV)
Prolipo+XGA	194.73 ± 63.41	0.23 ± 0.07	$-36.30 \pm 4,71$
Proliposome	176.97 ± 40.51	0.28 ± 0.02	-46.79 ± 12.64

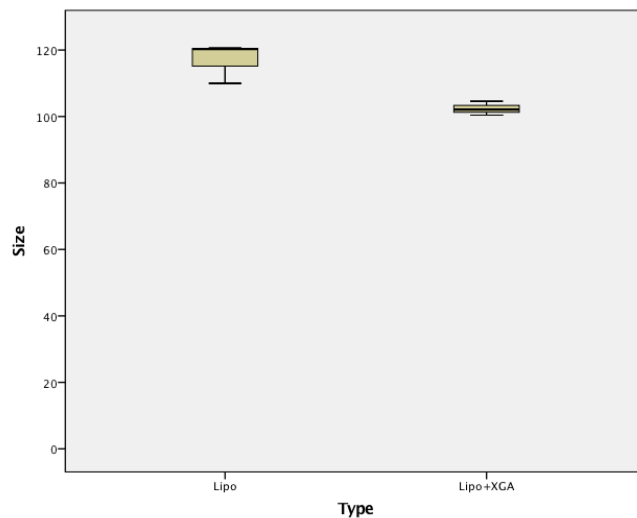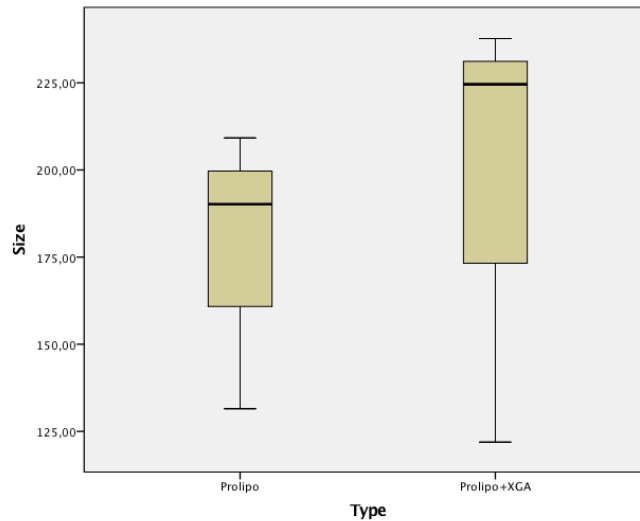Figure 22 - Box and whisker plot of effective diameter of liposomes formed by hydration of proliposomes produced by SD, with XGA and without XGA, at the day of production and at 3 months (p = 0.704).
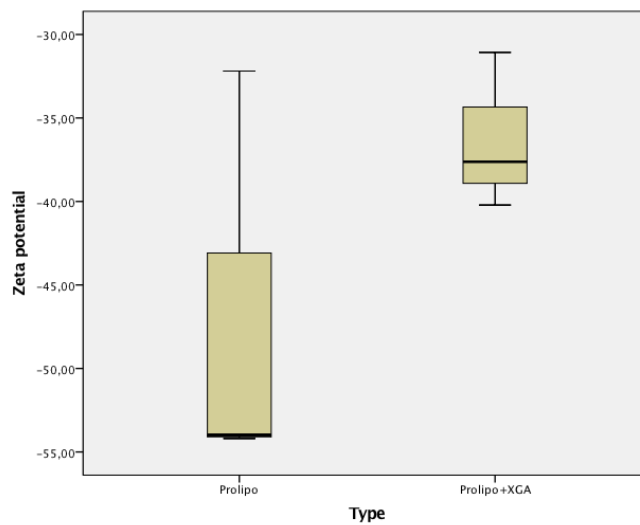
Figure 23 - Box and whisker plot of ZP of liposomes formed by hydration of proliposomes produced by SD, with XGA and without XGA, at the day of production and at 3 months (p = 0.249).

4.1.3   Particles morfology

The CryoSEM technique was used to capture images of the particles obtained after proliposomes hydration, in order to evaluate their morphology. Figure 24 shows the particles obtained from proliposomes produced by spray drying, without XGA. Particles having a spherical shape were observed. Figure 25 shows the morphology of the particles obtained by hydration of proliposomes produced by SD, with XGA. As observed, the

presence of XGA in proliposomes didn´t not altered the morphology. Both type of particles presented a very small size, but however, it is possible to observe particles of larger sizes.
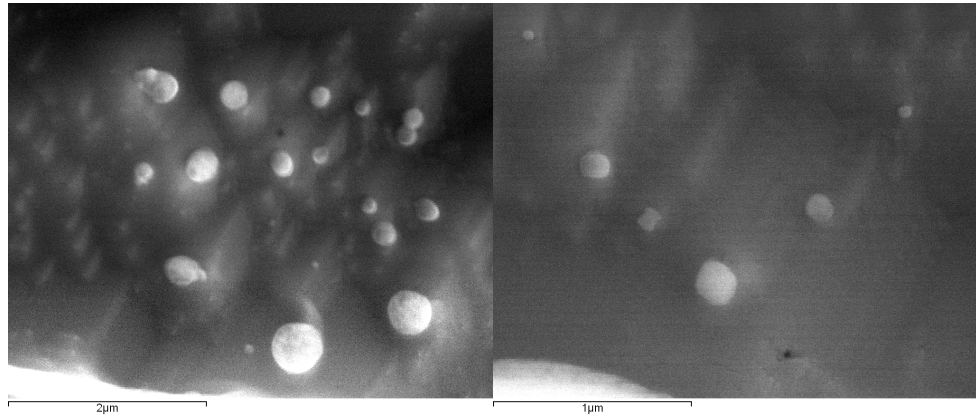
Figure 24 - CryoSEM images of liposomes formed by hydration of proliposomes produced by the SD method, without XGA at x 50000 magnification.
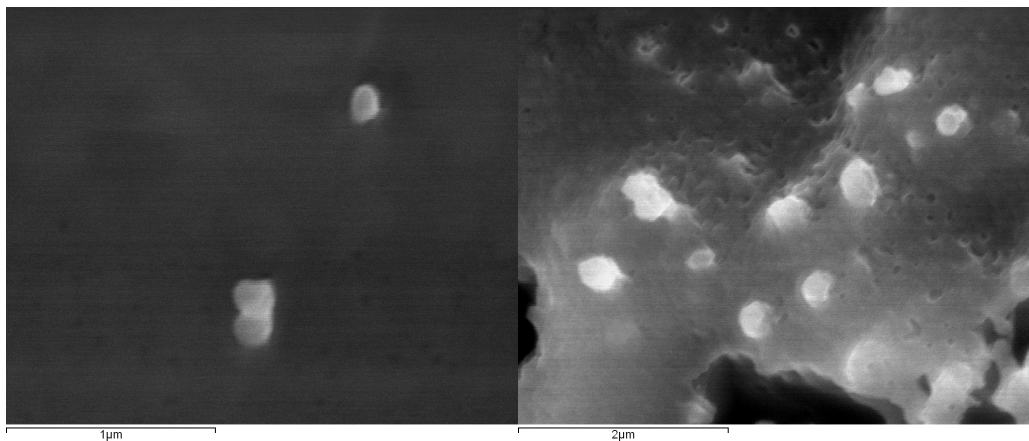
Figure 25 - CryoSEM images of liposomes formed by hydration of proliposomes produced by the SD method, with XGA at x 50000 and 25000 magnification, respectively.

Figure 26 and 27 shows the liposomes, without and with XGA, respectively. Particles having a spherical shape were observed, and it is possible to conclude that the presence of XGA in liposomes didn´t not alter their morphology.
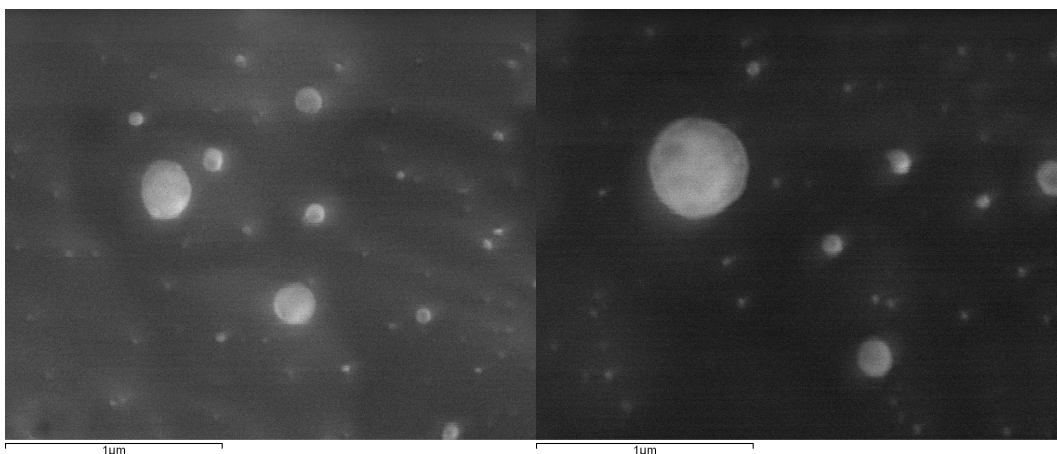
Figure 26: CryoSEM images of liposomes without XGA at x 50000 magnification.
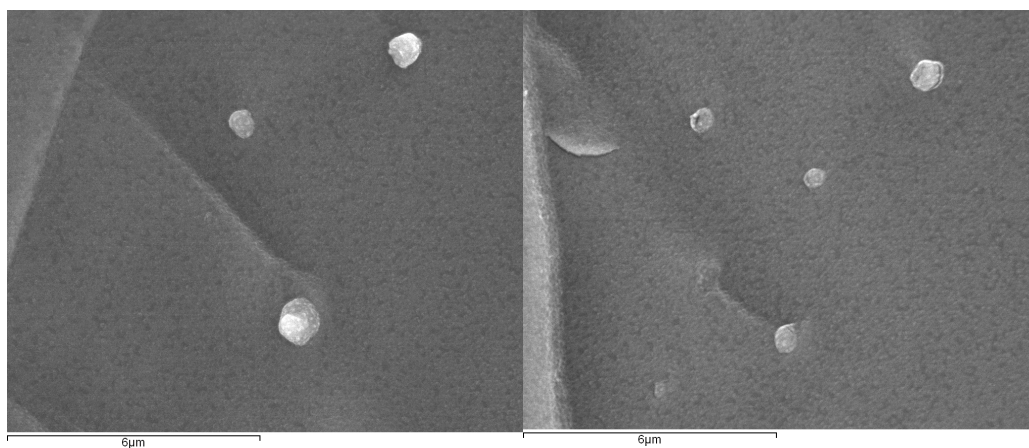
Figure 27 - CryoSEM images of liposomes with XGA at x 10000 magnification.

The surface morphology of proliposome powders without and with XGA produced from the spray drying method was examined by SEM. Figure 28 and 29 shows the spherical particles, with a high surface area. Also, the incorporation of XGA within proliposomes didn´t altered the morphology of the nanoparticles. The quantity of particles in the conventional SEM were much greater, when compared with CryoSEM, since they were not submitted to hydration. The SD seems to produce more uniform powdered particles, and allowed a fast dispersion of the powder when hydrated in order to form liposomes.
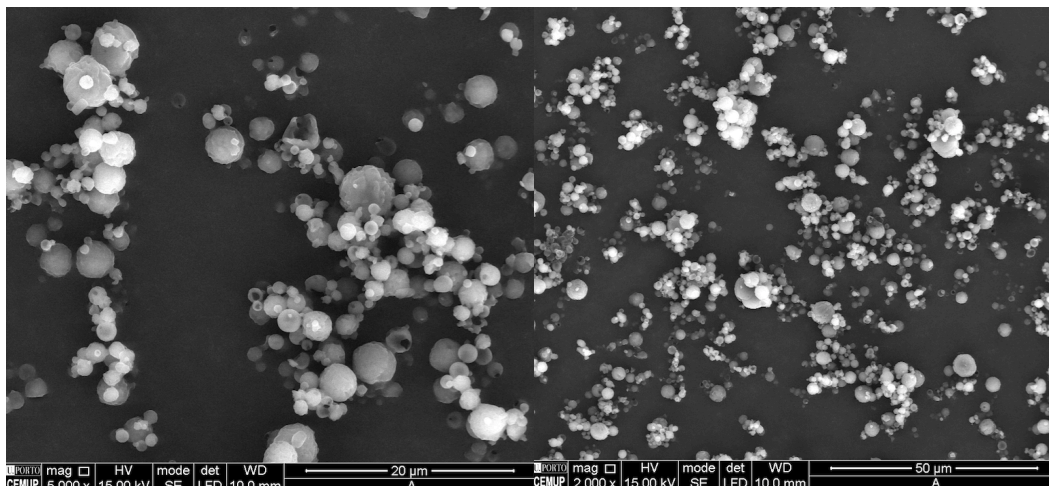
Figure 28 - SEM images of the surface of proliposome powders without XGA produced from the SD method.
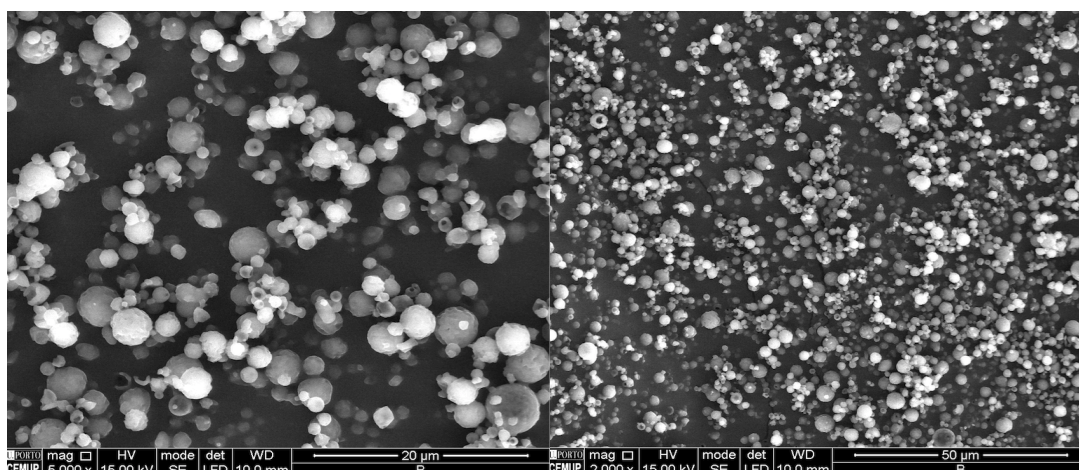
Figure 29 - SEM images of the surface of proliposome powders with XGA produced from the SD method.

4.1.4 Thermal behavior of proliposome powders

The thermal behavior of proliposome powders was analyzed by differential scanning calorimetry (DSC), which measures the onset temperature changes of the material (129, 130).

Figure 30 and Table X presents the DSC data from the components of proliposomal formulations. The mannitol peak in thermogram was used a as a reference peak for the thermal study of the proliposomal formulations.
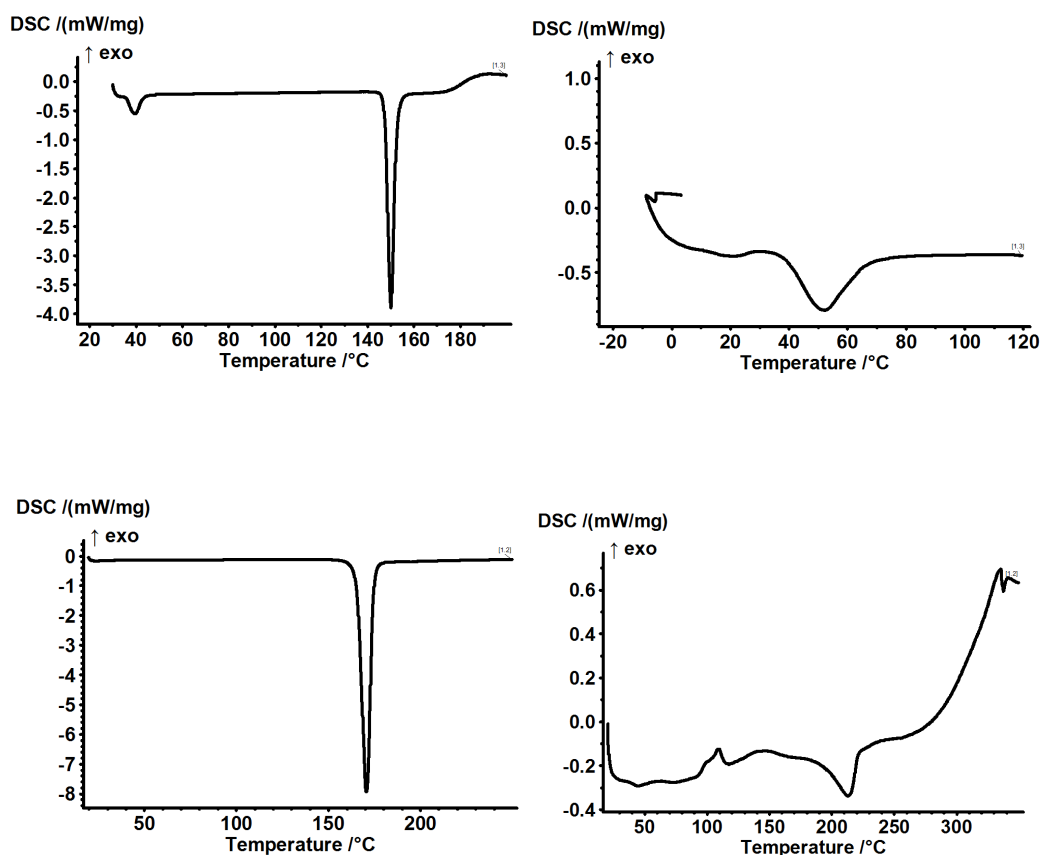
Figure 30 - DSC thermograms of cholesterol, egg phosphatidylcholine, mannitol and XGA.

Table X - DSC data of thermograms of cholesterol, egg phospatidylcholine, mannitol and XGA.

Formulation	Onset (ºC)
CH	147.3±0.17
PC	2.47±0.81
Mannitol	165.1±0.23
XGA	199.10±3.10
Proliposome without XGA	153.30±11.52
Proliposome with XGA	153.30±11.52
Liposome without XGA	Not visible
Liposome with XGA	Not visible

Figure 31 shows the mixture of components of the proliposomal formulation, where we can see all the peaks of each component; however in the proliposomal formulation

only the peak of mannitol (carrier) was visible, since this one was in much larger proportion compared with others. The presence of lipids in the formulation decreases the onset temperature of the mannitol peak, revealing the interaction between the lipid part and the carrier material of the formulation. What can be seen in the thermogram is that the lipids are well dispersed and present no crystalline forms, hence no peak for the lipids is visible (131). The presence of XGA in the formulation didn´t not altered the onset temperature of the mannitol peak. Other studies showed similar results (80, 131).

Figure 32 shows the DSC thermograms and DSC data of liposomes with and without XGA and each compound isolated (CH, PC, XGA).
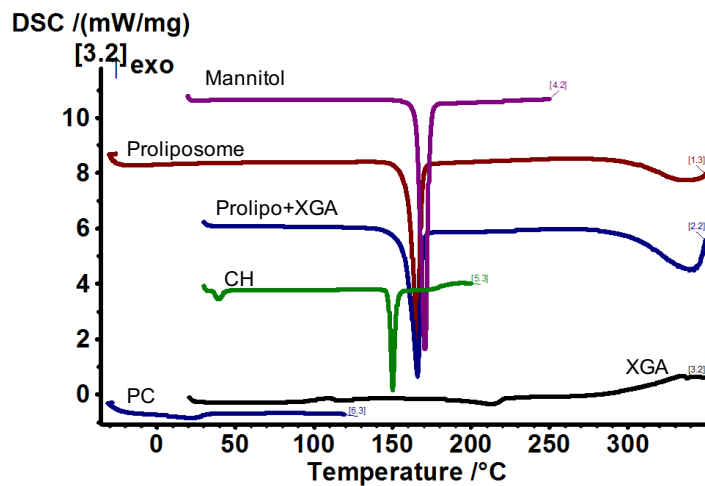
Figure 31 - Mixture of the components of the proliposomal formulation and their constituents.
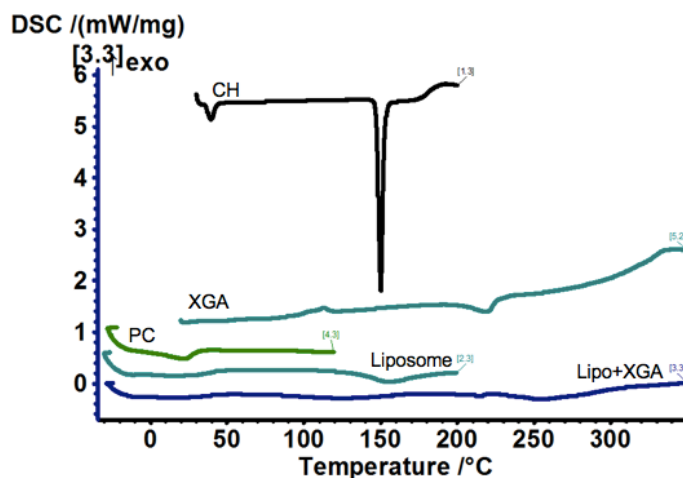
Figure 32 - Mixture of the components of the liposomal formulation and their constituents.

4.1.5 Entrapment efficiency

4.1.5.1 Quantification of XGA by HPLC

The UV spectrum of XGA was performed with the spectrophotometer, varying the wavelength from 200 to 400 nm (Figure 33). One of the peaks of absorption of XGA occured at 300 nm wavelength, which was chosen to detect the compound by the HPLC method for the EE.
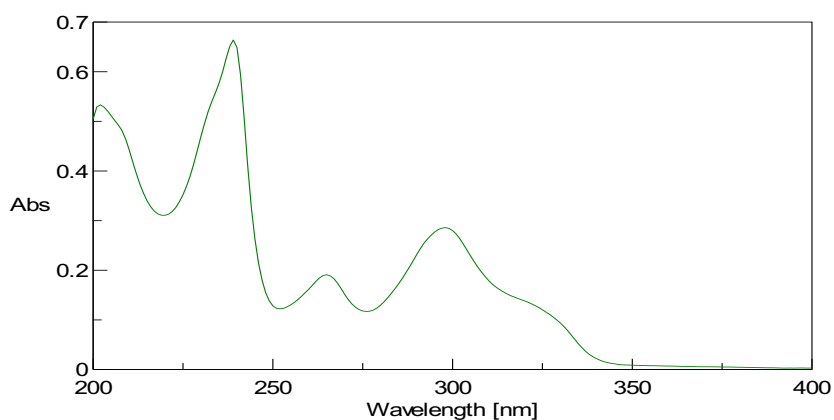
Figure 33 - Absorption spectrum between the wavelengths 200 to 400 nm.

As previously referred and in order to quantify XGA in proliposomal formulations, a methodology using HPLC equipped with a DAD detector was used. The results are shown in Table XI.

Table XI - Chromatographic parameters of 5 injections in the methanol / water (72:28) proportions of substance XGA.

t_r	Area (mAU.min)	Number of theorical plates	Resolution	Symmetry	K
5.21	2.5605	1435	3.9	1.04	2.47
5.23	2.5389	1519	3.9	1.03	2.49
5.23	2.5293	1527	3.9	1.03	2.49
5,23	2.6293	1494	3.7	1.12	2.49
5.23	2.5645	1493	3.9	1.06	2.49

The value of t_0 was estimated as follows: for a 15 cm x 4.6 mm column and a flow of 1.0 mL / min, obtaining:

$$V_m = 0.5 \text{ x } 15.0 \text{ x } 0.46^2 = 1,6 \text{ mL} \qquad \text{and} \qquad t_0 = 1.6/1.0 = 1.6 \text{ min}$$

The Table XII shows the concentration of XGA and respective mean peak area obtained from the chromatogram of XGA. Data were fitted to least squares linear regression and a calibration curve was obtained (Figure 34 – A), with the respective equation of the curve (Equation 5) having a correlation coefficient (R) of 0.9992 demonstrating good linearity in the tested range for XGA.

Table XII - Concentration of XGA and respective mean peak area.

Concentration (µg/ml)	Mean peak area
25.6	1.0813
30.0	1.3568
40.7	2.1650
50.6	2.7439
61.2	3.4443

$$y = 0.0665x - 0.6114 \qquad \text{Equation 8}$$

Figure 34 - B shows the residuals values of XGA standard solutions which were randomly dispersed, reinforcing the linearity of the method.
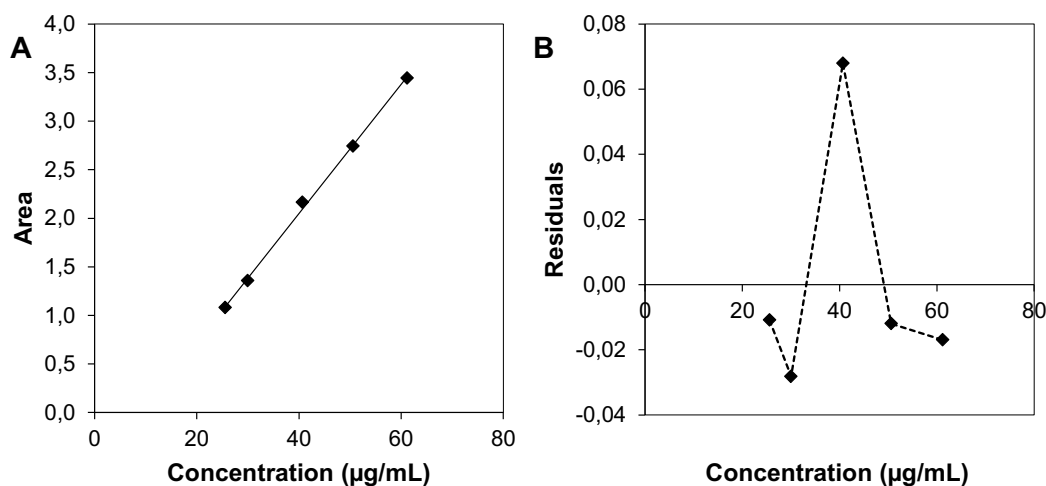
Figure 34 - Calibration curve (A) and residual plot (B) of XGA HPLC method.
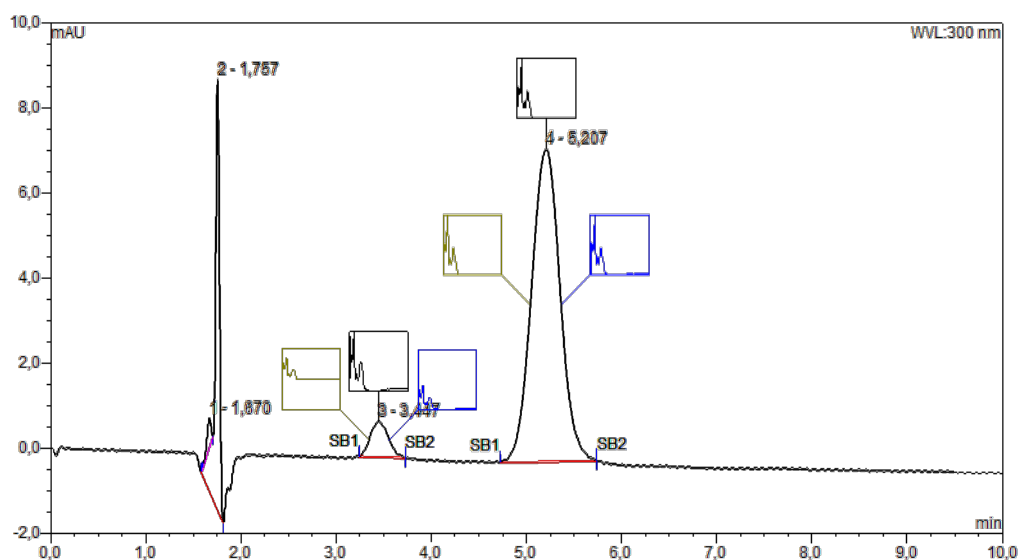
Figure 35 - Standard solution chromatogram and UV spectrum at 300nm for the specific detection of the compound.

The EE of XGA in liposomes obtained by hydration of proliposomes was determined by a direct measurement of the compound that was encapsulated in the formulation by an HPLC method. Figures 36 and 37 shows chromatograms of both the proliposome formulations which are subsequently hydrated and form liposomes, and from direct liposomes. Proliposome formulations demonstrated higher entrapment efficiency because XGA become more encapsulated. Table XIII shows that proliposomes have higher drug entrapment efficiency than liposomes, since the percentages are relatively higher than in liposome formulations.
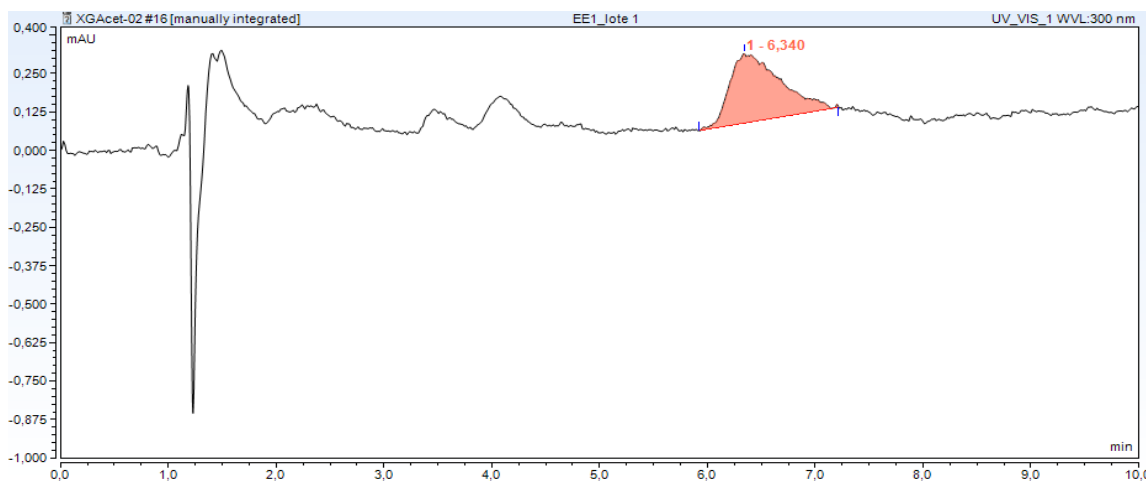
Figure 36 - HPLC chromatogram of the proliposome formulation.
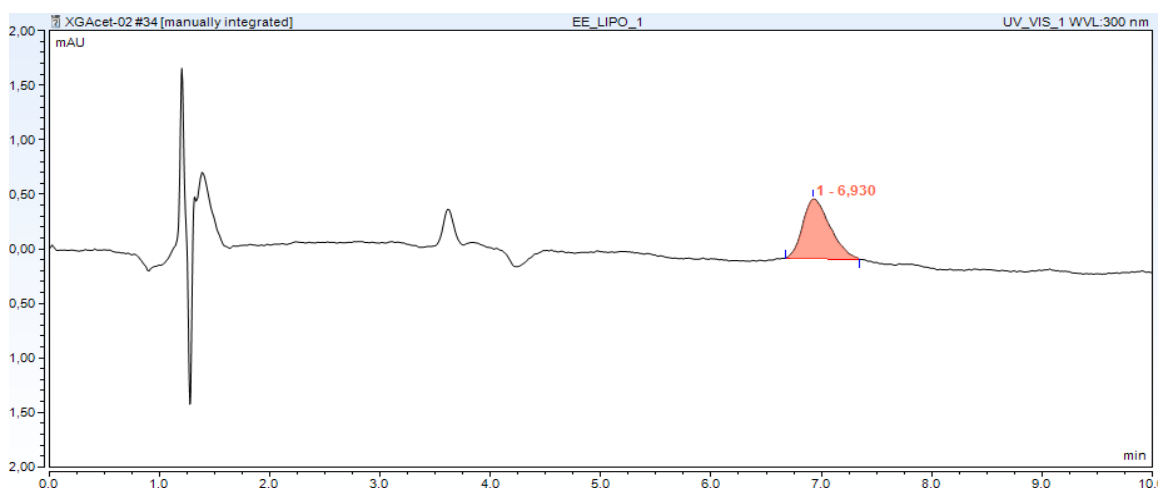
Figure 37 - HPLC chromatogram of the liposome formulation.

Table XIII - Entrapment Efficiency (EE) mean results.

EE Proliposomes				EE Liposomes			
1	87%	86%	87%	1	93%	80%	78%
2	87%	89%	88%	2	78%	79%	78%
3	88%	85%	87%	3	78%	77%	81%
Mean	87.1%			Mean	80.2%		

4.1.6 Cell viability

The different formulations of XGA, proliposomes with and without XGA and liposomes with and without XGA were evaluated in glioma cells, to verify their effects on cell viability.

Figure 39 shows the viability of XGA. In concentrations between 10 and 100 µM there is inhibition in the 3 tumor cell lines of the compound.
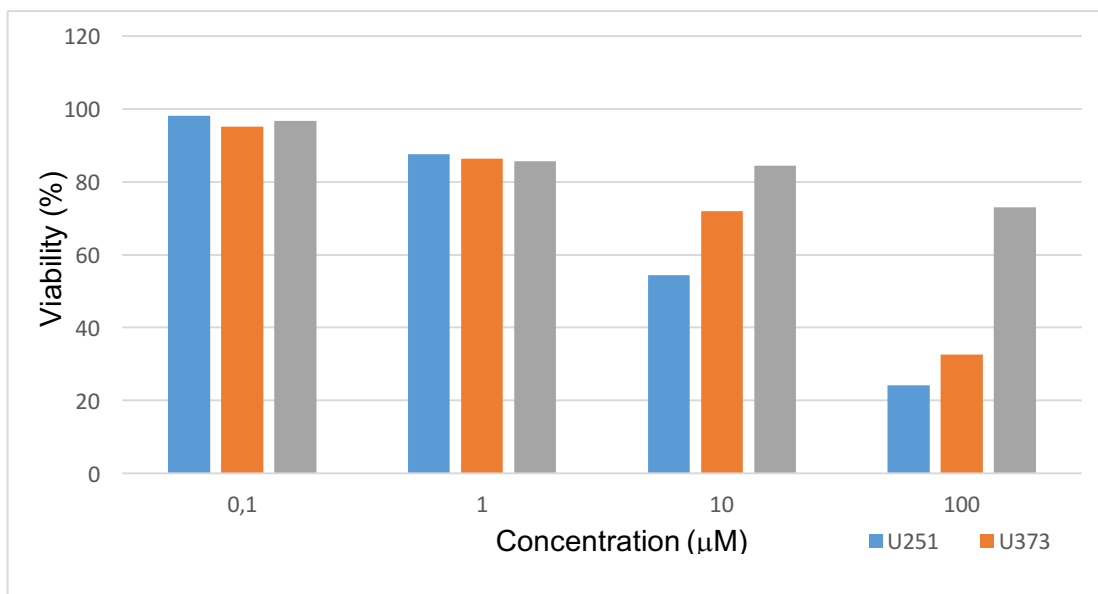
Figure 38 – Cell viability using XGA (glioma cell lines: U251, U373 and U87MG, with difference concentrations of 0.1, 1, 10 and 100 µM).

Figure 39 and 40 shows the cell viability (in percentage) when exposed to liposomes without and with XGA. The viability of the liposomes without drug (Figure 39) shows that there is no change in any concentration in the three tumor lines, as there was no inhibition of tumor cells. However, in XGA liposomes (Figure 40), there was inhibition in the three tumor lines in the concentration of 100 µM.
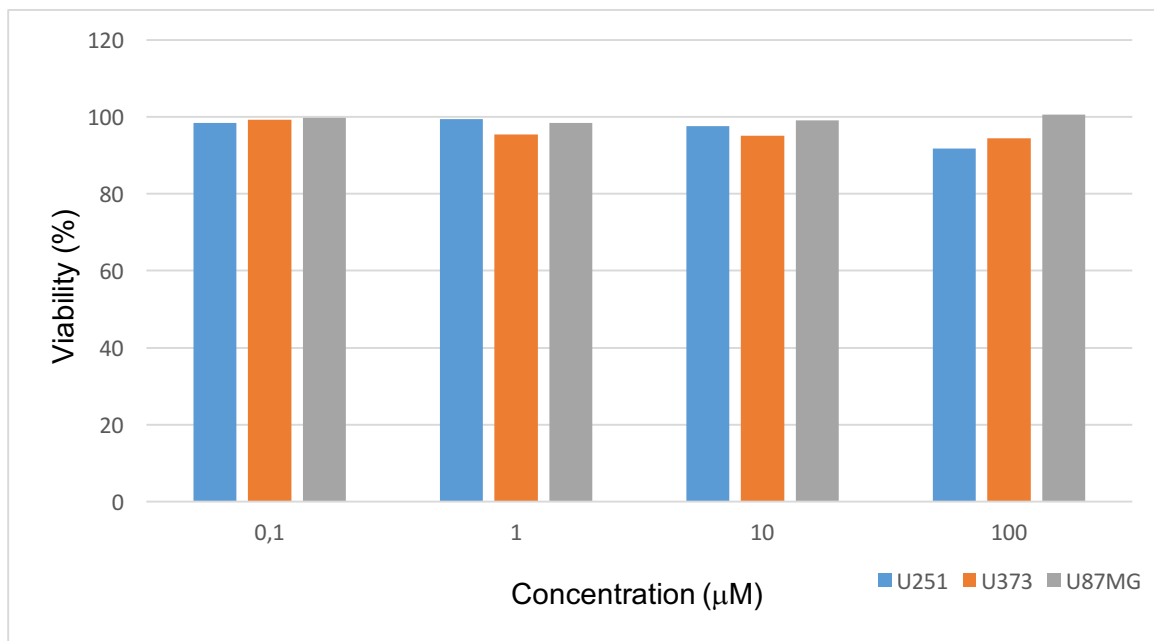
Figure 39 – Cell viability using liposomes without drug (glioma cell lines: U251, U373 and U87MG, with difference concentrations of, 0.1, 1, 10 and 100 μM).
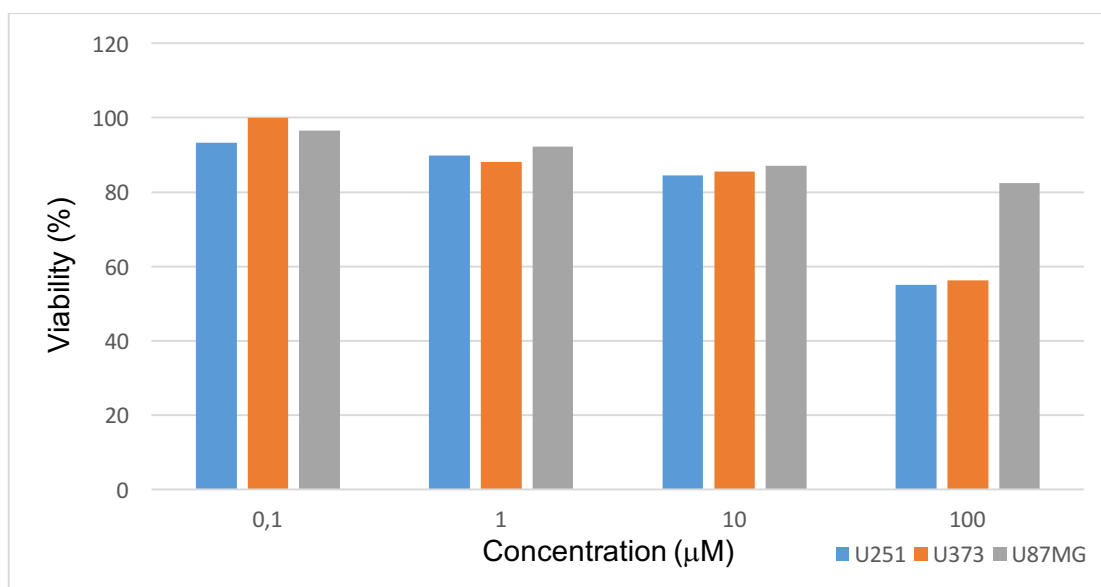
Figure 40 – Cell viability using liposomes with XGA (glioma cell lines: U251, U373 and U87MG, with difference concentrations of, 0.1, 1, 10 and 100 μM).

Figure 41 and 42 shows the cell viability when exposed to proliposomes without and with XGA. The viability of the proliposomes without drug (Figure 41) shows that there was a change in the 3 tumor lines, which may indicate that the empty proliposome showed some toxicity, and it may be due to mannitol. Because mannitol can have an osmotic effect, that is, as mannitol is a sugar, it causes the hyperosmotic effect, leading to cell

death. However, in XGA proliposomes (Figure 42), there was inhibition in the 3 tumor lines in the concentration between 10 and 100 μM.
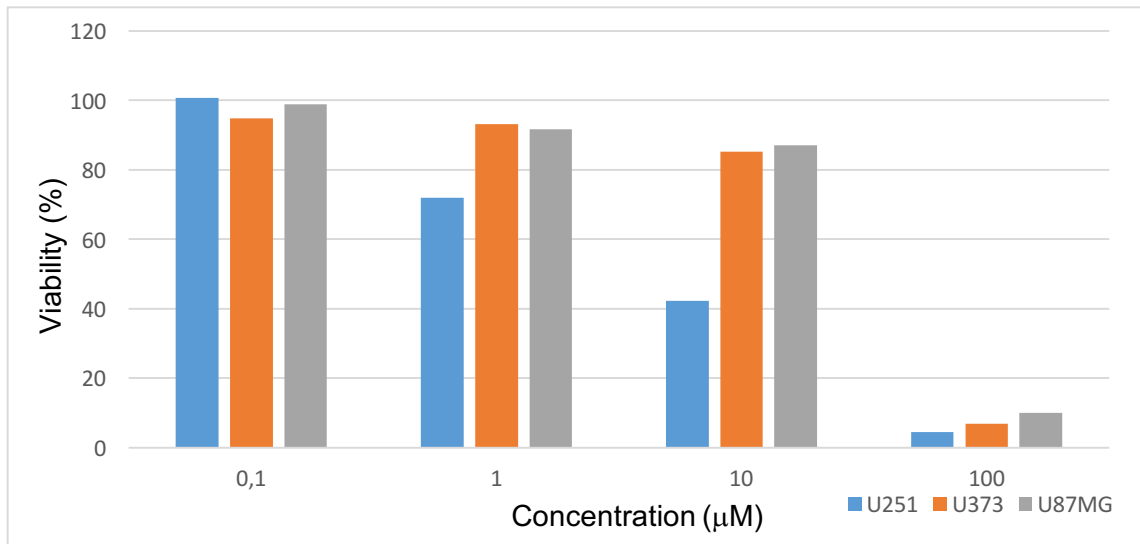
Figure 41 - Cell viability using proliposomes without XGA (glioma cell lines: U251, U373 and U87MG, with difference concentrations of, 0.1, 1, 10 and 100 μM).
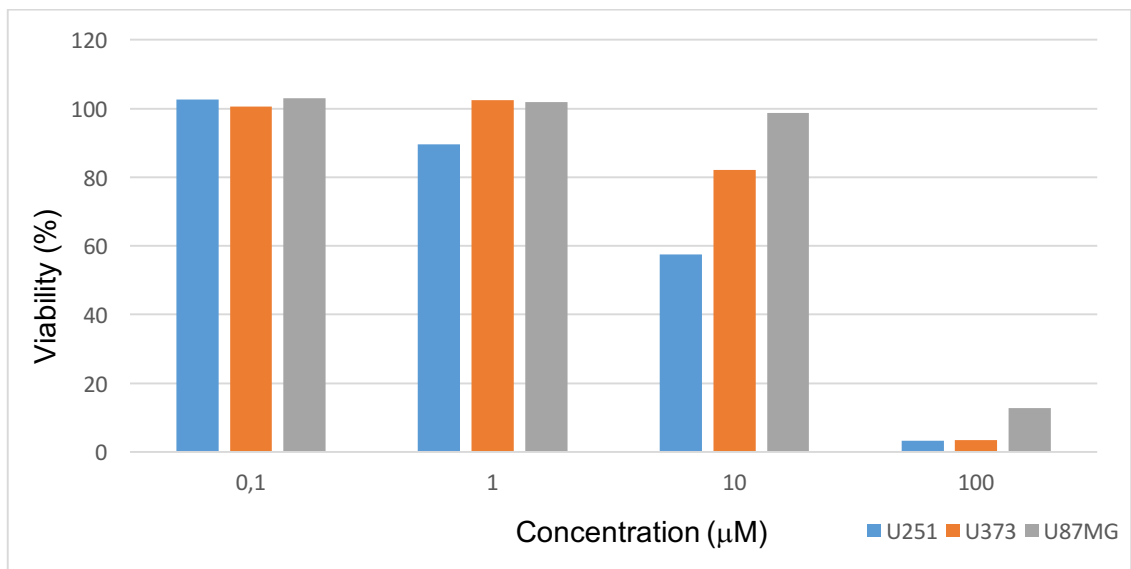
Figure 42 - Cell viability using proliposomes with XGA (glioma cell lines: U251, U373 and U87MG, with difference concentrations of, 0.1, 1, 10 and 100 μM).

5   Conclusion and future work

Liposomes have numerous advantages since they are similar with cell membranes. However, the physical and chemical instability limits their use, restricting their shelf-life and their clinical applications.

The proliposomes have been studied as an alternative to the conventional liposomes. They are solid particles formed by lipids and a transporter, that, when hydrated, originate liposomes. The fact that they are solid particles gives them more stability when compared to the traditional liposomes.

In this work, proliposomes and liposomes have been developed as a drug carrier of a promising antitumor synthetic xanthone derivate (XGA). Xanthone usually present poor water solubility and their encapsulation in nanosystems might be a strategy to solve this solubility problem.

Proliposomes and liposomes were produced with and without the drug. The proliposomes were produce by *Spray Drying* and the liposomes were produce by the conventional described method, thin lipid film hydration. After obtaining the proliposomes, they were hydrated to form the liposomes. Both formulations were characterized by size, zeta potential, encapsulation efficiency, morphology and cell viability. Viability was characterized in 3 different types of tumor cells: U251, U373 and U87MG. It has been found that when the concentration of compound is between 10 and 100 μM it inhibits the three types of cell lines.

The results showed that the liposomes obtained from the proliposomes have an average diameter of 200 nm. In comparison, the traditional liposomes presented an average size in the order of 100 nm. Both formulations presented good zeta potential values.

The stability of the proliposomes was tested and showed no significant changes in liposome properties after 15, 30 and 90 days.

The use of the CryoSEM and SEM techniques allowed the evaluation of the morphology of the proliposomes and liposomes formulations, showing them as spherical particles with a uniform morphology.

Both the liposomal formulations were able to inhibit the tumor cell lines. However, the drug-free proliposomal formulation showed some toxicity.

One of the next steps in the continuation of this work should be the study of the toxicity of the empty proliposomes and the toxicity of the carrier.

It is also necessary to verify the viability in normal cells to be able to compare with the results of the tumor cell lines tested. The antitumor activity of this novel drug could also be tested in other types of tumor cell lines.

6 Bibliographic references

1. Dimer FA, Friedrich RB, Beck RCR, Guterres SS, Pohlmann AR. Impact of nanotechnology on public health: Production of medicines. Quimica Nova. 2013;36(10):1520-6.
2. World Health Organization. Cancer 2017 [accessed on 15 May].
3. Beik J, Abed Z, Ghoreishi FS, Hosseini-Nami S, Mehrzadi S, Shakeri-Zadeh A, et al. Nanotechnology in hyperthermia cancer therapy: From fundamental principles to advanced applications. Journal of Controlled Release. 2016;235:205-21.
4. Ferrari M. Cancer nanotechnology: opportunities and challenges. Nature Reviews Cancer. 2005;5(3):161-71.
5. Vasir JK, Labhasetwar V. Biodegradable nanoparticles for cytosolic delivery of therapeutics. Adv Drug Deliv Rev. 2007;59(8):718-28.
6. Escriba PV. Membrane-lipid therapy: a new approach in molecular medicine. Trends in molecular medicine. 2006;12(1):34-43.
7. Galeotti T, Borrello S, Minotti G, Masotti L. Membrane alterations in cancer cells: the role of oxy radicals. Annals of the New York Academy of Sciences. 1986;488:468-80.
8. Mikirova N, Riordan HD, Jackson JA, Wong K, Miranda-Massari JR, Gonzalez MJ. Erythrocyte membrane fatty acid composition in cancer patients. Puerto Rico health sciences journal. 2004;23(2):107-13.
9. Gillies RJ, Raghunand N, Karczmar GS, Bhujwalla ZM. MRI of the tumor microenvironment. Journal of magnetic resonance imaging : JMRI. 2002;16(4):430-50.
10. Parks SK, Chiche J, Pouyssegur J. pH control mechanisms of tumor survival and growth. Journal of cellular physiology. 2011;226(2):299-308.
11. Estrella V, Chen T, Lloyd M, Wojtkowiak J, Cornnell HH, Ibrahim-Hashim A, et al. Acidity generated by the tumor microenvironment drives local invasion. Cancer research. 2013;73(5):1524-35.
12. Stubbs M, McSheehy PM, Griffiths JR, Bashford CL. Causes and consequences of tumour acidity and implications for treatment. Mol Med Today. 2000;6(1):15-9.
13. Cardone RA, Casavola V, Reshkin SJ. The role of disturbed pH dynamics and the Na+/H+ exchanger in metastasis. Nature reviews Cancer. 2005;5(10):786-95.
14. Seydel JK, Wiese M. Drug-membrane interactions: analysis, drug distribution, modeling: John Wiley & Sons; 2009.
15. Hendrich AB, Michalak K. Lipids as a target for drugs modulating multidrug resistance of cancer cells. Current drug targets. 2003;4(1):23-30.
16. Alves AC, Ribeiro D, Nunes C, Reis S. Biophysics in cancer: the relevance of drug-membrane interaction studies. Biochimica et Biophysica Acta (BBA)-Biomembranes. 2016;1858(9):2231-44.
17. Frezard F, Schettini DA, Rocha OGF, Demicheli C. Liposomes: Physicochemical and pharmacological properties, applications in antimony-based chemotherapy. Quimica Nova. 2005;28(3):511-8.
18. Batista CM, Carvalho CMBd, Magalhães NSS. Lipossomas e suas aplicações terapêuticas: estado da arte. Revista Brasileira de Ciências Farmacêuticas. 2007;43(2):167-79.
19. Dua J, Rana A, Bhandari A. Liposome: methods of preparation and applications. Int J Pharm Stud Res. 2012;3:14-20.
20. Sercombe L, Veerati T, Moheimani F, Wu SY, Sood AK, Hua S. Advances and challenges of liposome assisted drug delivery. Frontiers in pharmacology. 2015;6:286.
21. Koning GA, Storm G. Targeted drug delivery systems for the intracellular delivery of macromolecular drugs. Drug discovery today. 2003;8(11):482-3.

22. Machado LC, Gnoatto SA, Klüppel MLW. Lipossomas aplicados em farmacologia: uma revisão da literatura. Estudos de Biologia Ambiente e Diversidade. 2007;29(67):215-24.

23. Allen T, Hansen C, Martin F, Redemann C, Yau-Young A. Liposomes containing synthetic lipid derivatives of poly (ethylene glycol) show prolonged circulation half-lives in vivo. Biochimica et Biophysica Acta (BBA)-Biomembranes. 1991;1066(1):29-36.

24. Verkleij A, Ververgaert P, Van Deenen L, Elbers P. Phase transitions of phospholipid bilayers and membranes of Acholeplasma laidlawii B visualized by freeze fracturing electron microscopy. Biochimica et Biophysica Acta (BBA)-Biomembranes. 1972;288(2):326-32.

25. Allen TM, Cullis PR. Liposomal drug delivery systems: From concept to clinical applications. Advanced Drug Delivery Reviews. 2013;65(1):36-48.

26. Olson F, Hunt C, Szoka F, Vail W, Papahadjopoulos D. Preparation of liposomes of defined size distribution by extrusion through polycarbonate membranes. Biochimica et Biophysica Acta (BBA)-Biomembranes. 1979;557(1):9-23.

27. Hope M, Bally M, Webb G, Cullis P. Production of large unilamellar vesicles by a rapid extrusion procedure. Characterization of size distribution, trapped volume and ability to maintain a membrane potential. Biochimica et Biophysica Acta (BBA)-Biomembranes. 1985;812(1):55-65.

28. Samad A, Sultana Y, Aqil M. Liposomal drug delivery systems: an update review. Current drug delivery. 2007;4(4):297-305.

29. Li J, Wang X, Zhang T, Wang C, Huang Z, Luo X, et al. A review on phospholipids and their main applications in drug delivery systems. Asian Journal of Pharmaceutical Sciences. 2015;10(2):81-98.

30. Akbarzadeh A, Rezaei-Sadabady R, Davaran S, Joo SW, Zarghami N, Hanifehpour Y, et al. Liposome: classification, preparation, and applications. Nanoscale Res Lett. 2013;8:9.

31. Vemuri S, Rhodes CT. Preparation and characterization of liposomes as therapeutic delivery systems: a review. Pharm Acta Helv. 1995;70(2):95-111.

32. Vemuri S, Rhodes C. Preparation and characterization of liposomes as therapeutic delivery systems: a review. Pharmaceutica Acta Helvetiae. 1995;70(2):95-111.

33. Mufamadi MS, Pillay V, Choonara YE, Du Toit LC, Modi G, Naidoo D, et al. A review on composite liposomal technologies for specialized drug delivery. Journal of drug delivery. 2011;2011.

34. Christensen D, Foged C, Rosenkrands I, Nielsen HM, Andersen P, Agger EM. Trehalose preserves DDA/TDB liposomes and their adjuvant effect during freeze-drying. Biochimica et Biophysica Acta (BBA)-Biomembranes. 2007;1768(9):2120-9.

35. Vonarbourg A, Passirani C, Saulnier P, Benoit J-P. Parameters influencing the stealthiness of colloidal drug delivery systems. Biomaterials. 2006;27(24):4356-73.

36. American Cancer Society. How Chemotherapy Drugs Work 2017 [accessed on 11/07/2017]. Available from: https://www.cancer.org/treatment/treatments-and-side-effects/treatment-types/chemotherapy/how-chemotherapy-drugs-work.html.

37. Fuertes MA, Castilla J, Alonso C, Perez JM. Cisplatin biochemical mechanism of action: from cytotoxicity to induction of cell death through interconnections between apoptotic and necrotic pathways. Current medicinal chemistry. 2003;10(3):257-66.

38. Horwitz SB. Taxol (paclitaxel): mechanisms of action. Annals of oncology : official journal of the European Society for Medical Oncology. 1994;5 Suppl 6:S3-6.

39. Rose PG. Pegylated liposomal doxorubicin: optimizing the dosing schedule in ovarian cancer. The oncologist. 2005;10(3):205-14.

40. Kraft JC, Freeling JP, Wang Z, Ho RJY. Emerging Research and Clinical Development Trends of Liposome and Lipid Nanoparticle Drug Delivery Systems. Journal of Pharmaceutical Sciences. 2014;103(1):29-52.

41. Hann IM, Prentice HG. Lipid-based amphotericin B: a review of the last 10 years of use. International journal of antimicrobial agents. 2001;17(3):161-9.

42. Barenholz Y. Doxil(R)--the first FDA-approved nano-drug: lessons learned. Journal of controlled release : official journal of the Controlled Release Society. 2012;160(2):117-34.

43. Petre CE, Dittmer DP. Liposomal daunorubicin as treatment for Kaposi's sarcoma. Int J Nanomedicine. 2007;2(3):277-88.

44. Bowden R, Chandrasekar P, White MH, Li X, Pietrelli L, Gurwith M, et al. A double-blind, randomized, controlled trial of amphotericin B colloidal dispersion versus amphotericin B for treatment of invasive aspergillosis in immunocompromised patients. Clinical infectious diseases : an official publication of the Infectious Diseases Society of America. 2002;35(4):359-66.

45. Batist G, Ramakrishnan G, Rao CS, Chandrasekharan A, Gutheil J, Guthrie T, et al. Reduced cardiotoxicity and preserved antitumor efficacy of liposome-encapsulated doxorubicin and cyclophosphamide compared with conventional doxorubicin and cyclophosphamide in a randomized, multicenter trial of metastatic breast cancer. Journal of clinical oncology : official journal of the American Society of Clinical Oncology. 2001;19(5):1444-54.

46. N.M. Bressler VIPTSG. Verteporfin therapy of subfoveal choroidal neovascularization in age-related macular degeneration: two-year results of a randomized clinical trial including lesions with occult with no classic choroidal neovascularization--verteporfin in photodynamic therapy report 2. American journal of ophthalmology. 2001;131(5):541-60.

47. Gambling D, Hughes T, Martin G, Horton W, Manvelian G. A comparison of Depodur, a novel, single-dose extended-release epidural morphine, with standard epidural morphine for pain relief after lower abdominal surgery. Anesthesia and analgesia. 2005;100(4):1065-74.

48. Glantz MJ, LaFollette S, Jaeckle KA, Shapiro W, Swinnen L, Rozental JR, et al. Randomized trial of a slow-release versus a standard formulation of cytarabine for the intrathecal treatment of lymphomatous meningitis. Journal of clinical oncology : official journal of the American Society of Clinical Oncology. 1999;17(10):3110-6.

49. Simon JA. Estradiol in micellar nanoparticles: the efficacy and safety of a novel transdermal drug-delivery technology in the management of moderate to severe vasomotor symptoms. Menopause (New York, NY). 2006;13(2):222-31.

50. Sarris AH, Hagemeister F, Romaguera J, Rodriguez MA, McLaughlin P, Tsimberidou AM, et al. Liposomal vincristine in relapsed non-Hodgkin's lymphomas: early results of an ongoing phase II trial. Annals of oncology : official journal of the European Society for Medical Oncology. 2000;11(1):69-72.

51. Newman MS, Colbern GT, Working PK, Engbers C, Amantea MA. Comparative pharmacokinetics, tissue distribution, and therapeutic effectiveness of cisplatin encapsulated in long-circulating, pegylated liposomes (SPI-077) in tumor-bearing mice. Cancer chemotherapy and pharmacology. 1999;43(1):1-7.

52. Riviere K, Kieler-Ferguson HM, Jerger K, Szoka FC. Anti-tumor activity of liposome encapsulated fluoroorotic acid as a single agent and in combination with liposome irinotecan. Journal of controlled release. 2011;153(3):288-96.

53. Drummond DC, Noble CO, Guo Z, Hong K, Park JW, Kirpotin DB. Development of a highly active nanoliposomal irinotecan using a novel intraliposomal stabilization strategy. Cancer research. 2006;66(6):3271-7.

54. Suzuki R, Takizawa T, Kuwata Y, Mutoh M, Ishiguro N, Utoguchi N, et al. Effective anti-tumor activity of oxaliplatin encapsulated in transferrin-PEG-liposome. Int J Pharm. 2008;346(1-2):143-50.

55. Apostolidou E, Swords R, Alvarado Y, Giles FJ. Treatment of acute lymphoblastic leukaemia : a new era. Drugs. 2007;67(15):2153-71.

56. Poon RT, Borys N. Lyso-thermosensitive liposomal doxorubicin: an adjuvant to increase the cure rate of radiofrequency ablation in liver cancer. Future oncology (London, England). 2011;7(8):937-45.

57. Semple SC, Akinc A, Chen J, Sandhu AP, Mui BL, Cho CK, et al. Rational design of cationic lipids for siRNA delivery. Nature biotechnology. 2010;28(2):172-6.

58. Bradbury PA, Shepherd FA. Immunotherapy for lung cancer. Journal of thoracic oncology : official publication of the International Association for the Study of Lung Cancer. 2008;3(6 Suppl 2):S164-70.

59. Richard BM, Newton P, Ott LR, Haan D, Brubaker AN, Cole PI, et al. The Safety of EXPAREL (R) (Bupivacaine Liposome Injectable Suspension) Administered by Peripheral Nerve Block in Rabbits and Dogs. J Drug Deliv. 2012;2012:962101.

60. Payne NI, Ambrose CV, Timmins P, Ward MD, Ridgway F. Proliposomes: A Novel Solution to an Old Problem. Journal of Pharmaceutical Sciences. 1986;75(4):325-9.

61. Janga KY, Jukanti R, Velpula A, Sunkavalli S, Bandari S, Kandadi P, et al. Bioavailability enhancement of zaleplon via proliposomes: role of surface charge. European Journal of Pharmaceutics and Biopharmaceutics. 2012;80(2):347-57.

62. Falconer JR, Svirskis D, Adil AA, Wu Z. Supercritical Fluid Technologies to Fabricate Proliposomes. Journal of pharmacy & pharmaceutical sciences : a publication of the Canadian Society for Pharmaceutical Sciences, Societe canadienne des sciences pharmaceutiques. 2015;18(5):747-64.

63. Shaji J, Bhatia V. Proliposomes: a brief overview of novel delivery system. Int J Pharm Bio Sci. 2013;4(1):150-60.

64. Silva Moreira G. Desenvolvimento de prolipossomas com paclitaxel: uma nova abordagem na terapia do cancro. 2015.

65. Moreira A. Development of proliposomes as a vehicle to deliver new molecules with antitumor activity. 2015.

66. Manani H, Prajapati B, Patel R. Review of Preliposomes as novel drug delivery system. The Pharma Innovation Journal. 2015;4:61-7.

67. Sastry SV, Nyshadham JR, Fix JA. Recent technological advances in oral drug delivery–a review. Pharmaceutical science & technology today. 2000;3(4):138-45.

68. Storm G, Crommelin DJA. Liposomes: quo vadis? Pharmaceutical Science & Technology Today. 1998;1(1):19-31.

69. Verma RK, Garg S. Drug delivery technologies and future directions. Pharmaceut Technol On-Line. 2001;25(2):1-14.

70. Leopold CS. Coated dosage forms for colon-specific drug delivery. Pharmaceutical Science & Technology Today. 1999;2(5):197-204.

71. Deshmukh DD, Ravis WR, Betageri GV. Improved delivery of cromolyn from oral proliposomal beads. International journal of pharmaceutics. 2008;358(1):128-36.

72. Bernsdorff C, Wolf A, Winter R, Gratton E. Effect of hydrostatic pressure on water penetration and rotational dynamics in phospholipid-cholesterol bilayers. Biophysical journal. 1997;72(3):1264.

73. Yan-Yu X, Yun-mei S, Zhi-peng C, Qi-neng P. Preparation of silymarin proliposome: a new way to increase oral bioavailability of silymarin in beagle dogs. International journal of pharmaceutics. 2006;319(1):162-8.

74. Kumar R, Gupta RB, Betegeri G. Formulation, characterization, and in vitro release of glyburide from proliposomal beads. Drug delivery. 2001;8(1):25-7.

75. Hiremath PS, Soppimath KS, Betageri GV. Proliposomes of exemestane for improved oral delivery: formulation and in vitro evaluation using PAMPA, Caco-2 and rat intestine. International journal of pharmaceutics. 2009;380(1):96-104.

76. Payne NI, Timmins P, Ambrose CV, Ward MD, Ridgway F. Proliposomes: A novel solution to an old problem. Journal of Pharmaceutical Sciences. 1986;75(4):325-9.

77. Schaffazick SR, Guterres SS, Freitas LdL, Pohlmann AR. Physicochemical characterization and stability of the polymeric nanoparticle systems for drug administration. Química Nova. 2003;26(5):726-37.

78. Farr SJ, Kellaway IW, Carman-Meakin B. Assessing the potential of aerosol-generated liposomes from pressurised pack formulations. Journal of controlled release. 1987;5(2):119-27.

79. Rojanarat W, Changsan N, Tawithong E, Pinsuwan S, Chan H-K, Srichana T. Isoniazid proliposome powders for inhalation—preparation, characterization and cell culture studies. International journal of molecular sciences. 2011;12(7):4414-34.

80. Rojanarat W, Nakpheng T, Thawithong E, Yanyium N, Srichana T. Levofloxacin-proliposomes: opportunities for use in lung tuberculosis. Pharmaceutics. 2012;4(3):385-412.

81. King P, Lomovskaya O, Griffith DC, Burns JL, Dudley MN. In vitro pharmacodynamics of levofloxacin and other aerosolized antibiotics under multiple conditions relevant to chronic pulmonary infection in cystic fibrosis. Antimicrobial agents and chemotherapy. 2010;54(1):143-8.

82. Rastogi N, Goh KS, Bryskier A, Devallois A. In vitro activities of levofloxacin used alone and in combination with first- and second-line antituberculous drugs against Mycobacterium tuberculosis. Antimicrobial agents and chemotherapy. 1996;40(7):1610-6.

83. Albasarah YY, Somavarapu S, Stapleton P, Taylor KM. Chitosan-coated antifungal formulations for nebulisation. Journal of Pharmacy and Pharmacology. 2010;62(7):821-8.

84. Malam Y, Loizidou M, Seifalian AM. Liposomes and nanoparticles: nanosized vehicles for drug delivery in cancer. Trends in pharmacological sciences. 2009;30(11):592-9.

85. Wissing S, Kayser O, Müller R. Solid lipid nanoparticles for parenteral drug delivery. Advanced drug delivery reviews. 2004;56(9):1257-72.

86. Park JM, Ahn BN, Yoon EJ, Lee MG, Shim CK, Kim CK. The pharmacokinetics of methotrexate after intravenous administration of methotrexate-loaded proliposomes to rats. Biopharmaceutics & drug disposition. 1994;15(5):391-407.

87. Srinath P, Chary M, Vyas S, Diwan P. Long-circulating liposomes of indomethacin in arthritic rats—a biodisposition study. Pharmaceutica Acta Helvetiae. 2000;74(4):399-404.

88. Liua Q, Sua Q, Luoa G, Wanga Y, Zanga Q. Pharmacokinetics and tissue distribution of carboplatin liposomes after intravenous administration to mice. Asian J Pharm Sci. 2006;1(3-4):159-67.

89. Zhao L, Xiong H, Peng H, Wang Q, Han D, Bai C, et al. PEG-coated lyophilized proliposomes: preparation, characterizations and in vitro release evaluation of vitamin E. European Food Research and Technology. 2011;232(4):647-54.

90. Selek H, Sahin S, Kas HS, Hincal AA, Ponchel G, Ercan MT, et al. Formulation and characterization of formaldehyde cross-linked degradable starch microspheres containing terbutaline sulfate. Drug development and industrial pharmacy. 2007;33(2):147-54.

91. Lu Y, Li J, Wang G. In vitro and in vivo evaluation of mPEG-PLA modified liposomes loaded glycyrrhetinic acid. International journal of pharmaceutics. 2008;356(1):274-81.

92. Azevedo CMG, Afonso CMM, Sousa D, Lima RT, Helena Vasconcelos M, Pedro M, et al. Multidimensional optimization of promising antitumor xanthone derivatives. Bioorganic & Medicinal Chemistry. 2013;21(11):2941-59.

93. Goncalves AP, Silva N, Oliveira C, Kowbel DJ, Glass NL, Kijjoa A, et al. Transcription profiling of the Neurospora crassa response to a group of synthetic (thio)xanthones and a natural acetophenone. Genom Data. 2015;4:26-32.

94. Pinto MM, Sousa ME, Nascimento MS. Xanthone derivatives: new insights in biological activities. Current medicinal chemistry. 2005;12(21):2517-38.

95. Nicolaou K, Pfefferkorn J, Roecker A, Cao G-Q, Barluenga S, Mitchell H. Natural product-like combinatorial libraries based on privileged structures. 1. General principles and solid-phase synthesis of benzopyrans. Journal of the American Chemical Society. 2000;122(41):9939-53.

96. Na Y. Recent cancer drug development with xanthone structures. The Journal of pharmacy and pharmacology. 2009;61(6):707-12.

97. Li X-Y, Zhao Y, Sun M-G, Shi J-F, Ju R-J, Zhang C-X, et al. Multifunctional liposomes loaded with paclitaxel and artemether for treatment of invasive brain glioma. Biomaterials. 2014;35(21):5591-604.

98. Wrensch M, Minn Y, Chew T, Bondy M, Berger MS. Epidemiology of primary brain tumors: current concepts and review of the literature. Neuro-oncology. 2002;4(4):278-99.

99. Weil RJ, Palmieri DC, Bronder JL, Stark AM, Steeg PS. Breast cancer metastasis to the central nervous system. The American journal of pathology. 2005;167(4):913-20.

100. Agarwal S, Sane R, Oberoi R, Ohlfest JR, Elmquist WF. Delivery of molecularly targeted therapy to malignant glioma, a disease of the whole brain. Expert reviews in molecular medicine. 2011;13:e17.

101. Yan H, Wang L, Wang J, Weng X, Lei H, Wang X, et al. Two-order targeted brain tumor imaging by using an optical/paramagnetic nanoprobe across the blood brain barrier. ACS nano. 2012;6(1):410-20.

102. MacKay JA, Deen DF, Szoka FC, Jr. Distribution in brain of liposomes after convection enhanced delivery; modulation by particle charge, particle diameter, and presence of steric coating. Brain research. 2005;1035(2):139-53.

103. Saltzman WM, Mak MW, Mahoney MJ, Duenas ET, Cleland JL. Intracranial delivery of recombinant nerve growth factor: release kinetics and protein distribution for three delivery systems. Pharmaceutical research. 1999;16(2):232-40.

104. Wolburg H, Noell S, Fallier-Becker P, Mack AF, Wolburg-Buchholz K. The disturbed blood-brain barrier in human glioblastoma. Molecular aspects of medicine. 2012;33(5-6):579-89.

105. Moreira A. Development of proliposomes as a vehicle to deliver new molecules with antitumor activity. Faculty of Pharmacy: University of Porto 2015.

106. Silva Moreira G. Desenvolvimento de prolipossomas com paclitaxel: uma nova abordagem na terapia do cancro. Faculty of Pharmacy: University of Porto; 2015.

107. Geng F, Chai H, Ma L, Luo G, Li Y, Yuan Z. Simulation of dynamic transport of flexible ribbon particles in a rotary dryer. Powder Technology. 2016;297:115-25.

108. Shaji J, Bhatia V. Proliposomes: a brief overview of novel delivery system.

109. Fristsche; C. Operation Manual Nano Spray Dryer B-90. Switzerland2009.

110. Fritsche C. Spray Drier B-902009 16 November.

111. Xia Fei, Hu Daode, Jin Heyang, Zhao Yaping, Liang Jiamiao. Preparation of lutein proliposomes by supercritical anti-solvent technique. Food Hydrocolloids. 2012;26(2):456-63.

112. Berne BJ, Pecora R. Dynamic light scattering: with applications to chemistry, biology, and physics: Courier Corporation; 1976.

113. Son Kyonghee, Alkan Hayat. Liposomes prepared dynamically by interactions between bile salt and phospholipid molecules. Biochimica et Biophysica Acta (BBA)-Biomembranes. 1989;981(2):288-94.

114. Nagel Norbert E, Cevc Gregor, Kirchner Stephan. The mechanism of the solute-induced chain interdigitation in phosphatidylcholine vesicles and characterization of the isothermal phase transitions by means of dynamic light scattering. Biochimica et Biophysica Acta (BBA)-Biomembranes. 1992;1111(2):263-9.

115. Jones M. Dynamic light scattering: Malvern; 2017 [accessed on 21 July 2017]. Available from: https://www.malvern.com/en/products/technology/dynamic-light-scattering/?gclid=EAIaIQobChMIjsKx9L221gIVRxwbCh2PPAzAEAAYASAAEgJ77fD_BwE.

116. Luykx DM, Peters RJ, van Ruth SM, Bouwmeester H. A review of analytical methods for the identification and characterization of nano delivery systems in food. Journal of agricultural and food chemistry. 2008;56(18):8231-47.

117. Fei Xiong, Chen Xiong, Liang Ge, Yue-Jian Chen, Hao Wang, Ning Gu, et al. Preparation, characterization, and biodistribution of breviscapine proliposomes in heart. Journal of drug targeting. 2009;17(5):408-14.

118. Shah N. M, Parikh J, Namdeo A, Subramhnian N, Bhowmick S. Preparation, characterization and in vivo studies of proliposomes containing Cyclosporine A. Journal of nanoscience and nanotechnology. 2006;6(9-10):2967-73.

119. Keller BC. Liposomes in nutrition. Trends in Food Science & Technology. 2001;12(1):25-31.

120. Maherani B, Arab-Tehrany E, R Mozafari M, Gaiani C, Linder M. Liposomes: a review of manufacturing techniques and targeting strategies. Current Nanoscience. 2011;7(3):436-52.

121. Mozafari MR. Liposomes: an overview of manufacturing techniques. Cellular and Molecular Biology Letters. 2005;10(4):711.

122. Hunter RJ. Zeta potential in colloid science: principles and applications: Academic press; 2013.

123. Revil A, Pezard P, Glover P. Streaming potential in porous media: 1. Theory of the zeta potential. Journal of Geophysical Research: Solid Earth. 1999;104(B9):20021-31.

124. An C, Huang G, Yao Y, Zhao S. Emerging usage of electrocoagulation technology for oil removal from wastewater: A review. Science of The Total Environment. 2017;579(Supplement C):537-56.

125. Validation of Analytical Procedures: Text and Methodology Q2(R1) in ICH Harmonized Tripartite Guideline., (2005).

126. Validation of Chromatographic Methods, (1994).

127. Ahammed V, Narayan R, Paul J, Nayak Y, Roy B, Shavi GV, et al. Development and in vivo evaluation of functionalized ritonavir proliposomes for lymphatic targeting. Life Sciences. 2017;183:11-20.

128. Yang Y, Lu X, Liu Q, Dai Y, Zhu X, Wen Y, et al. Palmitoyl ascorbate and doxorubicin co-encapsulated liposome for synergistic anticancer therapy. European Journal of Pharmaceutical Sciences. 2017;105:219-29.

129. Davidsen J, Rosenkrands I, Christensen D, Vangala A, Kirby D, Perrie Y, et al. Characterization of cationic liposomes based on dimethyldioctadecylammonium and synthetic cord factor from M. tuberculosis (trehalose 6,6'-dibehenate)—A novel adjuvant inducing both strong CMI and antibody responses. Biochimica et Biophysica Acta (BBA) - Biomembranes. 2005;1718(1–2):22-31.

130. Gill P, Moghadam TT, Ranjbar B. Differential scanning calorimetry techniques: applications in biology and nanoscience. Journal of biomolecular techniques: JBT. 2010;21(4):167.

131. Rojanarat W, Changsan N, Tawithong E, Pinsuwan S, Chan HK, Srichana T. Isoniazid proliposome powders for inhalation-preparation, characterization and cell culture studies. Int J Mol Sci. 2011;12(7):4414-34.

7 Appendices

Appendix I – Statistical results characterization of liposomes formed by hydration of proliposomes at the day of production.

Size

Tests of Normality

	Type	Kolmogorov–Smirnov[a]			Shapiro–Wilk		
		Statistic	df	Sig.	Statistic	df	Sig.
Size	1	,248	3	.	,969	3	,659
	2	,272	3	.	,947	3	,556

a. Lilliefors Significance Correction

Independent Samples Test

		Levene's Test for Equality of Variances		t-test for Equality of Means					95% Confidence Interval of the Difference	
		F	Sig.	t	df	Sig. (2–tailed)	Mean Difference	Std. Error Difference	Lower	Upper
Size	Equal variances assumed	6,004	,070	−1,574	4	,191	−50,13333	31,84731	−138,55564	38,28897
	Equal variances not assumed			−1,574	2,061	,252	−50,13333	31,84731	−183,32506	83,05840

ZP

Tests of Normality

	Type	Kolmogorov–Smirnov[a]			Shapiro–Wilk		
		Statistic	df	Sig.	Statistic	df	Sig.
Size	1	,202	3	.	,994	3	,852
	2	,249	3	.	,968	3	,655

a. Lilliefors Significance Correction

Independent Samples Test

		Levene's Test for Equality of Variances		t-test for Equality of Means					95% Confidence Interval of the Difference	
		F	Sig.	t	df	Sig. (2–tailed)	Mean Difference	Std. Error Difference	Lower	Upper
Size	Equal variances assumed	4,406	,104	−1,891	4	,132	−7,88667	4,17048	−19,46577	3,69244
	Equal variances not assumed			−1,891	2,187	,188	−7,88667	4,17048	−24,43543	8,66210

Appendix II – Statistical results characterization of liposomes at the day of production.

Size

Tests of Normality

	Type	Kolmogorov–Smirnov[a]			Shapiro–Wilk		
		Statistic	df	Sig.	Statistic	df	Sig.
Size	1	,330	3	.	,866	3	,285
	2	,217	3	.	,988	3	,791

a. Lilliefors Significance Correction

Independent Samples Test

		Levene's Test for Equality of Variances		t-test for Equality of Means					95% Confidence Interval of the Difference	
		F	Sig.	t	df	Sig. (2–tailed)	Mean Difference	Std. Error Difference	Lower	Upper
Size	Equal variances assumed	12,503	,024	3,519	4	,024	135,40000	38,47976	28,56305	242,23695
	Equal variances not assumed			3,519	2,004	,072	135,40000	38,47976	−29,84695	300,64695

ZP

Tests of Normality

	Type	Kolmogorov–Smirnov[a]			Shapiro–Wilk		
		Statistic	df	Sig.	Statistic	df	Sig.
Size	1	,222	3	.	,986	3	,770
	2	,350	3	.	,830	3	,187

a. Lilliefors Significance Correction

Independent Samples Test

		Levene's Test for Equality of Variances		t-test for Equality of Means					95% Confidence Interval of the Difference	
		F	Sig.	t	df	Sig. (2-tailed)	Mean Difference	Std. Error Difference	Lower	Upper
Size	Equal variances assumed	3,031	,157	−3,626	4	,022	−18,24667	5,03286	−32,22012	−4,27322
	Equal variances not assumed			−3,626	2,270	,056	−18,24667	5,03286	−37,61266	1,11933

Appendix III – Statistical results characterization of liposomes formed by hydration of proliposomes after 15 days of production.

Size

Tests of Normality

	Type	Kolmogorov–Smirnov[a]			Shapiro–Wilk		
		Statistic	df	Sig.	Statistic	df	Sig.
Size	1	,282	3	.	,935	3	,509
	2	,335	3	.	,857	3	,260

a. Lilliefors Significance Correction

Independent Samples Test

		Levene's Test for Equality of Variances		t-test for Equality of Means					95% Confidence Interval of the Difference	
		F	Sig.	t	df	Sig. (2-tailed)	Mean Difference	Std. Error Difference	Lower	Upper
Size	Equal variances assumed	1,200	,335	,437	4	,685	11,00000	25,16894	−58,88018	80,88018
	Equal variances not assumed			,437	3,234	,690	11,00000	25,16894	−65,91650	87,91650

ZP

Tests of Normality

	Type	Kolmogorov–Smirnov[a]			Shapiro–Wilk		
		Statistic	df	Sig.	Statistic	df	Sig.
Size	1	,186	3	.	,998	3	,919
	2	,254	3	.	,964	3	,633

a. Lilliefors Significance Correction

Independent Samples Test

		Levene's Test for Equality of Variances		t-test for Equality of Means					95% Confidence Interval of the Difference	
		F	Sig.	t	df	Sig. (2-tailed)	Mean Difference	Std. Error Difference	Lower	Upper
Size	Equal variances assumed	,356	,583	1,344	4	,250	5,33333	3,96811	−5,68390	16,35057
	Equal variances not assumed			1,344	3,413	,261	5,33333	3,96811	−6,47245	17,13912

Appendix IV– Statistical results characterization of liposomes formed by hydration of proliposomes after 1 month of production.

Size

Tests of Normality

	Type	Kolmogorov–Smirnov[a]			Shapiro–Wilk		
		Statistic	df	Sig.	Statistic	df	Sig.
Size	1	,271	3	.	,947	3	,557
	2	,257	3	.	,960	3	,618

a. Lilliefors Significance Correction

Independent Samples Test

		Levene's Test for Equality of Variances		t-test for Equality of Means					95% Confidence Interval of the Difference	
		F	Sig.	t	df	Sig. (2-tailed)	Mean Difference	Std. Error Difference	Lower	Upper
Size	Equal variances assumed	6,004	,070	-1,574	4	,191	-50,13333	31,84731	-138,55564	38,28897
	Equal variances not assumed			-1,574	2,061	,252	-50,13333	31,84731	-183,32506	83,05840

ZP

Tests of Normality

		Kolmogorov-Smirnov[a]			Shapiro-Wilk		
	Type	Statistic	df	Sig.	Statistic	df	Sig.
Size	1	,260	3	.	,958	3	,607
	2	,222	3	.	,986	3	,771

a. Lilliefors Significance Correction

Independent Samples Test

		Levene's Test for Equality of Variances		t-test for Equality of Means					95% Confidence Interval of the Difference	
		F	Sig.	t	df	Sig. (2-tailed)	Mean Difference	Std. Error Difference	Lower	Upper
Size	Equal variances assumed	3,538	,133	-1,825	4	,142	-11,47333	6,28727	-28,92959	5,98292
	Equal variances not assumed			-1,825	2,184	,199	-11,47333	6,28727	-36,45066	13,50400

Appendix V– Statistical results characterization of liposomes formed by hydration of proliposomes after 3 month of production.

Size

Tests of Normality

		Kolmogorov-Smirnov[a]			Shapiro-Wilk		
	Type	Statistic	df	Sig.	Statistic	df	Sig.
Size	1	,295	3	.	,920	3	,452
	2	,348	3	.	,834	3	,198

a. Lilliefors Significance Correction

Independent Samples Test

		Levene's Test for Equality of Variances		t-test for Equality of Means					95% Confidence Interval of the Difference	
		F	Sig.	t	df	Sig. (2-tailed)	Mean Difference	Std. Error Difference	Lower	Upper
Size	Equal variances assumed	1,336	,312	-,409	4	,704	-17,76667	43,44378	-138,38594	102,85261
	Equal variances not assumed			-,409	3,399	,707	-17,76667	43,44378	-147,28016	111,74683

ZP

Tests of Normality

		Kolmogorov-Smirnov[a]			Shapiro-Wilk		
	Type	Statistic	df	Sig.	Statistic	df	Sig.
Size	1	,382	3	.	,757	3	,017
	2	,277	3	.	,941	3	,532

a. Lilliefors Significance Correction

Independent Samples Test

		Levene's Test for Equality of Variances		t-test for Equality of Means					95% Confidence Interval of the Difference	
		F	Sig.	t	df	Sig. (2-tailed)	Mean Difference	Std. Error Difference	Lower	Upper
Size	Equal variances assumed	5,387	,081	-1,347	4	,249	-10,49000	7,79046	-32,11978	11,13978
	Equal variances not assumed			-1,347	2,545	,285	-10,49000	7,79046	-37,99126	17,01126

Appendix VI– DLS graphics related to the size of proliposomes and liposomes.

Lipo_vazio_lote1 (Combined)
Dec 22, 2016   09:41:12

Effective Diameter:	139.8 nm
Polydispersity:	0.332
Avg. Count Rate:	464.4 kcps
Baseline Index:	2.0/ 98.63%
Elapsed Time:	00:12:00
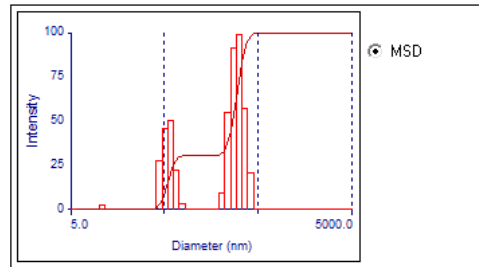
Run	Eff. Diam. (nm)	Half Width (nm)	Polydispersity	Baseline Index
1	139.3	79.6	0.326	1.2/100.00%
2	145.1	85.8	0.350	6.1/100.00%
3	139.0	80.6	0.336	0.6/100.00%
4	140.3	78.6	0.314	0.0/ 96.88%
5	137.0	79.7	0.338	2.5/ 96.88%
6	138.4	79.5	0.330	1.8/ 98.00%
Mean	139.8	80.6	0.332	2.0/ 98.63%
Std. Error	1.1	1.1	0.005	0.9/ 0.64
Combined	139.8	80.5	0.332	2.0/ 98.63%

Lipo_vazio_lote1 (Combined)
Dec 22, 2016   10:02:25

Effective Diameter:	120.8 nm
Polydispersity:	0.328
Avg. Count Rate:	429.6 kcps
Baseline Index:	6.7/ 99.11%
Elapsed Time:	00:12:00
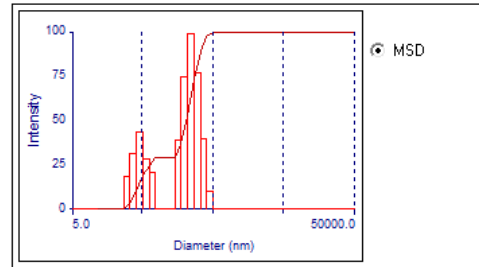
Run	Eff. Diam. (nm)	Half Width (nm)	Polydispersity	Baseline Index
1	119.5	68.7	0.330	7.7/ 97.77%
2	119.2	68.4	0.330	5.0/ 98.89%
3	118.9	67.8	0.326	7.1/100.00%
4	124.2	71.4	0.331	6.6/100.00%
5	121.0	68.8	0.323	5.2/ 98.00%
6	121.0	69.9	0.334	7.4/100.00%
Mean	120.6	69.2	0.329	6.5/ 99.11%
Std. Error	0.8	0.5	0.002	0.5/ 0.43
Combined	120.8	69.2	0.328	6.7/ 99.11%

Lipo_vazio_lote3 (Combined)
Dec 22, 2016   10:24:20

Effective Diameter:	120.3 nm
Polydispersity:	0.339
Avg. Count Rate:	482.4 kcps
Baseline Index:	4.1/ 97.63%
Elapsed Time:	00:12:00
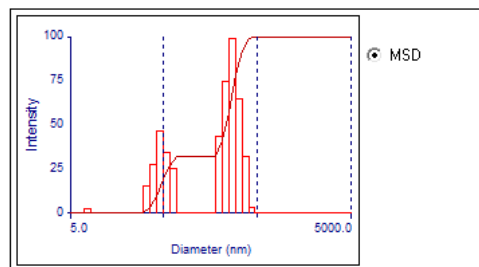
Run	Eff. Diam. (nm)	Half Width (nm)	Polydispersity	Baseline Index
1	118.4	68.5	0.335	6.3/100.00%
2	119.3	69.5	0.340	3.4/ 98.89%
3	120.9	71.8	0.353	6.0/ 96.67%
4	123.9	71.2	0.330	4.5/ 96.88%
5	119.8	69.4	0.335	1.0/ 95.55%
6	119.1	69.6	0.342	2.6/ 97.77%
Mean	120.3	70.0	0.339	4.0/ 97.63%
Std. Error	0.8	0.5	0.003	0.8/ 0.66
Combined	120.3	70.0	0.339	4.1/ 97.63%

proLipo_ lote 2 (Combined)
Jan 25, 2017   05:01:31

Effective Diameter: 200.9 nm
Polydispersity: 0.273

Avg. Count Rate: 483.9 kcps
Baseline Index: 6.2/ 98.70%

Elapsed Time: 00:12:00
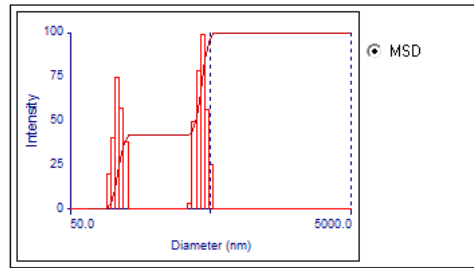
Run	Eff. Diam. (nm)	Half Width (nm)	Polydispersity	Baseline Index
1	204.8	107.8	0.277	8.6/ 98.89%
2	201.6	104.1	0.267	5.0/100.00%
3	202.8	108.7	0.288	6.1/ 99.11%
4	192.1	93.4	0.237	0.0/ 95.33%
5	202.3	107.8	0.284	9.7/100.00%
6	201.5	106.8	0.281	7.5/ 98.89%
Mean	200.8	104.8	0.272	6.1/ 98.70%
Std. Error	1.8	2.4	0.008	1.4/ 0.71
Combined	200.9	105.0	0.273	6.2/ 98.70%

proLipo_1 lio (Combined)
Jan 30, 2017   10:06:55

Effective Diameter: 178.5 nm
Polydispersity: 0.324

Avg. Count Rate: 402.3 kcps
Baseline Index: 1.7/ 98.40%

Elapsed Time: 00:12:00
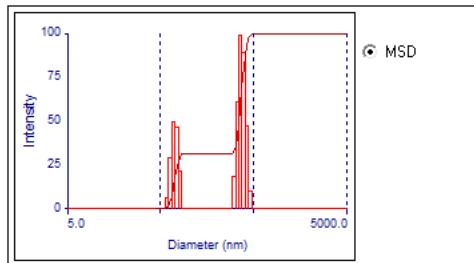
Run	Eff. Diam. (nm)	Half Width (nm)	Polydispersity	Baseline Index
1	195.4	110.6	0.320	5.7/ 98.89%
2	183.0	101.2	0.306	2.5/ 97.77%
3	181.0	100.1	0.306	0.9/ 97.77%
4	173.4	100.6	0.336	0.0/ 98.88%
5	168.6	97.3	0.333	2.6/ 99.11%
6	175.9	102.4	0.339	4.7/ 97.99%
Mean	179.6	102.0	0.323	2.7/ 98.40%
Std. Error	3.8	1.9	0.006	0.9/ 0.25
Combined	178.5	101.6	0.324	1.7/ 98.40%

proLipo_1 vazio atomizador (Combined)
Jan 30, 2017   10:39:13

Effective Diameter: 121.5 nm
Polydispersity: 0.281

Avg. Count Rate: 32.4 kcps
Baseline Index: 0.0/ 99.25%

Elapsed Time: 00:12:00
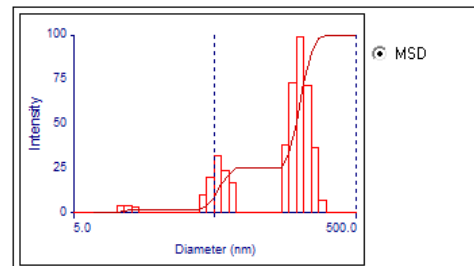
Run	Eff. Diam. (nm)	Half Width (nm)	Polydispersity	Baseline Index
1	206.4	112.7	0.298	0.0/ 98.96%
2	156.0	70.1	0.202	0.0/100.00%
3	130.1	70.3	0.292	0.0/ 98.78%
4	117.1	62.5	0.285	6.5/ 98.78%
5	111.0	61.0	0.302	5.5/100.00%
6	112.6	59.3	0.278	5.5/ 98.95%
Mean	138.9	72.6	0.276	2.9/ 99.25%
Std. Error	15.1	8.2	0.015	1.3/ 0.24
Combined	121.5	64.4	0.281	0.0/ 99.25%

ProLipo_lote 2 vazio (nano) (Combined)
Feb 2, 2017   14:11:08

Effective Diameter:	**169.5 nm**
Polydispersity:	**0.231**
Avg. Count Rate:	**360.5 kcps**
Baseline Index:	**4.5/ 97.28%**
Elapsed Time:	**00:12:00**
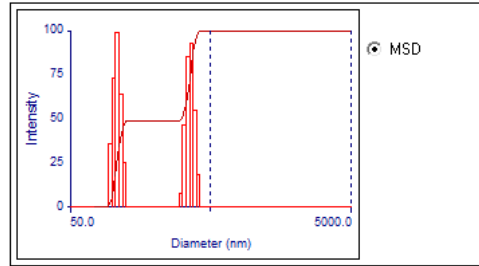
Run	Eff. Diam. (nm)	Half Width (nm)	Polydispersity	Baseline Index
1	165.6	77.7	0.220	4.4/ 96.87%
2	170.4	84.9	0.248	8.4/ 97.76%
3	169.4	81.3	0.230	3.9/ 97.76%
4	169.6	81.8	0.232	5.3/ 96.64%
5	170.1	81.7	0.231	3.4/ 95.75%
6	171.3	82.1	0.230	2.8/ 98.88%
Mean	169.4	81.6	0.232	4.7/ 97.28%
Std. Error	0.8	0.9	0.004	0.8/ 0.45
Combined	169.5	81.5	0.231	4.5/ 97.28%

lipo_vazio1 nano(estab) (Combined)
Feb 8, 2017   10:03:13

Effective Diameter:	**195.4 nm**
Polydispersity:	**0.260**
Avg. Count Rate:	**395.7 kcps**
Baseline Index:	**7.5/ 98.03%**
Elapsed Time:	**00:12:00**
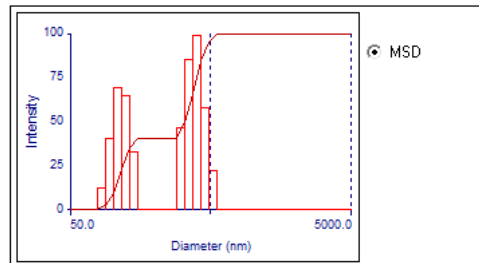
Run	Eff. Diam. (nm)	Half Width (nm)	Polydispersity	Baseline Index
1	202.2	108.3	0.287	9.8/ 97.99%
2	196.7	103.9	0.279	7.0/ 95.76%
3	194.3	98.7	0.258	5.9/ 98.88%
4	194.6	100.6	0.267	7.9/ 96.65%
5	195.7	92.3	0.222	7.2/100.00%
6	189.6	96.1	0.257	8.5/ 98.88%
Mean	195.5	100.0	0.262	7.7/ 98.03%
Std. Error	1.7	2.3	0.009	0.5/ 0.64
Combined	195.4	99.7	0.260	7.5/ 98.03%

lipo_farmaco_1_nano (Combined)
Feb 8, 2017   12:04:46

Effective Diameter:	**154.0 nm**
Polydispersity:	**0.298**
Avg. Count Rate:	**524.1 kcps**
Baseline Index:	**6.8/ 95.60%**
Elapsed Time:	**00:12:00**
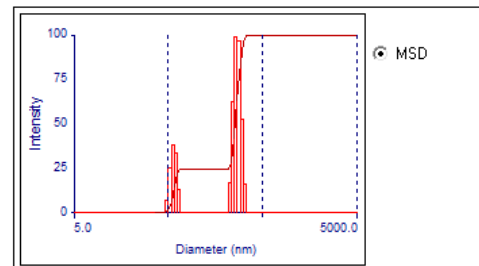
Run	Eff. Diam. (nm)	Half Width (nm)	Polydispersity	Baseline Index
1	132.6	77.5	0.341	7.0/ 95.56%
2	151.3	80.6	0.284	3.4/ 95.57%
3	165.4	82.4	0.248	8.9/ 96.67%
4	166.5	88.9	0.285	7.7/ 96.90%
5	169.0	89.5	0.281	6.5/ 95.57%
6	162.4	81.8	0.254	9.4/ 93.33%
Mean	157.9	83.5	0.282	7.1/ 95.60%
Std. Error	5.6	1.9	0.014	0.9/ 0.52
Combined	154.0	84.0	0.298	6.8/ 95.60%

lipo_farmaco_1_lio (Combined)
Feb 9, 2017   18:14:37

Effective Diameter:	**231.3 nm**
Polydispersity:	**0.252**
Avg. Count Rate:	**367.2 kcps**
Baseline Index:	**1.3/ 97.02%**
Elapsed Time:	**00:12:00**
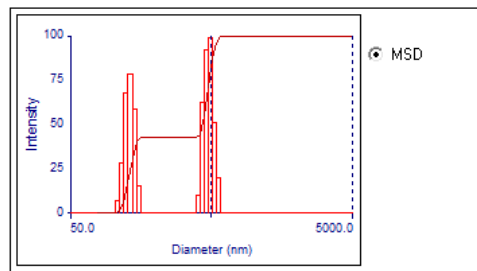
Run	Eff. Diam. (nm)	Half Width (nm)	Polydispersity	Baseline Index
1	228.7	117.9	0.266	0.0/ 92.19%
2	229.6	118.6	0.267	2.8/ 97.54%
3	228.6	113.2	0.245	9.5/ 98.88%
4	232.3	117.0	0.254	8.3/100.00%
5	233.4	110.9	0.226	3.2/ 97.99%
6	235.2	118.8	0.255	0.0/ 95.53%
Mean	231.3	116.1	0.252	4.0/ 97.02%
Std. Error	1.1	1.3	0.006	1.7/ 1.14
Combined	231.3	116.2	0.252	1.3/ 97.02%

Prolipo_vazio 2 (liofiliz) (Combined)
Feb 16, 2017   14:45:18

Effective Diameter:	**217.4 nm**
Polydispersity:	**0.311**
Avg. Count Rate:	**513.0 kcps**
Baseline Index:	**6.7/ 97.78%**
Elapsed Time:	**00:12:00**
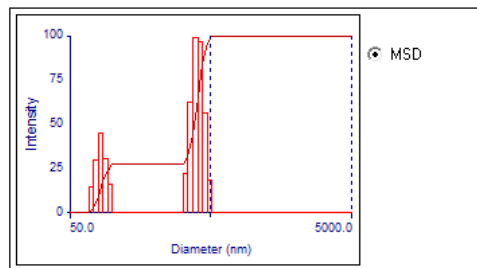
Run	Eff. Diam. (nm)	Half Width (nm)	Polydispersity	Baseline Index
1	203.4	111.8	0.302	7.5/ 95.56%
2	208.5	121.3	0.339	9.4/ 97.78%
3	218.1	119.3	0.299	6.3/ 98.67%
4	227.1	124.3	0.300	6.0/ 98.00%
5	225.2	123.6	0.301	5.3/100.00%
6	224.6	124.5	0.307	7.1/ 96.67%
Mean	217.8	120.8	0.308	6.9/ 97.78%
Std. Error	4.0	2.0	0.006	0.6/ 0.63
Combined	217.4	121.3	0.311	6.7/ 97.78%

Prolipo_com farmaco2 (latomi) (Combined)
Feb 16, 2017   15:10:27

Effective Diameter:	**185.0 nm**
Polydispersity:	**0.205**
Avg. Count Rate:	**386.3 kcps**
Baseline Index:	**9.1/ 98.32%**
Elapsed Time:	**00:12:00**
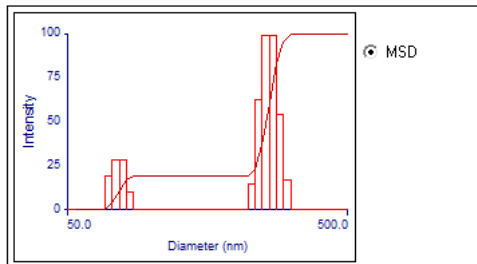
Run	Eff. Diam. (nm)	Half Width (nm)	Polydispersity	Baseline Index
1	170.6	81.8	0.230	7.2/ 96.65%
2	181.8	84.1	0.214	9.8/ 97.76%
3	188.6	81.4	0.186	8.6/ 98.88%
4	185.9	79.1	0.181	9.4/ 98.88%
5	189.7	87.3	0.212	8.1/ 97.76%
6	192.5	89.0	0.214	8.1/100.00%
Mean	184.9	83.8	0.206	8.5/ 98.32%
Std. Error	3.2	1.5	0.008	0.4/ 0.48
Combined	185.0	83.8	0.205	9.1/ 98.32%

Prolipo_farmaco_2(liof) (Combined)
Feb 16, 2017   15:41:32

Effective Diameter:	202.4 nm
Polydispersity:	0.278
Avg. Count Rate:	349.3 kcps
Baseline Index:	6.8/ 99.48%
Elapsed Time:	00:12:00
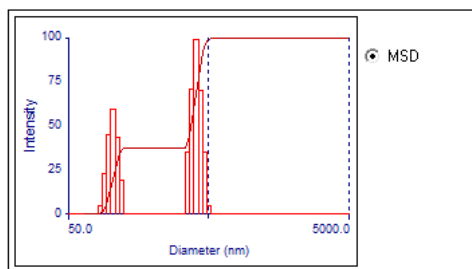
Run	Eff. Diam. (nm)	Half Width (nm)	Polydispersity	Baseline Index
1	196.2	103.4	0.278	5.3/100.00%
2	207.4	106.9	0.266	7.5/ 98.88%
3	208.5	106.1	0.259	8.0/100.00%
4	206.0	109.0	0.280	7.6/100.00%
5	197.4	106.4	0.291	7.9/ 99.11%
6	199.4	108.6	0.297	6.9/ 98.88%
Mean	202.5	106.7	0.278	7.2/ 99.48%
Std. Error	2.2	0.8	0.006	0.4/ 0.24
Combined	202.4	106.7	0.278	6.8/ 99.48%

Prolipo_vazio_2(atomizador) (Combined)
Feb 16, 2017   16:04:11

Effective Diameter:	176.1 nm
Polydispersity:	0.250
Avg. Count Rate:	480.5 kcps
Baseline Index:	1.3/ 98.04%
Elapsed Time:	00:12:00
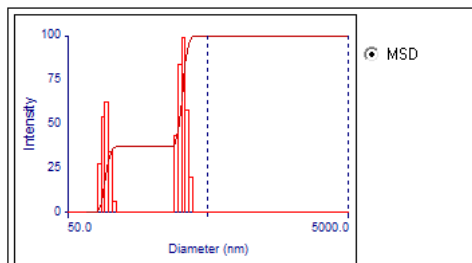
Run	Eff. Diam. (nm)	Half Width (nm)	Polydispersity	Baseline Index
1	168.4	83.0	0.243	6.4/ 98.89%
2	175.4	84.2	0.231	5.5/ 98.88%
3	179.2	85.4	0.227	9.3/ 98.89%
4	177.1	90.4	0.261	5.9/ 96.89%
5	177.9	93.4	0.276	7.6/ 96.90%
6	176.3	88.9	0.254	9.0/ 97.78%
Mean	175.7	87.6	0.249	7.3/ 98.04%
Std. Error	1.6	1.6	0.008	0.7/ 0.40
Combined	176.1	88.0	0.250	1.3/ 98.04%

prolipo_farmaco_lote1 (atomi) (Combined)
Feb 22, 2017   10:04:04

Effective Diameter:	151.0 nm
Polydispersity:	0.316
Avg. Count Rate:	426.2 kcps
Baseline Index:	5.8/ 98.77%
Elapsed Time:	00:12:00
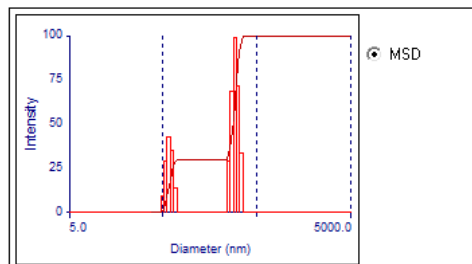
Run	Eff. Diam. (nm)	Half Width (nm)	Polydispersity	Baseline Index
1	143.6	82.7	0.332	3.2/100.00%
2	147.0	83.1	0.320	3.8/100.00%
3	177.2	93.9	0.281	6.5/ 97.77%
4	156.7	86.1	0.302	4.7/100.00%
5	149.3	83.7	0.314	8.8/ 95.98%
6	141.4	79.1	0.313	6.5/ 98.88%
Mean	152.5	84.8	0.310	5.6/ 98.77%
Std. Error	5.4	2.0	0.007	0.9/ 0.67
Combined	151.0	84.8	0.316	5.8/ 98.77%

Prolipo_vazio lote1 (atomza) (Combined)
Feb 24, 2017   10:46:32

Effective Diameter: 170.0 nm
Polydispersity: 0.286

Avg. Count Rate: 486.0 kcps
Baseline Index: 5.3/ 96.63%

Elapsed Time: 00:12:00
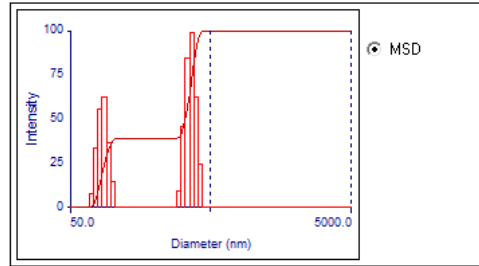
Run	Eff. Diam. (nm)	Half Width (nm)	Polydispersity	Baseline Index
1	153.3	83.4	0.296	6.5/ 93.54%
2	166.5	88.8	0.284	5.6/100.00%
3	173.3	91.0	0.276	5.5/ 98.00%
4	175.6	92.9	0.280	5.8/ 97.11%
5	177.2	93.7	0.280	5.5/ 94.44%
6	173.1	95.2	0.302	7.0/ 96.67%
Mean	169.8	90.8	0.286	6.0/ 96.63%
Std. Error	3.6	1.7	0.004	0.3/ 0.96
Combined	170.0	90.8	0.286	5.3/ 96.63%

Proli_farmaco_atomi_lote 2 (Combined)
Mar 1, 2017   10:45:41

Effective Diameter: 169.5 nm
Polydispersity: 0.273

Avg. Count Rate: 428.9 kcps
Baseline Index: 5.4/ 99.37%

Elapsed Time: 00:12:00
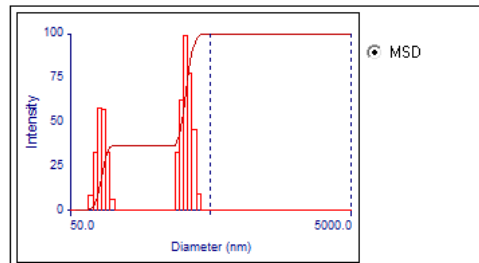
Run	Eff. Diam. (nm)	Half Width (nm)	Polydispersity	Baseline Index
1	177.0	92.1	0.271	6.9/100.00%
2	172.8	90.5	0.274	9.9/100.00%
3	169.3	89.3	0.278	4.6/ 98.88%
4	165.1	85.6	0.269	3.6/100.00%
5	164.5	84.1	0.262	5.5/ 97.33%
6	169.4	89.6	0.280	4.8/100.00%
Mean	169.7	88.5	0.272	5.9/ 99.37%
Std. Error	1.9	1.2	0.003	0.9/ 0.45
Combined	169.5	88.5	0.273	5.4/ 99.37%

Proli_vazio_atomi_lote 2 (Combined)
Mar 2, 2017   11:07:54

Effective Diameter: 172.5 nm
Polydispersity: 0.253

Avg. Count Rate: 358.8 kcps
Baseline Index: 7.1/ 95.86%

Elapsed Time: 00:12:00
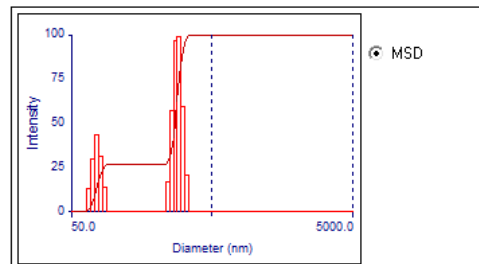
Run	Eff. Diam. (nm)	Half Width (nm)	Polydispersity	Baseline Index
1	165.2	79.4	0.231	7.0/ 97.76%
2	170.5	77.7	0.207	3.4/ 95.75%
3	175.4	89.7	0.261	9.1/ 95.75%
4	176.1	91.4	0.269	8.2/ 97.76%
5	175.9	95.8	0.297	8.9/ 89.26%
6	179.1	93.0	0.270	8.0/ 98.88%
Mean	173.7	87.8	0.256	7.4/ 95.86%
Std. Error	2.0	3.1	0.013	0.9/ 1.41
Combined	172.5	86.7	0.253	7.1/ 95.86%

Proli_farmaco_atomi_lote 3 (Combined)
Mar 2, 2017   11:29:21

Effective Diameter: 173.6 nm
Polydispersity: 0.264

Avg. Count Rate: 431.7 kcps
Baseline Index: 5.6/ 98.89%

Elapsed Time: 00:12:00
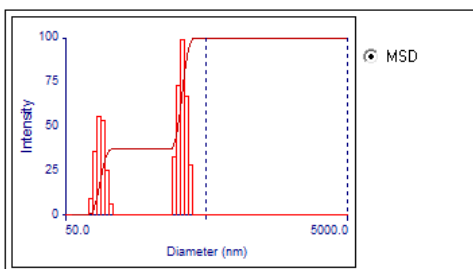
Run	Eff. Diam. (nm)	Half Width (nm)	Polydispersity	Baseline Index
1	169.1	86.1	0.259	5.8/ 98.89%
2	171.0	90.6	0.281	6.2/100.00%
3	172.5	91.1	0.279	7.2/ 98.66%
4	174.0	87.7	0.254	3.6/ 98.88%
5	178.5	90.2	0.256	4.3/ 98.89%
6	176.5	88.2	0.249	6.2/ 98.00%
Mean	173.6	89.0	0.263	5.6/ 98.89%
Std. Error	1.4	0.8	0.006	0.5/ 0.26
Combined	173.6	89.2	0.264	5.6/ 98.89%

prolipo_lote1_farmaco_atomiz (Combined)
Mar 8, 2017   10:41:25

Effective Diameter: 163.6 nm
Polydispersity: 0.223

Avg. Count Rate: 543.2 kcps
Baseline Index: 6.3/ 98.89%

Elapsed Time: 00:12:00
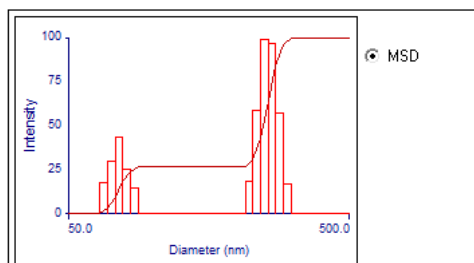
Run	Eff. Diam. (nm)	Half Width (nm)	Polydispersity	Baseline Index
1	158.7	76.6	0.233	8.4/ 96.67%
2	160.1	73.2	0.209	4.3/100.00%
3	164.8	78.5	0.227	7.1/ 97.78%
4	169.1	78.4	0.215	7.3/100.00%
5	165.9	83.1	0.251	8.3/ 98.89%
6	164.1	73.7	0.201	4.4/100.00%
Mean	163.8	77.2	0.223	6.6/ 98.89%
Std. Error	1.6	1.5	0.007	0.8/ 0.57
Combined	163.6	77.2	0.223	6.3/ 98.89%

Prolipo_3_vazio_atomi (Combined)
Mar 9, 2017   11:20:47

Effective Diameter: 229.0 nm
Polydispersity: 0.299

Avg. Count Rate: 475.6 kcps
Baseline Index: 1.7/ 96.74%

Elapsed Time: 00:12:00
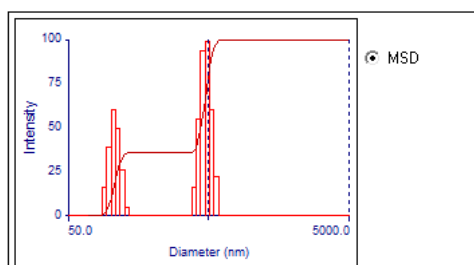
Run	Eff. Diam. (nm)	Half Width (nm)	Polydispersity	Baseline Index
1	204.2	106.7	0.273	0.0/ 95.54%
2	212.9	114.2	0.288	5.1/ 94.88%
3	232.8	129.1	0.308	5.0/ 95.56%
4	225.4	117.2	0.271	4.1/ 96.66%
5	253.2	141.7	0.313	1.3/ 98.89%
6	236.9	133.3	0.316	2.5/ 98.89%
Mean	227.6	123.7	0.295	3.0/ 96.73%
Std. Error	7.2	5.4	0.008	0.8/ 0.72
Combined	229.0	125.1	0.299	1.7/ 96.74%

Prolip:_3_vazio (atomiz) (Combined)
Mar 22, 2017   15:08:09

Effective Diameter: 237.5 nm
Polydispersity: 0.292

Avg. Count Rate: 537.9 kcps
Baseline Index: 0.0/ 99.26%

Elapsed Time: 00:12:00
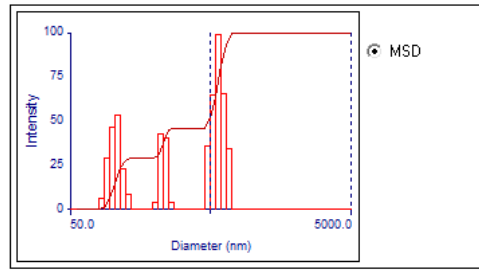
Run	Eff. Diam. (nm)	Half Width (nm)	Polydispersity	Baseline Index
1	213.0	106.0	0.248	4.7/100.00%
2	211.6	105.8	0.250	6.6/ 98.89%
3	414.7	233.2	0.316	0.0/ 98.89%
4	217.1	112.2	0.267	6.7/100.00%
5	215.9	103.2	0.228	2.6/100.00%
6	218.0	115.2	0.279	5.5/ 97.78%
Mean	248.4	129.3	0.265	4.4/ 99.26%
Std. Error	33.3	20.9	0.013	1.1/ 0.37
Combined	237.5	128.4	0.292	0.0/ 99.26%

Prolip:_1_XGA (atomizad) (Combined)
Mar 22, 2017   17:16:13

Effective Diameter: 181.1 nm
Polydispersity: 0.257

Avg. Count Rate: 498.7 kcps
Baseline Index: 8.4/ 98.33%

Elapsed Time: 00:12:00

Run	Eff. Diam. (nm)	Half Width (nm)	Polydispersity	Baseline Index
1	165.5	82.3	0.248	6.9/ 96.67%
2	181.2	92.2	0.259	6.7/ 95.57%
3	187.7	94.7	0.254	8.4/100.00%
4	185.1	94.2	0.259	9.5/ 98.89%
5	184.8	93.6	0.257	8.9/ 98.89%
6	188.4	95.7	0.258	9.1/100.00%
Mean	182.1	92.1	0.256	8.3/ 98.33%
Std. Error	3.5	2.0	0.002	0.5/ 0.74
Combined	181.1	91.8	0.257	8.4/ 98.33%

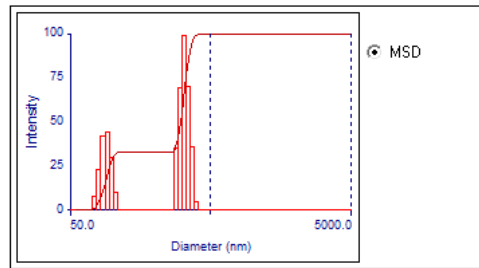**Prolipo_lote2_XGA_atomi (Combined)**
Apr 3, 2017   15:02:34

Effective Diameter: 223.1 nm
Polydispersity: 0.271

Avg. Count Rate: 483.3 kcps
Baseline Index: 3.6/ 96.04%

Elapsed Time: 00:12:00
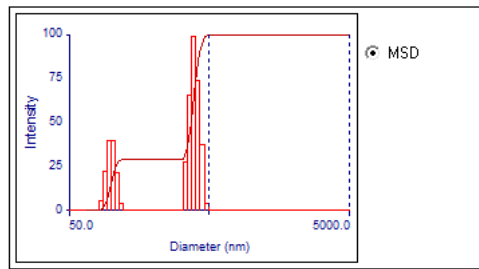
Run	Eff. Diam. (nm)	Half Width (nm)	Polydispersity	Baseline Index
1	210.3	105.2	0.250	0.0/ 93.33%
2	210.1	109.6	0.272	5.2/ 92.67%
3	223.2	118.9	0.284	4.5/ 93.56%
4	225.2	116.9	0.270	6.2/ 98.89%
5	230.2	117.1	0.259	3.0/ 98.89%
6	233.5	120.0	0.264	1.7/ 98.89%
Mean	222.1	114.6	0.266	3.4/ 96.04%
Std. Error	4.1	2.4	0.005	0.9/ 1.28
Combined	223.1	116.1	0.271	3.6/ 96.04%

Prolipo_1_XGA (atomizad) (Combined)
Apr 4, 2017   10:02:01

Effective Diameter: 219.4 nm
Polydispersity: 0.256

Avg. Count Rate: 484.5 kcps
Baseline Index: 5.2/ 96.89%

Elapsed Time: 00:12:00
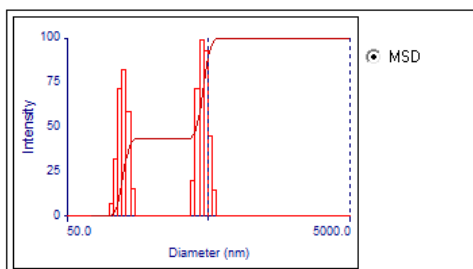
Run	Eff. Diam. (nm)	Half Width (nm)	Polydispersity	Baseline Index
1	214.4	104.9	0.239	2.8/ 96.44%
2	231.1	125.3	0.294	6.9/ 97.78%
3	216.1	105.8	0.240	8.2/ 98.89%
4	226.3	117.5	0.270	9.3/ 98.00%
5	225.2	116.2	0.266	1.4/ 93.56%
6	211.4	103.7	0.240	5.3/ 96.67%
Mean	220.8	112.2	0.258	5.7/ 96.89%
Std. Error	3.2	3.6	0.009	1.3/ 0.76
Combined	219.4	111.1	0.256	5.2/ 96.89%

Prolipo_XGA_3 (atomiz) (Combined)
Apr 5, 2017   11:30:11

Effective Diameter: 193.3 nm
Polydispersity: 0.249

Avg. Count Rate: 444.8 kcps
Baseline Index: 7.2/ 98.59%

Elapsed Time: 00:12:00

Run	Eff. Diam. (nm)	Half Width (nm)	Polydispersity	Baseline Index
1	187.9	100.3	0.285	6.9/ 98.89%
2	183.7	90.2	0.241	8.2/100.00%
3	193.0	95.5	0.245	7.2/ 99.11%
4	194.8	94.6	0.236	8.4/ 96.66%
5	199.8	95.5	0.228	8.5/ 96.88%
6	203.9	104.5	0.263	5.9/100.00%
Mean	193.9	96.8	0.250	7.5/ 98.59%
Std. Error	3.0	2.0	0.009	0.4/ 0.60
Combined	193.3	96.5	0.249	7.2/ 98.59%

Lipo_vazio1_ final (Combined)
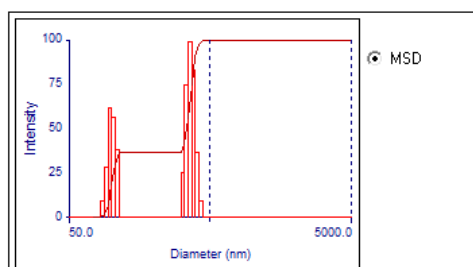Apr 12, 2017   13:01:21

Effective Diameter: 161.5 nm
Polydispersity: 0.115

Avg. Count Rate: 435.6 kcps
Baseline Index: 8.9/ 98.37%

Elapsed Time: 00:12:00
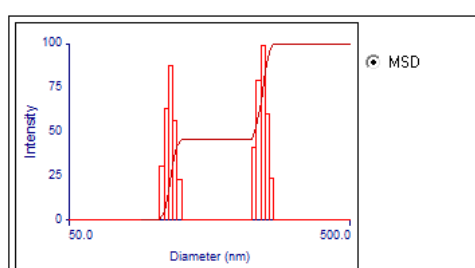
Run	Eff. Diam. (nm)	Half Width (nm)	Polydispersity	Baseline Index
1	144.7	42.8	0.087	9.2/100.00%
2	159.2	47.9	0.091	9.2/100.00%
3	162.7	45.3	0.077	8.9/ 93.54%
4	164.0	57.7	0.124	8.9/ 97.77%
5	167.7	60.8	0.132	5.7/ 98.89%
6	172.0	71.6	0.173	9.6/100.00%
Mean	161.7	54.3	0.114	8.6/ 98.37%
Std. Error	3.8	4.5	0.015	0.6/ 1.03
Combined	161.5	54.7	0.115	8.9/ 98.37%

Lipo_vazio2_ final (Combined)
Apr 12, 2017   13:22:41

Effective Diameter: 285.3 nm
Polydispersity: 0.235

Avg. Count Rate: 462.1 kcps
Baseline Index: 7.1/ 97.63%

Elapsed Time: 00:12:00
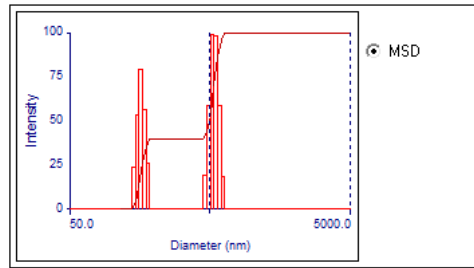
Run	Eff. Diam. (nm)	Half Width (nm)	Polydispersity	Baseline Index
1	259.7	131.4	0.256	5.1/ 97.77%
2	280.8	138.7	0.244	8.3/ 94.43%
3	284.0	132.1	0.216	4.0/100.00%
4	298.1	141.6	0.225	9.5/ 96.89%
5	289.6	145.6	0.253	6.1/ 97.77%
6	302.1	142.2	0.222	9.5/ 98.89%
Mean	285.7	138.6	0.236	7.1/ 97.63%
Std. Error	6.2	2.4	0.007	1.0/ 0.77
Combined	285.3	138.3	0.235	7.1/ 97.63%

Lipo_vazio3_ final (Combined)
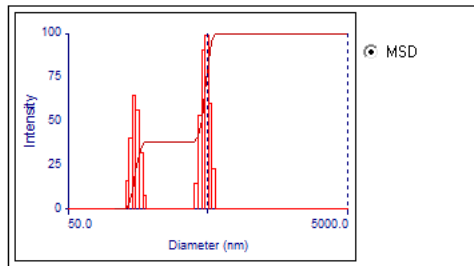Apr 12, 2017   14:30:27

Effective Diameter: 267.2 nm
Polydispersity: 0.230

Avg. Count Rate: 512.5 kcps
Baseline Index: 7.4/ 98.82%

Elapsed Time: 00:12:00

Run	Eff. Diam. (nm)	Half Width (nm)	Polydispersity	Baseline Index
1	243.4	121.6	0.249	8.6/100.00%
2	258.4	130.2	0.254	7.5/ 98.89%
3	269.4	130.8	0.236	9.2/ 98.89%
4	278.1	131.6	0.224	5.1/100.00%
5	276.6	120.3	0.189	6.4/ 95.56%
6	269.3	126.0	0.219	6.6/ 99.56%
Mean	265.9	126.7	0.229	7.2/ 98.82%
Std. Error	5.3	2.0	0.010	0.6/ 0.68
Combined	267.2	128.2	0.230	7.4/ 98.82%

Prolipo_2_XGA(atomi) (Combined)
Apr 18, 2017   14:00:55

Effective Diameter: 177.3 nm
Polydispersity: 0.323

Avg. Count Rate: 404.8 kcps
Baseline Index: 7.4/ 97.81%

Elapsed Time: 00:12:00
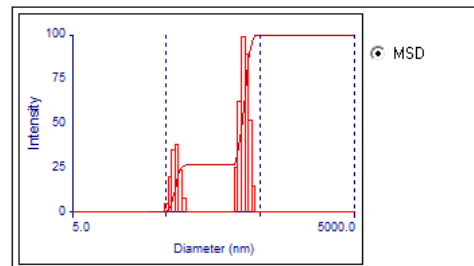
Run	Eff. Diam. (nm)	Half Width (nm)	Polydispersity	Baseline Index
1	196.4	102.9	0.274	6.4/ 98.88%
2	167.5	97.0	0.336	7.9/ 92.41%
3	165.9	96.5	0.338	9.2/ 96.65%
4	172.7	100.0	0.335	9.9/100.00%
5	176.3	98.9	0.315	5.0/ 98.88%
6	200.7	106.9	0.283	6.8/100.00%
Mean	179.9	100.4	0.314	7.5/ 97.81%
Std. Error	6.1	1.6	0.012	0.7/ 1.19
Combined	177.3	100.8	0.323	7.4/ 97.81%

Prolipo_3_XGA(atomi) (Combined)
Apr 18, 2017   14:20:14

Effective Diameter: 182.3 nm
Polydispersity: 0.304

Avg. Count Rate: 467.5 kcps
Baseline Index: 7.4/ 99.67%

Elapsed Time: 00:12:00
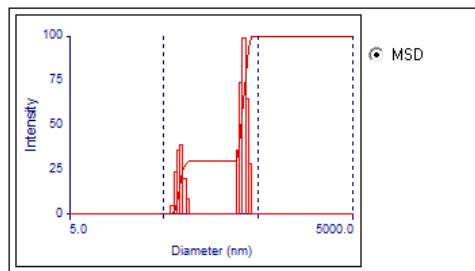
Run	Eff. Diam. (nm)	Half Width (nm)	Polydispersity	Baseline Index
1	174.1	98.4	0.320	8.0/100.00%
2	172.0	92.1	0.286	6.8/100.00%
3	170.8	95.1	0.310	8.8/ 99.11%
4	200.5	109.5	0.298	7.8/100.00%
5	201.2	106.6	0.281	7.1/ 98.89%
6	196.8	108.6	0.304	8.1/100.00%
Mean	185.9	101.7	0.300	7.8/ 99.67%
Std. Error	6.1	3.0	0.006	0.3/ 0.21
Combined	182.3	100.5	0.304	7.4/ 99.67%

Prolipo_vazio_1_atomizado (Combined)
Apr 24, 2017   11:09:16

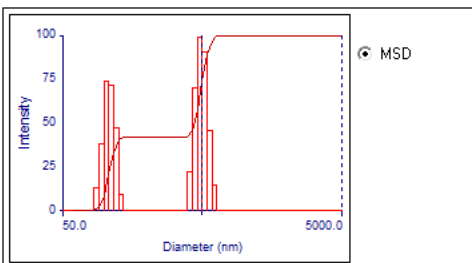**Effective Diameter:**   209.4 nm
Polydispersity: 0.301

Avg. Count Rate: 453.6 kcps
Baseline Index: 1.8/ 98.33%

Elapsed Time: 00:12:00

Run	Eff. Diam. (nm)	Half Width (nm)	Polydispersity	Baseline Index
1	199.9	114.0	0.325	5.2/ 98.89%
2	207.4	112.3	0.293	1.7/100.00%
3	216.6	118.6	0.300	3.3/ 96.66%
4	211.1	114.5	0.294	0.9/ 97.10%
5	209.2	112.1	0.287	0.0/ 97.77%
6	210.8	118.1	0.314	2.5/ 99.55%
Mean	209.2	114.9	0.302	2.3/ 98.33%
Std. Error	2.2	1.1	0.006	0.8/ 0.55
Combined	209.4	114.8	0.301	1.8/ 98.33%

Prolipo_XGA_1 (Combined)
Apr 24, 2017   11:47:26

Effective Diameter: 272.8 nm
Polydispersity: 0.302

Avg. Count Rate: 509.7 kcps
Baseline Index: 5.0/ 98.00%

Elapsed Time: 00:12:00
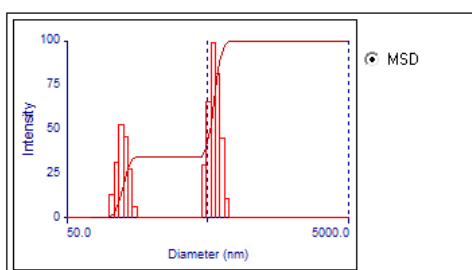
Run	Eff. Diam. (nm)	Half Width (nm)	Polydispersity	Baseline Index
1	260.9	143.4	0.302	7.2/ 97.78%
2	265.8	143.1	0.290	2.9/100.00%
3	274.5	149.8	0.298	3.7/ 98.89%
4	276.3	151.1	0.299	4.5/ 97.78%
5	281.6	161.3	0.328	6.5/ 96.67%
6	278.7	152.1	0.298	5.6/ 96.89%
Mean	273.0	150.1	0.302	5.1/ 98.00%
Std. Error	3.3	2.7	0.005	0.7/ 0.51
Combined	272.8	149.8	0.302	5.0/ 98.00%

Lipo_XGA_1 (Combined)
Apr 26, 2017   16:14:38

Effective Diameter: 102.1 nm
Polydispersity: 0.098

Avg. Count Rate: 378.1 kcps
Baseline Index: 10.0/ 97.02%

Elapsed Time: 00:12:00
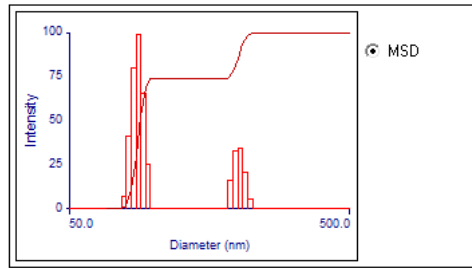
Run	Eff. Diam. (nm)	Half Width (nm)	Polydispersity	Baseline Index
1	96.9	28.9	0.089	8.9/ 97.76%
2	101.2	24.5	0.059	9.1/ 96.64%
3	103.0	37.3	0.131	9.2/ 94.41%
4	102.8	39.4	0.147	10.0/ 97.76%
5	103.5	36.6	0.125	8.7/ 95.53%
6	105.4	26.4	0.063	9.0/100.00%
Mean	102.1	32.2	0.102	9.1/ 97.02%
Std. Error	1.2	2.6	0.015	0.2/ 0.80
Combined	102.1	32.0	0.098	10.0/ 97.02%

Lipo_XGA_2 (Combined)
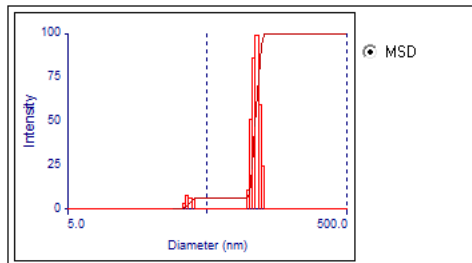Apr 26, 2017   16:34:15

Effective Diameter: 100.4 nm
Polydispersity: 0.095

Avg. Count Rate: 279.8 kcps
Baseline Index: 9.8/ 96.50%

Elapsed Time: 00:12:00

Run	Eff. Diam. (nm)	Half Width (nm)	Polydispersity	Baseline Index
1	95.6	27.8	0.085	8.3/ 98.88%
2	97.5	30.4	0.097	9.3/ 94.85%
3	100.1	27.2	0.074	8.9/ 94.85%
4	102.2	38.6	0.143	7.9/ 97.54%
5	103.7	26.9	0.067	7.5/100.00%
6	103.3	32.2	0.097	9.1/ 92.84%
Mean	100.4	30.5	0.094	8.5/ 96.50%
Std. Error	1.3	1.8	0.011	0.3/ 1.12
Combined	100.4	31.0	0.095	9.8/ 96.50%

Lipo_XGA_3 (Combined)
Apr 26, 2017   16:53:54

Effective Diameter: 105.0 nm
Polydispersity: 0.111

Avg. Count Rate: 23.1 kcps
Baseline Index: 4.9/ 88.15%

Elapsed Time: 00:12:00
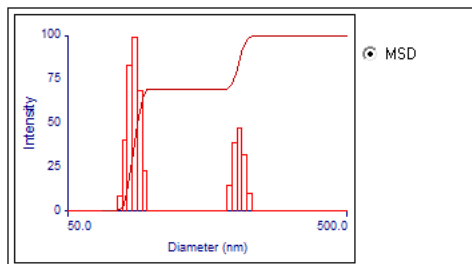
Run	Eff. Diam. (nm)	Half Width (nm)	Polydispersity	Baseline Index
1	98.3	38.5	0.154	1.5/ 82.78%
2	103.4	29.1	0.079	1.3/ 86.26%
3	104.5	34.3	0.108	2.4/ 88.13%
4	105.9	37.5	0.125	3.9/ 91.32%
5	107.3	34.7	0.105	9.2/ 89.06%
6	108.2	40.5	0.140	8.8/ 91.33%
Mean	104.6	35.8	0.118	4.5/ 88.15%
Std. Error	1.5	1.6	0.011	1.5/ 1.33
Combined	105.0	35.0	0.111	4.9/ 88.15%

Prolipo_XGA_2 (Combined)
May 3, 2017   10:16:32

Effective Diameter: 237.6 nm
Polydispersity: 0.304

Avg. Count Rate: 455.2 kcps
Baseline Index: 3.4/ 97.96%

Elapsed Time: 00:12:00
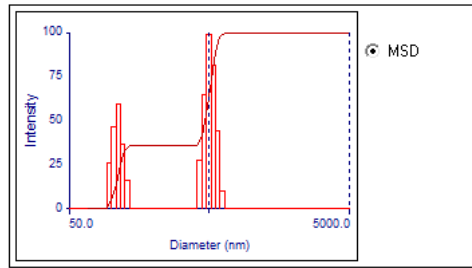
Run	Eff. Diam. (nm)	Half Width (nm)	Polydispersity	Baseline Index
1	236.5	132.1	0.312	9.7/ 97.77%
2	232.7	125.6	0.291	4.5/ 98.89%
3	243.8	133.4	0.299	1.8/ 95.55%
4	239.5	131.2	0.300	3.8/ 96.66%
5	235.9	128.1	0.295	0.0/ 98.89%
6	241.0	137.3	0.324	7.1/100.00%
Mean	238.2	131.3	0.304	4.5/ 97.96%
Std. Error	1.6	1.7	0.005	1.4/ 0.67
Combined	237.6	131.0	0.304	3.4/ 97.96%

Prolipo_XGA_3 (estab) (Combined)
May 3, 2017   10:47:10

Effective Diameter: 166.8 nm
Polydispersity: 0.005

Avg. Count Rate: 315.5 kcps
Baseline Index: 8.5/ 98.73%

Elapsed Time: 00:12:00
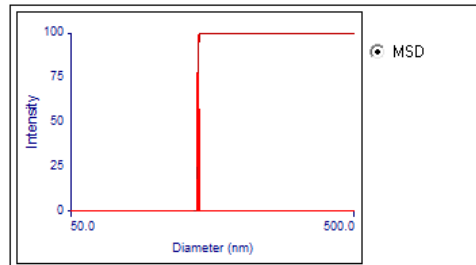
Run	Eff. Diam. (nm)	Half Width (nm)	Polydispersity	Baseline Index
1	160.6	11.4	0.005	8.6/ 98.88%
2	168.6	11.9	0.005	7.6/100.00%
3	170.2	12.0	0.005	6.5/ 94.63%
4	160.2	11.3	0.005	6.9/ 98.88%
5	166.6	11.8	0.005	9.8/100.00%
6	167.6	11.9	0.005	8.2/100.00%
Mean	165.7	11.7	0.005	7.9/ 98.73%
Std. Error	1.7	0.1	0.000	0.5/ 0.85
Combined	166.8	11.8	0.005	8.5/ 98.73%

Prolipo_vazio_atomizado_2 (Combined)
May 3, 2017   11:05:36

Effective Diameter: 190.5 nm
Polydispersity: 0.278

Avg. Count Rate: 65.3 kcps
Baseline Index: 3.6/ 99.01%

Elapsed Time: 00:12:00
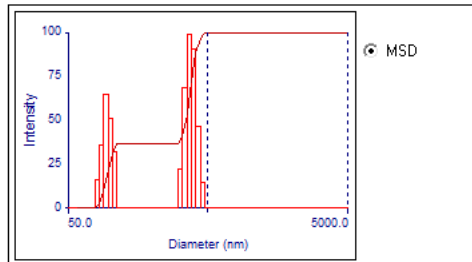
Run	Eff. Diam. (nm)	Half Width (nm)	Polydispersity	Baseline Index
1	180.0	89.1	0.245	7.9/ 98.96%
2	188.7	99.2	0.276	4.9/ 97.74%
3	191.4	104.5	0.298	0.0/ 98.96%
4	193.0	101.2	0.275	2.3/100.00%
5	189.9	98.3	0.268	1.3/100.00%
6	198.0	107.9	0.297	4.7/ 98.43%
Mean	190.2	100.0	0.276	3.5/ 99.01%
Std. Error	2.4	2.6	0.008	1.2/ 0.36
Combined	190.5	100.4	0.278	3.6/ 99.01%

Atomizado_prolipo_3 (Combined)
Jun 8, 2017   15:03:34

Effective Diameter: 132.5 nm
Polydispersity: 0.289

Avg. Count Rate: 404.4 kcps
Baseline Index: 3.3/ 96.65%

Elapsed Time: 00:12:00
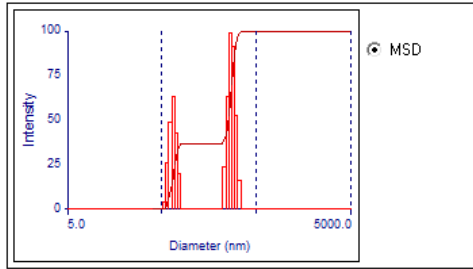
Run	Eff. Diam. (nm)	Half Width (nm)	Polydispersity	Baseline Index
1	104.3	56.4	0.293	8.0/ 96.21%
2	106.6	56.2	0.278	6.2/100.00%
3	118.8	60.3	0.258	7.1/ 95.54%
4	136.1	70.3	0.267	4.8/ 95.76%
5	151.4	81.0	0.286	4.7/ 98.88%
6	171.6	88.9	0.269	2.8/ 93.54%
Mean	131.5	68.9	0.275	5.6/ 96.65%
Std. Error	10.9	5.6	0.005	0.8/ 0.97
Combined	132.5	71.2	0.289	3.3/ 96.65%

Prolipo_1_xga(estab) (Combined)
Jun 21, 2017   11:25:28

Effective Diameter: 224.6 nm
Polydispersity: 0.272

Avg. Count Rate: 375.0 kcps
Baseline Index: 8.4/ 97.58%

Elapsed Time: 00:12:00
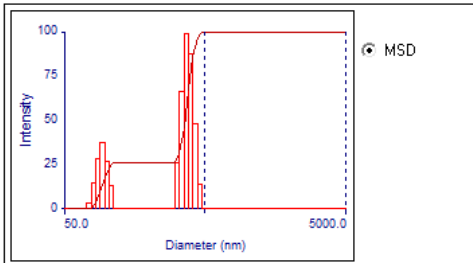
Run	Eff. Diam. (nm)	Half Width (nm)	Polydispersity	Baseline Index
1	249.4	131.0	0.276	9.1/ 97.76%
2	228.5	118.5	0.269	7.8/ 96.64%
3	223.8	114.6	0.262	6.9/100.00%
4	217.0	114.1	0.277	7.8/ 95.53%
5	212.3	109.3	0.265	7.1/ 98.88%
6	216.9	114.3	0.278	8.0/ 96.64%
Mean	224.6	117.0	0.271	7.8/ 97.58%
Std. Error	5.5	3.1	0.003	0.3/ 0.67
Combined	224.6	117.1	0.272	8.4/ 97.58%

Prolipo_xga_2 (estab) (Combined)
Jul 3, 2017   14:09:26

Effective Diameter: 237.6 nm
Polydispersity: 0.272

Avg. Count Rate: 396.0 kcps
Baseline Index: 3.7/ 97.25%

Elapsed Time: 00:12:00
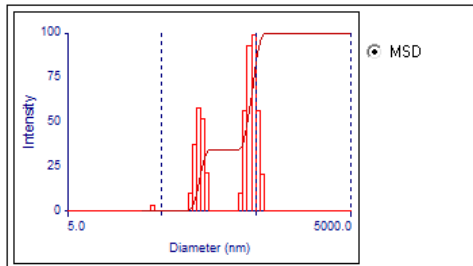
Run	Eff. Diam. (nm)	Half Width (nm)	Polydispersity	Baseline Index
1	215.8	106.8	0.245	0.6/ 94.42%
2	228.7	114.2	0.250	5.1/ 95.54%
3	236.8	123.6	0.273	2.4/100.00%
4	245.1	128.9	0.276	5.0/ 97.99%
5	251.3	134.5	0.286	9.0/ 98.88%
6	248.4	136.5	0.302	0.0/ 96.65%
Mean	237.7	124.1	0.272	3.7/ 97.25%
Std. Error	5.5	4.8	0.009	1.4/ 0.86
Combined	237.6	123.9	0.272	3.7/ 97.25%

Prolipo_xga_3(estab) (Combined)
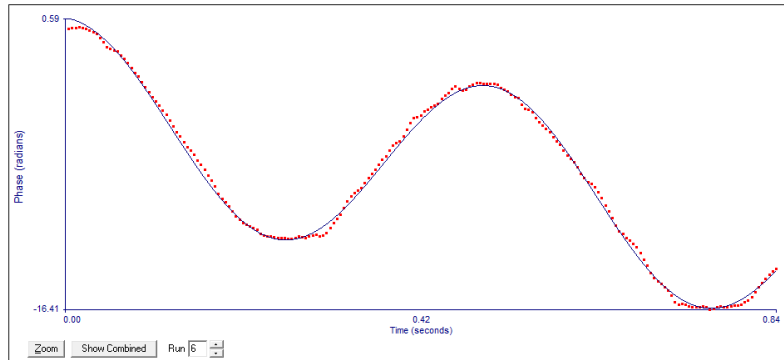**Jul 3, 2017   14:46:02**

Effective Diameter: 117.6 nm
Polydispersity: 0.184

Avg. Count Rate: 316.4 kcps
Baseline Index: 7.2/ 99.22%

Elapsed Time: 00:12:00
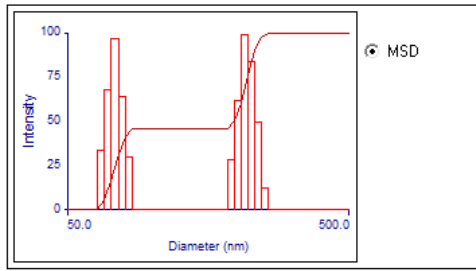
Run	Eff. Diam. (nm)	Half Width (nm)	Polydispersity	Baseline Index
1	88.5	29.1	0.108	0.3/100.00%
2	116.0	34.1	0.086	9.8/ 98.43%
3	124.8	49.1	0.155	9.6/ 98.88%
4	131.0	51.0	0.152	9.1/100.00%
5	136.2	57.0	0.175	6.7/ 97.98%
6	134.1	60.6	0.204	9.7/100.00%
Mean	121.8	46.8	0.147	7.5/ 99.22%
Std. Error	7.3	5.1	0.018	1.5/ 0.37
Combined	117.6	50.4	0.184	7.2/ 99.22%

75

Appendix VII– DLS graphics related to the zeta potential of proliposomes and liposomes.
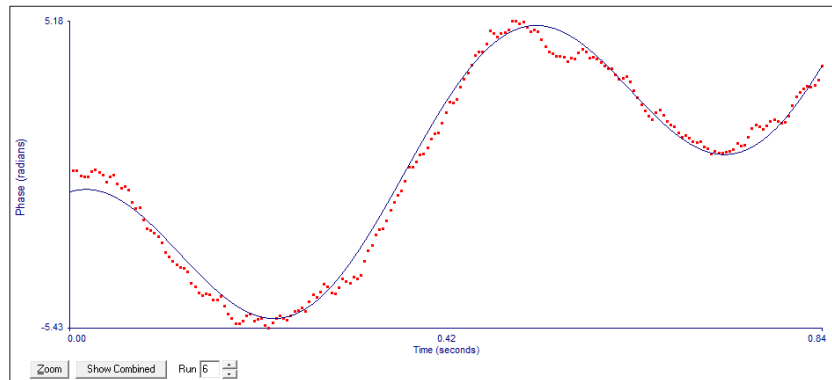
ProLipo (lote 2 vazio nano) (Run 6)
Measurement Completed
Runs Completed: 6
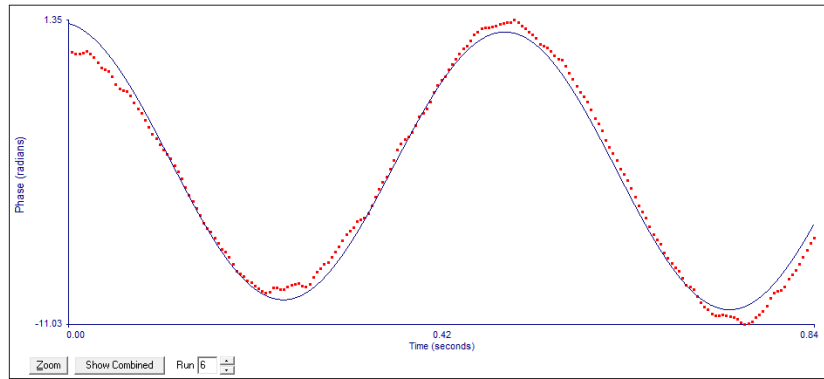
Run	Mobility	Zeta Potential (mV)	Rel. Residual
1	- 3.16	- 44.48	0.0145
2	- 3.46	- 48.67	0.0330
3	- 3.48	- 49.03	0.0156
4	- 3.53	- 49.67	0.0212
5	- 3.42	- 48.16	0.0225
6	- 3.67	- 51.73	0.0293
Mean	- 3.45	- 48.62	0.0227
Std. Error	0.07	0.97	0.0030
Combined	- 3.45	- 48.58	0.0152

Start   Runs   Hide Graph

Clear   Parameters   Copy To Clipboard

lipo_farmaco_1_nano (Run 6)
Measurement Completed
Runs Completed: 6
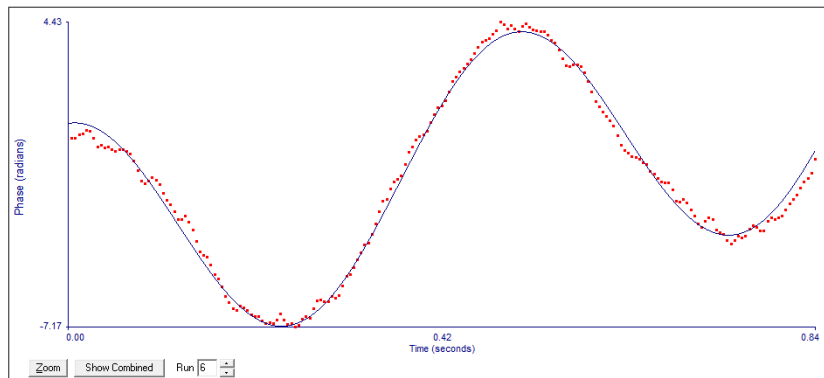
Run	Mobility	Zeta Potential (mV)	Rel. Residual
1	- 2.38	- 33.58	0.0311
2	- 2.85	- 40.11	0.0520
3	- 2.98	- 41.96	0.0297
4	- 3.28	- 46.21	0.0332
5	- 2.82	- 39.65	0.0447
6	- 3.62	- 50.99	0.0219
Mean	- 2.99	- 42.08	0.0354
Std. Error	0.17	2.44	0.0045
Combined	- 2.97	- 41.85	0.0175

Start   Runs   Hide Graph

Clear   Parameters   Copy To Clipboard

77

lipo_farmaco_1_lio (Run 6)
Measurement Completed
Runs Completed: 6
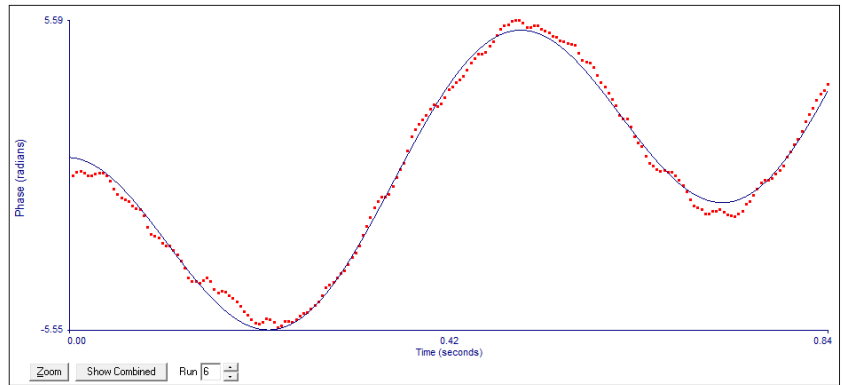
Run	Mobility	Zeta Potential (mV)	Rel. Residual
1	-2.93	-41.26	0.0185
2	-3.25	-45.81	0.0113
3	-2.83	-39.86	0.0222
4	-3.08	-43.40	0.0201
5	-3.01	-42.38	0.0186
6	-3.11	-43.79	0.0200
Mean	-3.04	-42.75	0.0185
Std. Error	0.06	0.85	0.0015
Combined	-3.03	-42.72	0.0110

Start   Runs   Hide Graph
Clear   Parameters   Copy To Clipboard

Prolipo_3_farmaco(atomiz) (Run 6)
Measurement Completed
Runs Completed: 6
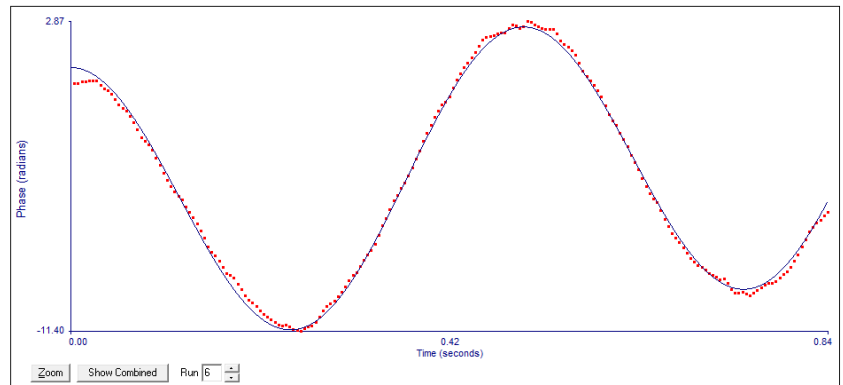
Run	Mobility	Zeta Potential (mV)	Rel. Residual
1	-3.52	-49.61	0.0109
2	-3.47	-48.82	0.0169
3	-3.40	-47.89	0.0119
4	-3.65	-51.37	0.0292
5	-3.76	-52.96	0.0311
6	-3.75	-52.77	0.0160
Mean	-3.59	-50.57	0.0193
Std. Error	0.06	0.86	0.0036
Combined	-3.59	-50.56	0.0135

Start   Runs   Hide Graph
Clear   Parameters   Copy To Clipboard

78

Prolip_3_vazio(atomizad) (Run 6)
Measurement Completed
Runs Completed: 6

Phase (radians)

1.98

-5.73

0.00   0.42   0.84
Time (seconds)

Zoom   Show Combined   Run 6
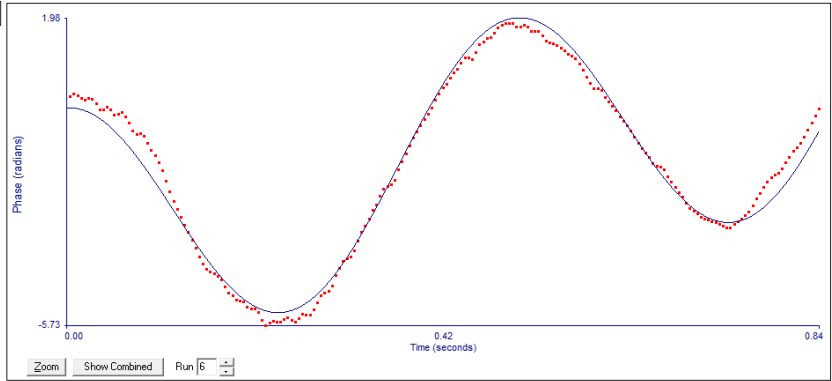
Run	Mobility	Zeta Potential (mV)	Rel. Residual
1	-2.55	-35.94	0.0196
2	-2.82	-39.75	0.0230
3	-2.55	-35.96	0.0177
4	-2.75	-38.74	0.0269
5	-2.61	-36.70	0.0157
6	-2.48	-34.91	0.0199
Mean	-2.63	-37.00	0.0205
Std. Error	0.05	0.76	0.0016
Combined	-2.62	-36.96	0.0074

Start   Runs   Hide Graph

Clear   Parameters   Copy To Clipboard

Prolip_1_XGA(atomizad) (Run 6)
Measurement Completed
Runs Completed: 6

Phase (radians)

1.23

-5.19

0.00   0.42   0.84
Time (seconds)

Zoom   Show Combined   Run 6
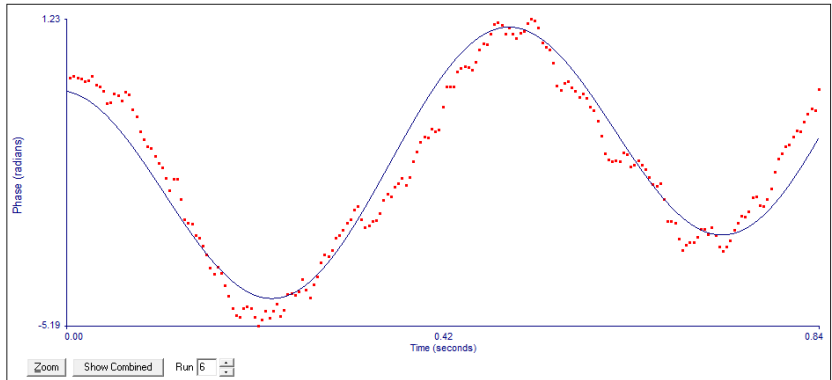
Run	Mobility	Zeta Potential (mV)	Rel. Residual
1	-2.48	-34.95	0.0198
2	-2.53	-35.63	0.0164
3	-2.41	-33.95	0.0371
4	-1.98	-27.92	0.0547
5	-2.29	-32.30	0.0278
6	-1.76	-24.84	0.0332
Mean	-2.24	-31.60	0.0315
Std. Error	0.12	1.76	0.0056
Combined	-2.21	-31.14	0.0125

Start   Runs   Hide Graph

Clear   Parameters   Copy To Clipboard

Prolipo_lote2_XGA_atomi (Run 6)
Measurement Completed
Runs Completed: 6
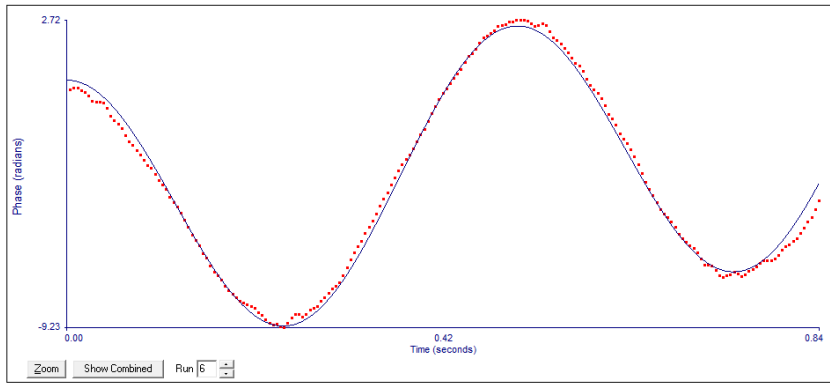
Run	Mobility	Zeta Potential (mV)	Rel. Residual
1	-3.34	-47.06	0.0357
2	-3.28	-46.16	0.0182
3	-3.28	-46.14	0.0155
4	-3.08	-43.42	0.0195
5	-3.22	-45.29	0.0163
6	-3.19	-44.88	0.0191
Mean	-3.23	-45.49	0.0207
Std. Error	0.04	0.52	0.0031
Combined	-3.23	-45.45	0.0124

Start   Runs   Hide Graph
Clear   Parameters   Copy To Clipboard

Prolipo_1_XGA (atomizad) (Run 6)
Measurement Completed
Runs Completed: 6
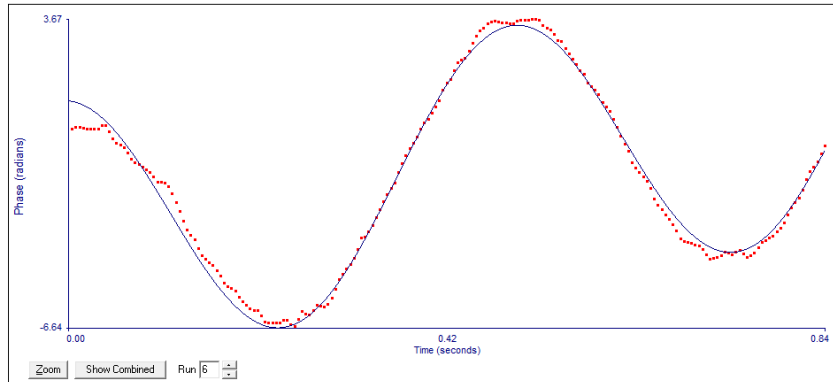
Run	Mobility	Zeta Potential (mV)	Rel. Residual
1	-2.38	-33.49	0.0210
2	-2.42	-34.01	0.0214
3	-2.87	-40.43	0.0189
4	-2.85	-40.07	0.0163
5	-2.92	-41.10	0.0182
6	-2.76	-38.85	0.0205
Mean	-2.70	-37.99	0.0194
Std. Error	0.10	1.38	0.0008
Combined	-2.70	-37.98	0.0090

Start   Runs   Hide Graph
Clear   Parameters   Copy To Clipboard

Prolipo_XGA_3 (atomiza) (Run 6)
Measurement Completed
Runs Completed: 6

Zoom | Show Combined | Run 6
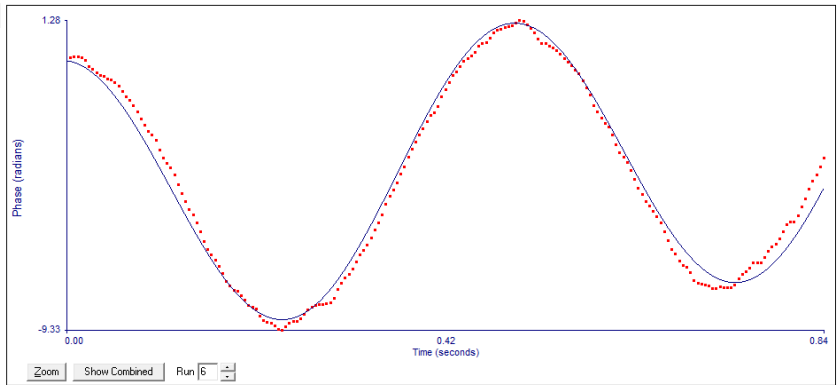
Run	Mobility	Zeta Potential (mV)	Rel. Residual
1	-2.57	-36.16	0.0117
2	-3.07	-43.17	0.0169
3	-3.05	-43.00	0.0265
4	-2.65	-37.27	0.0269
5	-2.87	-40.41	0.0262
6	-3.17	-44.60	0.0267
Mean	-2.90	-40.77	0.0225
Std. Error	0.10	1.40	0.0027
Combined	-2.89	-40.74	0.0058

Start | Runs | Hide Graph
Clear | Parameters | Copy To Clipboard

Prolipo_3_vazio (atomiz-est) (Run 6)
Measurement Completed
Runs Completed: 6

Zoom | Show Combined | Run 6
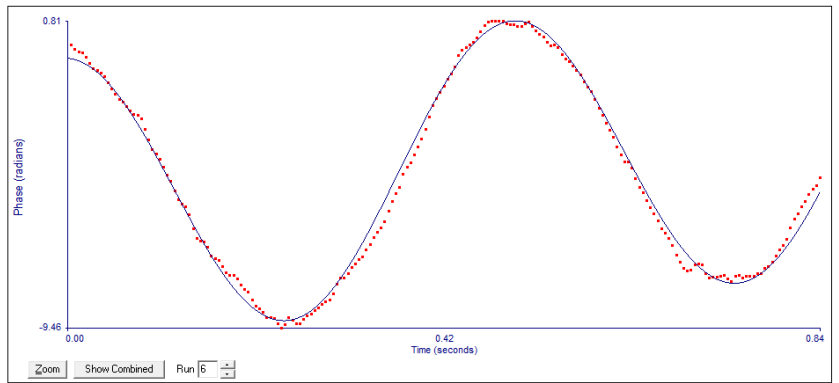
Run	Mobility	Zeta Potential (mV)	Rel. Residual
1	-2.62	-36.83	0.0120
2	-2.69	-37.93	0.0174
3	-2.50	-35.24	0.0358
4	-2.59	-36.44	0.0152
5	-2.74	-38.64	0.0170
6	-2.82	-39.66	0.0187
Mean	-2.66	-37.46	0.0193
Std. Error	0.05	0.65	0.0034
Combined	-2.66	-37.41	0.0085

Start | Runs | Hide Graph
Clear | Parameters | Copy To Clipboard

81

Lipo 24Fev17 - 6 semanas dp (Run 6)
Measurement Completed
Runs Completed: 6
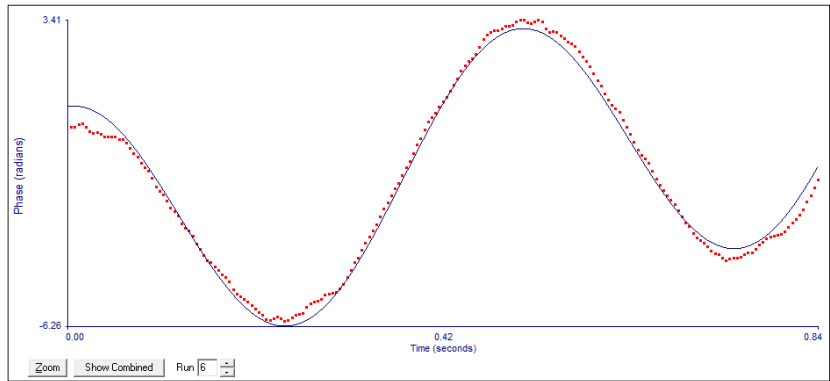
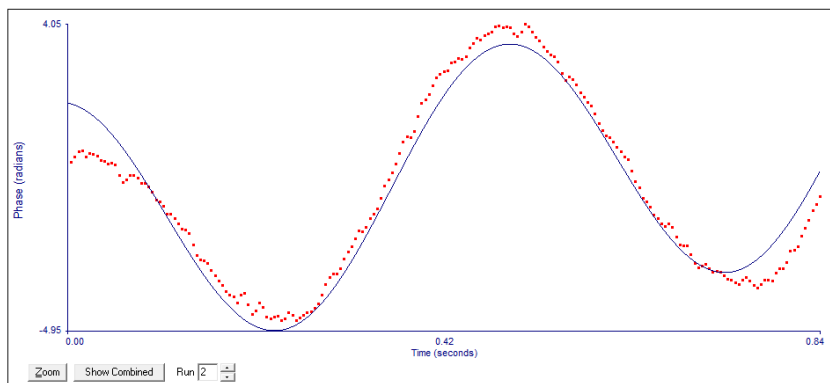| Run	Mobility	Zeta Potential (mV)	Rel. Residual
1	-2.44	-34.34	0.0150
2	-2.37	-33.40	0.0197
3	-2.17	-30.51	0.0170
4	-2.11	-29.71	0.0202
5	-2.49	-35.07	0.0205
6	-2.32	-32.69	0.0199
Mean	-2.32	-32.62	0.0187
Std. Error	0.06	0.87	0.0009
Combined	-2.31	-32.57	0.0074

Start Runs Hide Graph
Clear Parameters Copy To Clipboard

Lipo_vazio1_ final (Run 2)
Measurement Completed
Runs Completed: 2

Run	Mobility	Zeta Potential (mV)	Rel. Residual
1	-3.17	-44.69	0.0289
2	-2.91	-40.94	0.0391
Mean	-3.04	-42.82	0.0340
Std. Error	0.13	1.88	0.0051
Combined	-3.04	-42.74	0.0223

Start Runs Hide Graph
Clear Parameters Copy To Clipboard

82

Lipo_vazio1_ final (Run 6)
Measurement Completed
Runs Completed: 6

Phase (radians) — 3.29 ... -4.80
Time (seconds) 0.00 0.42 0.84

Zoom | Show Combined | Run 6
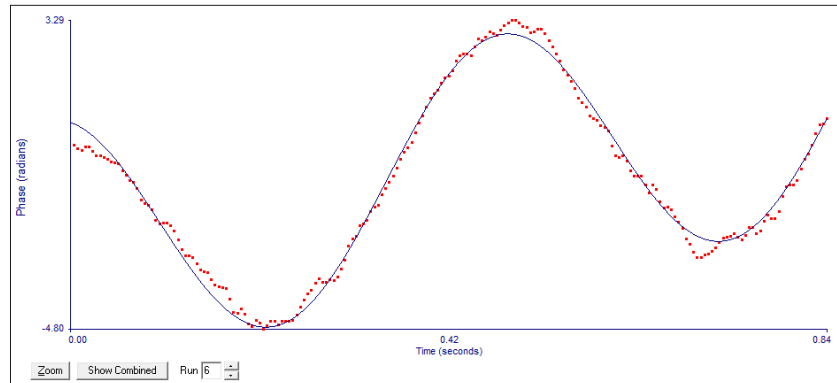
Run	Mobility	Zeta Potential (mV)	Rel. Residual
1	-2.98	-42.02	0.0158
2	-2.67	-37.65	0.0430
3	-2.49	-35.02	0.0379
4	-2.35	-33.02	0.0218
5	-2.37	-33.36	0.0345
6	-2.61	-36.81	0.0161
Mean	-2.58	-36.32	0.0282
Std. Error	0.10	1.36	0.0048
Combined	-2.57	-36.14	0.0138

Start | Runs | Hide Graph
Clear | Parameters | Copy To Clipboard

Lipo_vazio2_ final (Run 6)
Measurement Completed
Runs Completed: 6

Phase (radians) — 4.27 ... -5.83
Time (seconds) 0.00 0.42 0.84

Zoom | Show Combined | Run 6
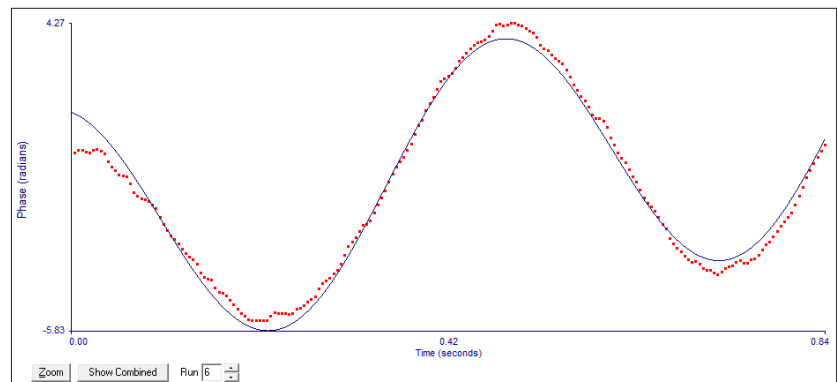
Run	Mobility	Zeta Potential (mV)	Rel. Residual
1	-3.08	-43.32	0.0211
2	-3.11	-43.78	0.0157
3	-3.07	-43.28	0.0172
4	-3.12	-43.97	0.0206
5	-3.16	-44.49	0.0120
6	-3.29	-46.32	0.0251
Mean	-3.14	-44.19	0.0186
Std. Error	0.03	0.46	0.0019
Combined	-3.14	-44.18	0.0130

Start | Runs | Hide Graph
Clear | Parameters | Copy To Clipboard

83

Lipo_vazio3_ final (Run 6)
Measurement Completed
Runs Completed: 6
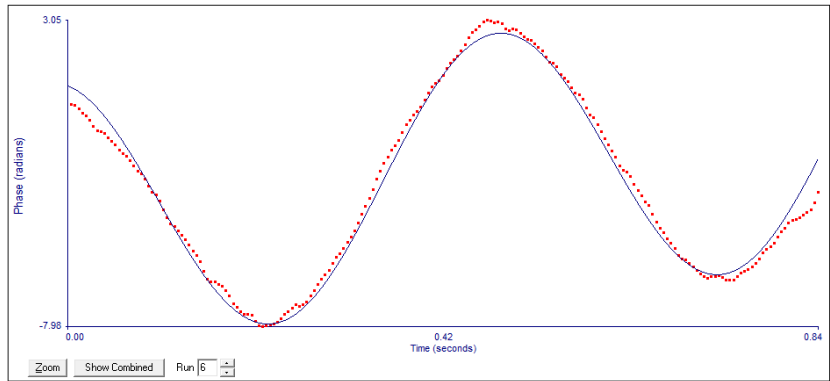
Run	Mobility	Zeta Potential (mV)	Rel. Residual
1	-3.47	-48.81	0.0221
2	-3.74	-52.66	0.0203
3	-3.99	-56.15	0.0322
4	-3.81	-53.70	0.0346
5	-3.80	-53.50	0.0267
6	-3.80	-53.53	0.0260
Mean	-3.77	-53.06	0.0270
Std. Error	0.07	0.98	0.0023
Combined	-3.77	-53.05	0.0232

Start   Runs   Hide Graph
Clear   Parameters   Copy To Clipboard

Prolipo_2_XGA(atomi) (Run 6)
Measurement Completed
Runs Completed: 6
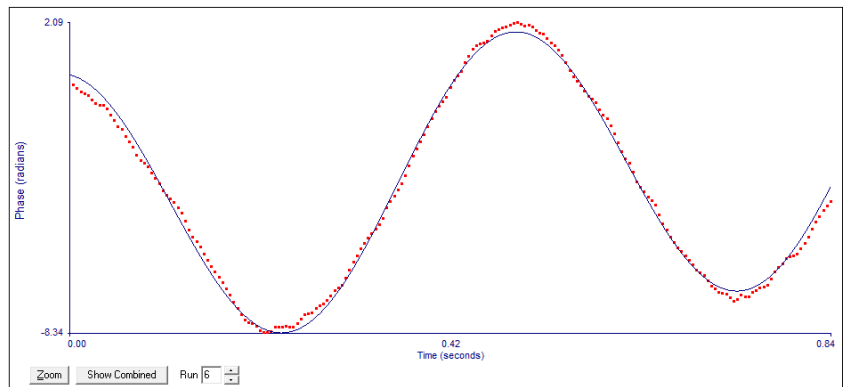
Run	Mobility	Zeta Potential (mV)	Rel. Residual
1	-2.89	-40.64	0.0153
2	-3.26	-45.84	0.0132
3	-2.99	-42.07	0.0142
4	-3.33	-46.83	0.0120
5	-3.59	-50.51	0.0279
6	-3.26	-45.87	0.0147
Mean	-3.22	-45.29	0.0162
Std. Error	0.10	1.44	0.0024
Combined	-3.21	-45.23	0.0066

Start   Runs   Hide Graph
Clear   Parameters   Copy To Clipboard

Prolipo_3_XGA(atomi) (Run 6)
Measurement Completed
Runs Completed: 6
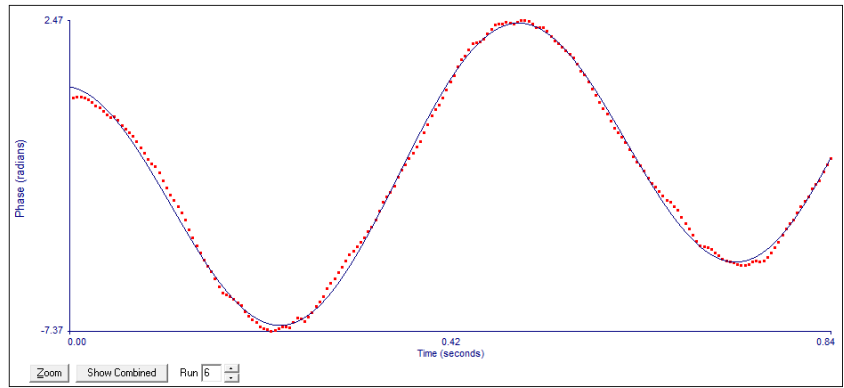
Run	Mobility	Zeta Potential (mV)	Rel. Residual
1	-3.02	-42.56	0.0142
2	-3.07	-43.29	0.0114
3	-2.98	-41.96	0.0174
4	-2.87	-40.38	0.0135
5	-3.14	-44.16	0.0154
6	-3.18	-44.84	0.0115
Mean	-3.04	-42.87	0.0139
Std. Error	0.05	0.65	0.0009
Combined	-3.04	-42.83	0.0071

Prolipo_vazio_1_atomizado (Run 6)
Measurement Completed
Runs Completed: 6
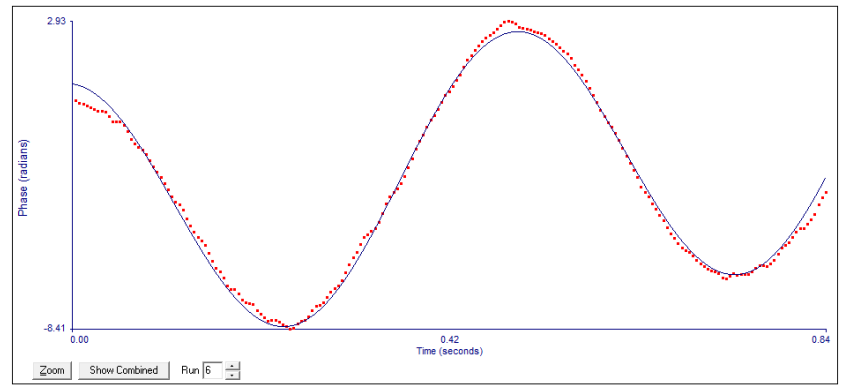
Run	Mobility	Zeta Potential (mV)	Rel. Residual
1	-3.97	-55.93	0.0192
2	-3.73	-52.57	0.0250
3	-3.78	-53.26	0.0186
4	-3.68	-51.84	0.0153
5	-3.79	-53.43	0.0206
6	-4.13	-58.16	0.0169
Mean	-3.85	-54.20	0.0193
Std. Error	0.07	0.97	0.0014
Combined	-3.85	-54.16	0.0074

Prolipo_vazio_1_liofiliz (Run 6)
Measurement Completed
Runs Completed: 6
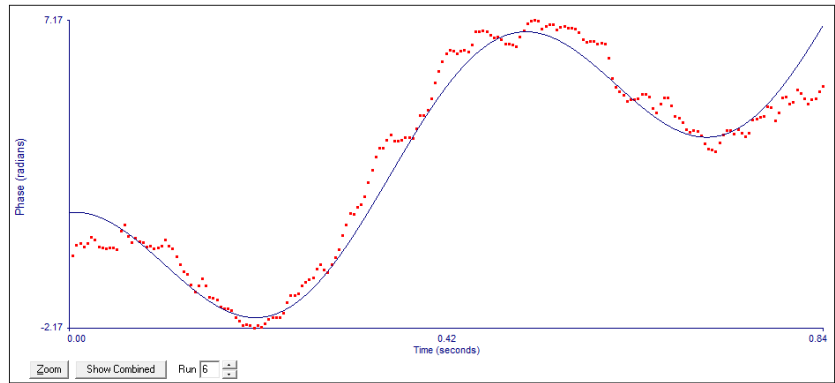
Run	Mobility	Zeta Potential (mV)	Rel. Residual
1	-1.59	-22.39	0.0486
2	-1.82	-25.57	0.0364
3	-2.05	-28.87	0.0492
4	-2.04	-28.78	0.0653
5	-1.79	-25.21	0.0380
6	-2.15	-30.26	0.0411
Mean	-1.91	-26.85	0.0465
Std. Error	0.09	1.21	0.0044
Combined	-1.85	-26.07	0.0240

Start Runs Hide Graph
Clear Parameters Copy To Clipboard

Prolipo_XGA_1 (Run 6)
Measurement Completed
Runs Completed: 6
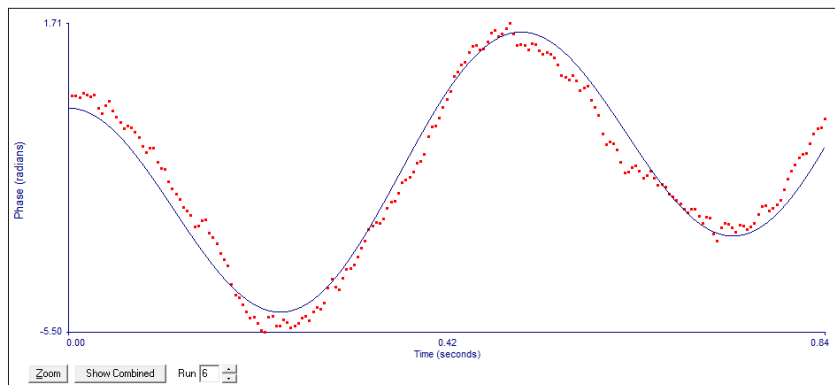
Run	Mobility	Zeta Potential (mV)	Rel. Residual
1	-2.27	-31.96	0.0200
2	-1.97	-27.79	0.0252
3	-2.15	-30.26	0.0207
4	-2.02	-28.43	0.0203
5	-2.12	-29.91	0.0227
6	-2.00	-28.19	0.0281
Mean	-2.09	-29.43	0.0228
Std. Error	0.05	0.65	0.0013
Combined	-2.08	-29.33	0.0079

Start Runs Hide Graph
Clear Parameters Copy To Clipboard

Lipo_XGA_1 (Run 6)
Measurement Completed
Runs Completed: 6
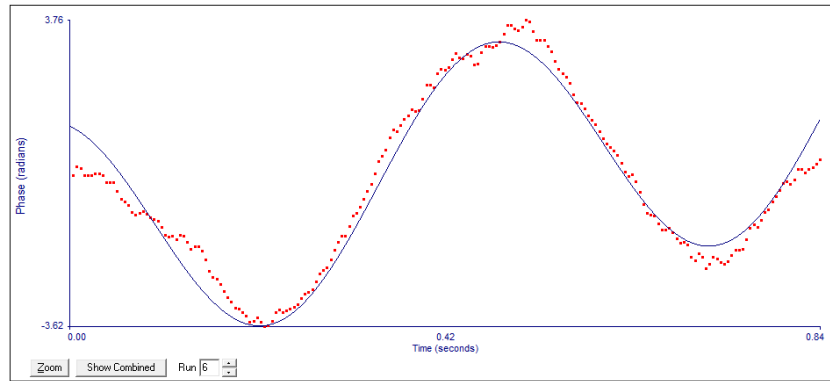
Run	Mobility	Zeta Potential (mV)	Rel. Residual
1	-1.99	-27.97	0.0232
2	-1.66	-23.41	0.0213
3	-1.81	-25.44	0.0257
4	-2.09	-29.49	0.0213
5	-1.59	-22.43	0.0207
6	-2.32	-32.68	0.0283
Mean	-1.91	-26.90	0.0234
Std. Error	0.11	1.59	0.0012
Combined	-1.90	-26.82	0.0167

Zoom Show Combined Run 6

Start Runs Hide Graph
Clear Parameters Copy To Clipboard

Lipo_XGA_2 (Run 6)
Measurement Completed
Runs Completed: 6
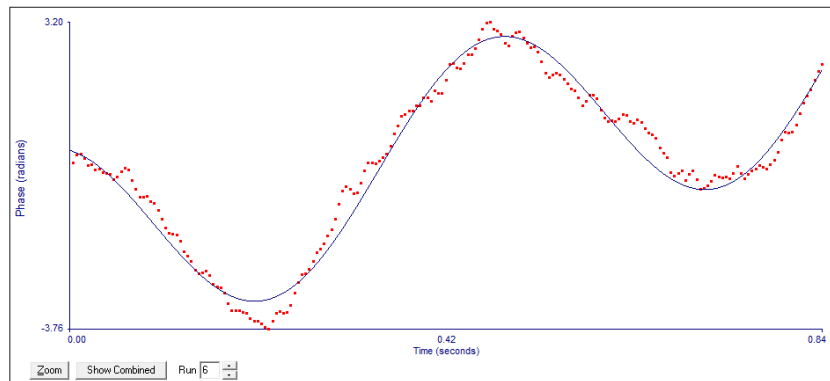
Run	Mobility	Zeta Potential (mV)	Rel. Residual
1	-1.35	-19.02	0.0244
2	-1.84	-25.89	0.0289
3	-1.99	-27.98	0.0325
4	-1.44	-20.31	0.0276
5	-1.41	-19.88	0.0335
6	-1.91	-26.87	0.0219
Mean	-1.66	-23.33	0.0281
Std. Error	0.12	1.64	0.0018
Combined	-1.61	-22.63	0.0111

Zoom Show Combined Run 6

Start Runs Hide Graph
Clear Parameters Copy To Clipboard

87

Lipo_XGA_3 (Run 6)
Measurement Completed
Runs Completed: 6

Phase (radians) | 1.94 ... -5.20 | Time (seconds) 0.00 ... 0.42 ... 0.84

Zoom | Show Combined | Run 6
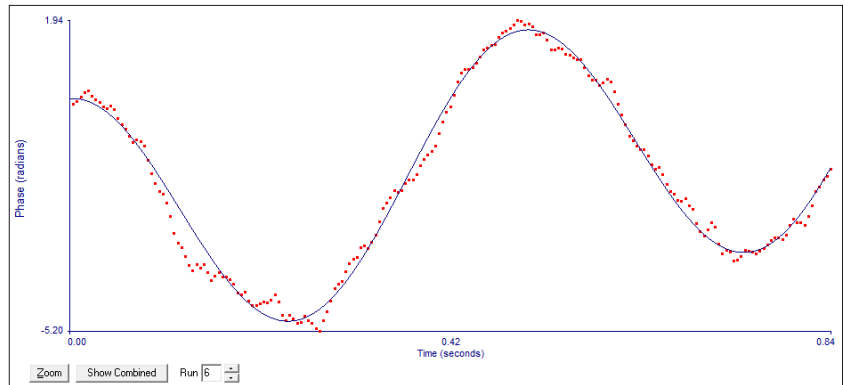
Run	Mobility	Zeta Potential (mV)	Rel. Residual
1	-1.90	-26.82	0.0252
2	-1.75	-24.60	0.0385
3	-1.71	-24.08	0.0310
4	-2.10	-29.54	0.0256
5	-2.22	-31.28	0.0178
6	-1.92	-27.08	0.0180
Mean	-1.93	-27.23	0.0260
Std. Error	0.08	1.14	0.0032
Combined	-1.93	-27.16	0.0133

Start | Runs | Hide Graph
Clear | Parameters | Copy To Clipboard

Prolipo_XGA_2 (Run 6)
Measurement Completed
Runs Completed: 6

Phase (radians) | 2.06 ... -1.82 | Time (seconds) 0.00 ... 0.42 ... 0.84

Zoom | Show Combined | Run 6
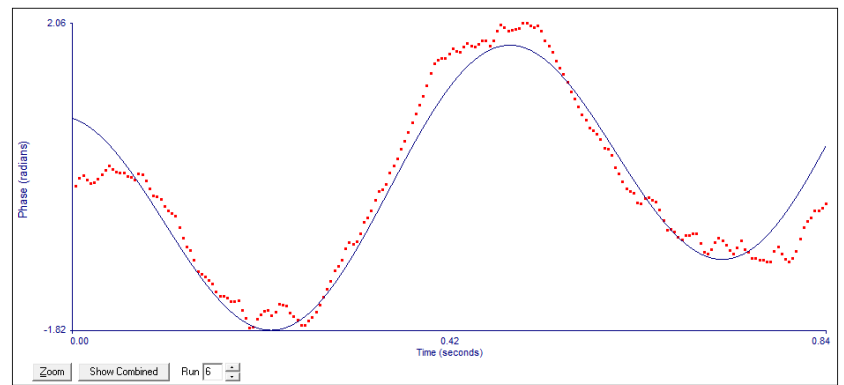
Run	Mobility	Zeta Potential (mV)	Rel. Residual
1	-1.24	-17.43	0.0087
2	-1.24	-17.51	0.0101
3	-1.12	-15.77	0.0220
4	-1.30	-18.28	0.0162
5	-0.98	-13.79	0.0124
6	-1.22	-17.14	0.0201
Mean	-1.18	-16.65	0.0149
Std. Error	0.05	0.66	0.0022
Combined	-1.18	-16.64	0.0092

Start | Runs | Hide Graph
Clear | Parameters | Copy To Clipboard

Prolipo_XGA_3 (Run 6)
Measurement Completed
Runs Completed: 6
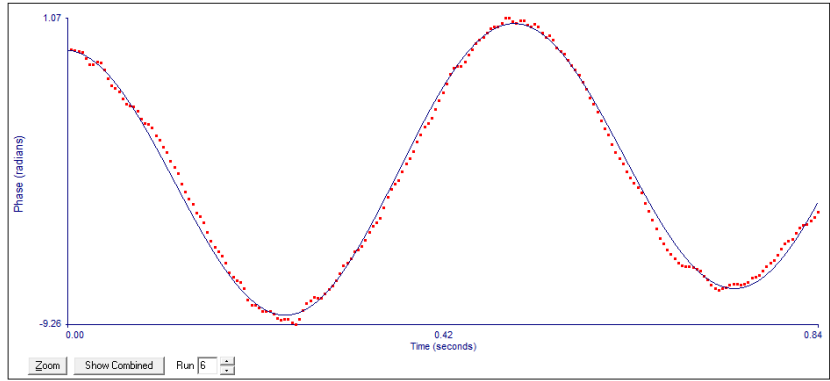
Run	Mobility	Zeta Potential (mV)	Rel. Residual
1	-2.59	-36.48	0.0194
2	-2.66	-37.40	0.0209
3	-2.38	-33.54	0.0173
4	-2.64	-37.15	0.0269
5	-2.75	-38.71	0.0406
6	-3.09	-43.45	0.0165
Mean	-2.68	-37.79	0.0236
Std. Error	0.09	1.33	0.0037
Combined	-2.68	-37.73	0.0114

Start   Runs   Hide Graph
Clear   Parameters   Copy To Clipboard

Prolipo_vazio_atomizado_2 (Run 6)
Measurement Completed
Runs Completed: 6
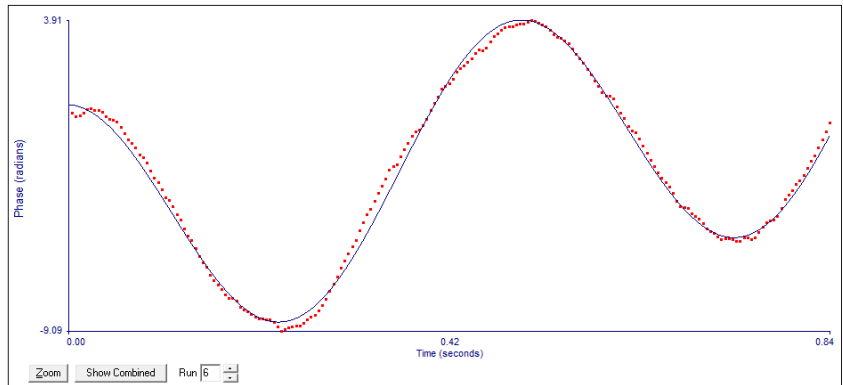
Run	Mobility	Zeta Potential (mV)	Rel. Residual
1	-3.82	-53.79	0.0206
2	-3.64	-51.22	0.0189
3	-3.80	-53.48	0.0174
4	-3.85	-54.26	0.0330
5	-3.95	-55.67	0.0183
6	-3.94	-55.47	0.0212
Mean	-3.83	-53.98	0.0216
Std. Error	0.05	0.66	0.0024
Combined	-3.83	-53.93	0.0121

Start   Runs   Hide Graph
Clear   Parameters   Copy To Clipboard

atomizadi_prolipo_3 (Run 6)
Measurement Completed
Runs Completed: 6
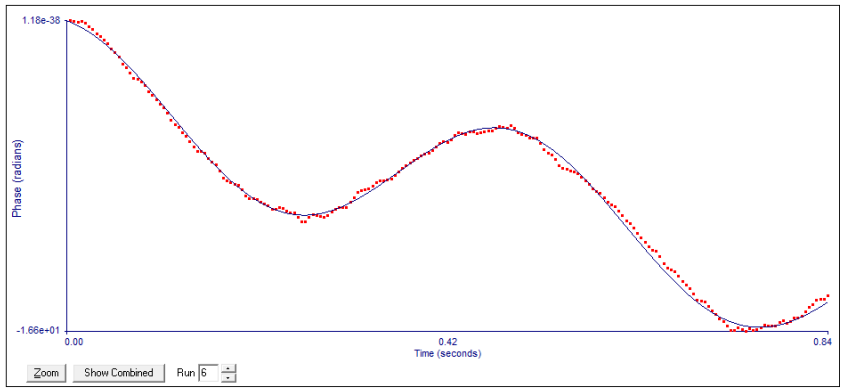
Run	Mobility	Zeta Potential (mV)	Rel. Residual
1	-1.84	-25.89	0.0282
2	-2.27	-31.95	0.0290
3	-2.38	-33.46	0.0310
4	-2.46	-34.71	0.0210
5	-2.57	-36.13	0.0199
6	-2.21	-31.12	0.0156
Mean	-2.29	-32.21	0.0241
Std. Error	0.10	1.47	0.0025
Combined	-2.29	-32.19	0.0109

Start   Runs   Hide Graph
Clear   Parameters   Copy To Clipboard

Prolipo_1_xga(estab) (Run 6)
Measurement Completed
Runs Completed: 6
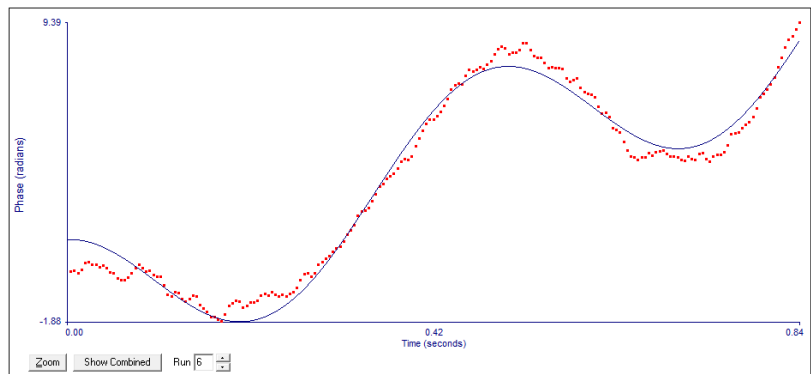
Run	Mobility	Zeta Potential (mV)	Rel. Residual
1	-2.32	-32.66	0.0303
2	-3.00	-42.21	0.0283
3	-2.90	-40.85	0.0392
4	-2.72	-38.26	0.0519
5	-2.50	-35.22	0.0294
6	-2.60	-36.55	0.0343
Mean	-2.67	-37.62	0.0356
Std. Error	0.10	1.45	0.0037
Combined	-2.66	-37.49	0.0184

Start   Runs   Hide Graph
Clear   Parameters   Copy To Clipboard

90

Prolipo_xga_2 (estab) (Run 6)
Measurement Completed
Runs Completed: 6

3.23

Phase (radians)

-6.75

0.00   0.42   0.84
Time (seconds)

Zoom   Show Combined   Run 6
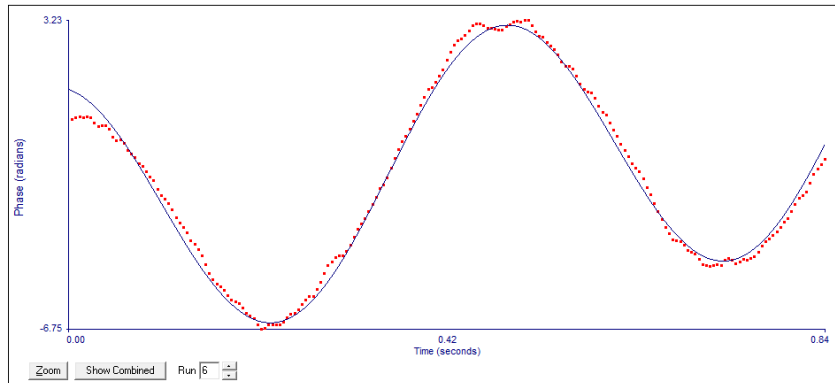
Run	Mobility	Zeta Potential (mV)	Rel. Residual
1	-2.88	-40.61	0.0279
2	-2.72	-38.28	0.0169
3	-2.48	-34.97	0.0207
4	-3.19	-44.89	0.0260
5	-2.73	-38.41	0.0203
6	-3.13	-44.07	0.0190
Mean	-2.86	-40.21	0.0218
Std. Error	0.11	1.54	0.0017
Combined	-2.85	-40.16	0.0150

Start   Runs   Hide Graph
Clear   Parameters   Copy To Clipboard

Prolipo_xga_3 (estab) (Run 6)
Measurement Completed
Runs Completed: 6

2.84

Phase (radians)

-5.16

0.00   0.42   0.84
Time (seconds)

Zoom   Show Combined   Run 6
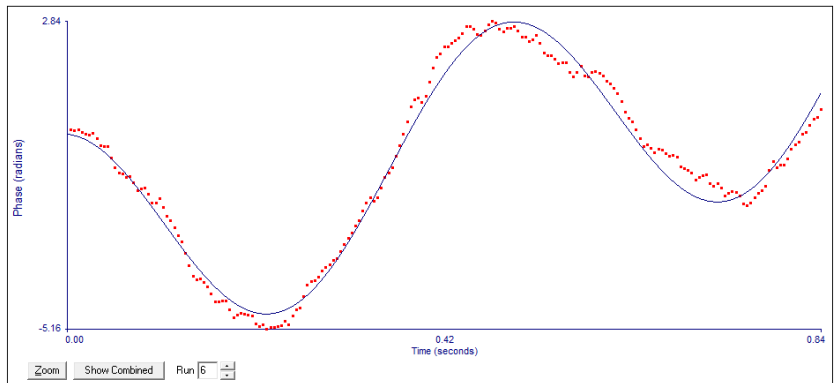
Run	Mobility	Zeta Potential (mV)	Rel. Residual
1	-2.29	-32.27	0.0387
2	-2.21	-31.07	0.0298
3	-2.26	-31.86	0.0259
4	-2.11	-29.66	0.0383
5	-2.09	-29.47	0.0295
6	-2.28	-32.08	0.0233
Mean	-2.21	-31.07	0.0309
Std. Error	0.04	0.50	0.0026
Combined	-2.20	-31.01	0.0094

Start   Runs   Hide Graph
Clear   Parameters   Copy To Clipboard

91